The role of energy & fatty acid metabolism in obesity and insulin resistance

"The role of energy & fatty acid metabolism in obesity and insulin resistance"
Cover design & Layout: Marcel IJssennagger & Mattijs M. Heemskerk
Printed by: Gildeprint Drukkerijen
ISBN: 9789462330351

The role of energy & fatty acid metabolism in obesity and insulin resistance

PROEFSCHRIFT

ter verkrijging van
de graad van Doctor aan de Universiteit Leiden,
op gezag van Rector Magnificus prof.mr. C.J.J.M. Stolker,
volgens besluit van het College voor Promoties
te verdedigen op dinsdag 6 oktober 2015
klokke 16.15 uur

door

Mattijs Maria Heemskerk

geboren te Rijpwetering
in 1985

Promotie commissie

Promotor:	Prof. dr. ir. J.A.P Willems van Dijk
Co-promotor:	dr. V.J.A. van Harmelen
Overige leden:	Prof. dr. P.C.N. Rensen Prof. dr. ir. A.H. Kersten (Universiteit Wageningen, Wageningen) Prof. dr. M. van Eck dr. M.A. Giera dr. ing. S.A.A. van den Berg (Amphia ziekenhuis, Breda)

The research described in this thesis was performed at the department of Human Genetics and at the Einthoven Laboratory for Experimental Vascular Medicine, Leiden University Medical Center, Leiden, The Netherlands. The research was financially supported by grants from the Netherlands Center for Systems Biology.

Financial support by the Dutch Heart Foundation and the Netherlands Association for the Study of Obesity for the publication of this thesis is gratefully acknowledged. The printing of this thesis was kindly supported by TSE Systems and Beun-De Ronde.

Table of contents

Voorwoord

Het leven staat in een delicate relatie tot zijn omgeving. Maar dit betekent niet dat het leven in balans is met de omgeving. Integendeel, de staat waarin cellen verkeren die in perfecte balans zijn met hun omgeving wordt in wetenschappelijke terminologie dan ook "dood" genoemd. Om te kunnen overleven moeten cellen hun inwendige omgeving stabiel houden, ondanks de veranderlijke buitenwereld. Alleen in een stabiele inwendige omgeving kunnen de complexe chemische reacties plaatsvinden die het voedsel wat we eten omzetten tot de cellen van ons lichaam. Het proces van het behouden van een stabiele inwendige omgeving heet **homeostase** en de som van alle chemische reacties die plaatsvinden in een organisme noemt men het **metabolisme**.

Het behouden van homeostase kan alleen door continu energie aan te voeren via een ononderbroken metabolisme van voedingsstoffen. Maar omdat ononderbroken aanvoer van voedingsstoffen niet altijd gegarandeerd kan worden in de natuur is een **buffer** van opgeslagen energie van cruciaal belang, bijvoorbeeld in de vorm van vet. Het goed reguleren van de opbouw en afbraak van deze energievoorraden zou een groot evolutionair voordeel opleveren als periodes van overvloed en schaarste elkaar afwisselen. Er wordt zelfs gedacht dat een goede regulatie van energievoorraden aan de basis heeft gestaan van de evolutionaire ontwikkeling van het relatief grote menselijke brein: menselijke baby's worden als één van de vetste landdieren geboren, wat het mogelijk maakt om onze energieverslindende hersenen te kunnen voeden en te laten ontwikkelen [1,2]. Het is dus duidelijk dat energievoorraden in de vorm van vet essentieel zijn voor de mens.

1 Leonard, W. R., Robertson et al. **2003**; Metabolic correlates of hominid brain evolution. *Comparative Biochemistry and Physiology Part A: Molecular & Integrative Physiology* 136:5

2 Cunnane, S. C., and Crawford, M. A. **2003**; Survival of the fattest: fat babies were the key to evolution of the large human brain. *Comparative Biochemistry and Physiology Part A: Molecular & Integrative Physiology* 136:17

1

General introduction

Metabolic diseases

In today's world, more people die from complications of overweight than from underweight. Overweight and obesity significantly increase the risk for type 2 diabetes and cardiovascular disease (CVD). Globally, CVD is the number one cause of death (World Health Organization, March 2013). Preventing obesity-related diseases is estimated to save a substantial amount of medical care costs, but also diminish environmental, labor productivity and human capital loss [1]. Therefore, obesity is a growing societal and political point of concern. Understanding how susceptibility to obesity-related diseases arises and how to tip the balance back in favor of a more healthy energetic state is crucial.

Energy metabolism

Energy is taken up by the body by digesting energy-rich nutrients in the diet. These digestion products can be further metabolized according to the requirement at that time. Nutrients can be used either as building blocks for biomass, or oxidized for generating heat and/or the cellular chemical energy currency: Adenosine triphosphate (**ATP**). Nutrients can also be stored. The metabolic fates (oxidation, biomass and storage) of dietary protein, carbohydrates and fats are depicted in figure 1.

In the post-prandial state, dietary fats and carbohydrates are broken down in the gastrointestinal tract to fatty acids and monosaccharides, respectively. Monosaccharides such as glucose enters the blood stream directly, but fatty acids are first converted to triglycerides in the small intestine and loaded into chylomicron lipoprotein particles (built around apolipoprotein (apo) B48), used to transport water-insoluble lipids. The lipoprotein particles are then transported via lymph and the water soluble nutrients via the blood to all organs, which will take up nutrients according to their need. Chylomicrons adhere to the vascular endothelial wall to release fatty acids near the cell membrane. Adipocytes can store excess fatty acid as triglycerides. The liver can store excess glucose as glycogen.

In the fasting state, the body relies on the release of stored glycogen and triglycerides to fulfill the energy requirements of each cell. Adipocytes can hydrolyze the stored triglycerides, releasing non-esterified fatty acids (NEFA). As NEFAs are toxic, they are quickly shielded from the environment. For example, NEFAs in the blood complex with albumin. The liver can rapidly take up NEFAs from albumin complexes. The NEFAs are then esterified to glycerol to reform triglycerides. These TGs are loaded by the liver onto very low density lipoprotein particles (VLDL, built around apoB100) and secreted into the blood. Similarly, glycogen can be broken down, thus secreting glucose.

The energy-rich lipids and carbohydrates are important building materials. The cells of the body grow, divide and develop by metabolizing dietary nutrients. Lipids are important components of the cell membrane, creating a closed compartment wherein homeostasis is possible. Carbohydrates are important components for nucleotides. Amino acids are essential

for the synthesis of enzymes and other proteins.

Fatty acids and glucose are mostly used as fuel. They can both be metabolized to acetyl-CoA, which is the main input metabolite of the mitochondrial tricarboxylic acid (TCA) cycle. In the TCA cycle acetyl-CoA is oxidized in a step-wise controlled fashion generating carbon dioxide, water, but also reducing equivalents (NADH). The reducing equivalents are fed into in the mitochondrial electron transfer chain to generate a proton gradient which drives the conversion of ADP to ATP or the generation of heat. ATP is the central energy currency of the cell, needed to maintain homeostasis.

The energy buffer capacity of available intracellular ATP is generally very small. Therefore an energy buffer of triglycerides and glycogen is stored mostly in adipose tissue and liver, respectively. Since the energy density of triglycerides is about six times higher than glycogen, triglycerides are the preferred energy storage form. Glucose can be converted to fatty acids as storage, but it is impossible to convert fatty acids back to glucose. As the brain is mostly dependent on glucose, a glucose storage in the form of glycogen is vital.

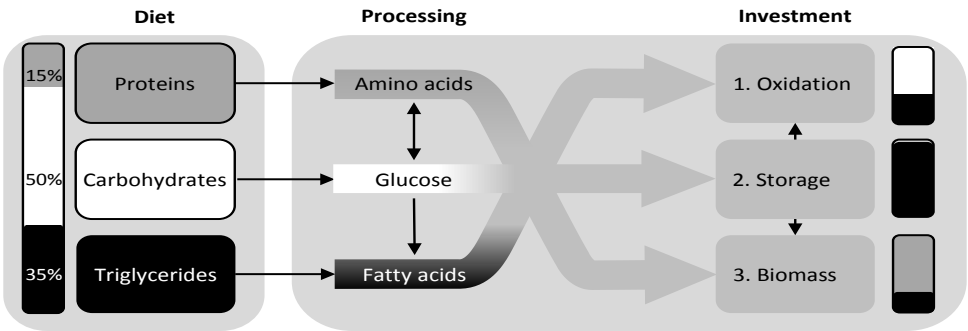

Figure 1: Macronutrient composition of the human diet, which is absorbed and processed in the body and subsequently allocated to fuel oxidation for energy, energy storage or to growth of biomass. The macronutrient composition is given as a stacked bar graph: Carbohydrates (C, White), Protein (P, Grey) and Fat (F, Black). Western Diet (Standard American Diet) composition in C/P/F = 50/15/35 kcal% [2]*. Average muscle biomass composition in C/P/F = 0/75/25 kcal%* [3] *and average human storage composition in C/P/F = 1/0/99 kcal%* [4]*. Average human oxidative respiratory quotient in C/P/F = 40/0/60 kcal%* [5, 6]*.*

Figure 1 describes the schematic roadmap that dietary nutrients follow, from nutrient intake to nutrient usage and storage. It does not describe how the decision is made to allocate certain nutrients to certain processes under certain conditions. In order to gain more insight in this allocation process, it is useful to determine the energy balance. If the balance has shifted from the homeostatic set point, nutrient allocation should be adjusted to regain balance. The energy balance describes how the energy intake from the diet compares to the energy expended in order to fuel the nutrient usage:

$$\Delta Energy\ storage(kJ/h) = Energy\ intake(kJ/h) - Energy\ expenditure(kJ/h)$$

If the energy intake of an organism over a period of time is in balance with the energy expenditure, the amount of energy storage will stay the same. In the case of a positive energy balance the energy storage will increase over time.

Balancing energy metabolism

Regulating the energy storage and release is crucial to keep up with the ATP demand of every cell in the organism. To regulate most processes in biology, negative feedback loops have evolved. The concentration of a certain metabolite is sensed by a sensor. If the concentration (input) increases beyond a threshold, the sensor will elicit a response (feedback) leading to increased consumption and/or decreased production of the metabolite, thereby bringing the input concentration back to the set-point homeostatic level. Due to its robustness, negative feedback loops are the most abundant regulatory mechanism to balance consumption and production at a homeostatic level [7].

The first step in the regulation of energy metabolism is therefore to sense the energy balance. Sensing the energy balance is done at multiple levels: The intracellular energy availability, the energy available circulating in the blood and the energy available in storage. It is important to sense the energy balance at these different levels, so that energy allocation can be adjusted to fit the local and global requirements of the organism, but also to fit the acute and long-term requirements of the organism.

In the post-prandial state, more energy intake has occurred than required for energy expenditure at that moment. When the digestion products enter the bloodstream, the concentration of glucose, amino acids and lipids will rise. Pancreatic β-cells taking up increasing levels of glucose will sense an increase in their intracellular ATP/AMP energy balance [8]. This leads to the secretion of insulin, which will bind to the insulin receptor present on the cell membranes. Insulin will signal the switch from a catabolic state (burning nutrients for fuel) to an anabolic state (use nutrients to build up storage and biomass), required during the switch from fasting to feeding. This results in an increased nutrient uptake and a decrease of the blood nutrient concentrations back to homeostatic set-point levels, at which insulin secretion is not stimulated any longer.

In contrast, in the fasting state, more energy is expended than is taken up via the intestine. This might cause cells to use up their ATP supply faster than they rebuild ATP. Each cell can sense the drop in ATP/AMP energy balance via amongst others the enzyme AMPK. Activated AMPK will locally stimulate the cell's insulin sensitivity, thereby increasing insulin-induced glucose import from the circulation into the cell [9]. AMPK signaling can also activate the production of extracellular energy demanding hormones, namely glucagon (by pancreatic α-cells), adrenaline and cortisol (by the adrenal glands). These hormones will travel via the blood to the storage cells, signaling the release of fatty acids and glucose into the blood, from where they can be processed and absorbed by the cells.

The energy balance is also sensed at the storage level. Storage cells must also be able to signal the total amount of stored nutrients present, otherwise the buffer capacity might not be sufficient for unforeseen fasting conditions. The glycogen buffer in the liver is small, but crucial. Therefore, when the glycogen content is low, hepatocytes stimulate adipocyte lipolysis forcing a switch from oxidizing low-abundant glucose to oxidizing fatty acids [10]. Reversely, when the glycogen content is high, hepatocytes stimulate adipocyte lipogenesis to convert high-abundant glucose to triglycerides [11]. The mechanism for sensing and signaling according to glycogen content are not yet completely known. Adipocytes release leptin, an adipokine, according to their lipid content. Therefore, sensing the adipocyte lipid content is possible by sensing the blood leptin concentration. When stored energy is in abundance, it can be used for growth, development and reproduction processes. These global and long-term responses are indeed stimulated by leptin [12].

The response to sensing the energy balance is mostly mediated via blood hormones, which can manipulate the cellular energy metabolism. However the response can also be mediated via neuronal signaling, which could manipulate not only energy metabolism, but also behavior [13]. Leptin for example acts as an extracellular hormone, inducing a neuronal satiety signal in the brain. Low leptin levels will not signal satiety, thereby steering behavior to finding food. High leptin levels induce satiety behavior [12]. Many different hormones have been found to manipulate neuronal satiety signaling. Even in anticipation of nutrients entering the blood, different gastro-intestinal sensory cells secrete ghrelin, cholecystokinin and peptide YY in response to nutrients, which are all stimulatory signals of satiety [13]. In response to high levels of blood nutrients insulin also acts as a stimulus of satiety. The default signal in food intake regulation is appetite signaling, which can be suppressed by for example the satiety mechanisms described above.

Negative feedback is present in many different energy balance sensing processes, ranging from neuronal and hormonal to intracellular processes. Although it is a very robust regulatory mechanism, resistance to negative feedback can occur. Resistance can be useful physiologically to adapt to a short-term overwhelming response. However, resistance can also occur if certain environmental triggers become chronic triggers. For example, in the event of a chronic overconsumption of energy-rich nutrients. Resistance to some of the regulatory hormonal, neuronal and intracellular feedback responses described above can have adverse metabolic effects, such as insulin resistance, leptin resistance and neuronal satiety resistance [14]. With negative feedback, an altered level of the input (for example a high glucose concentration) is sensed and accordingly feedback is given (for example a higher insulin concentration). With resistance to feedback, a chronically elevated level of the feedback (for example a high insulin concentration) is sensed and accordingly feedback resistance arises (for example a lower insulin receptor concentration). Therefore, resistance to negative feedback is paradoxically governed by negative feedback itself. It is an adaptation to chronically altered (environmental) feedback triggers. And it is precisely this altered 'obesogenic environment' that has led to a sudden rise in the prevalence of obesity and the metabolic syndrome since the late 1970's.

Unbalanced energy metabolism

Metabolic syndrome

Starting from the 1920's, the recognition of a particular clustering of metabolic abnormalities in patients led to a new diagnosis: Metabolic syndrome (MetS) [15]. There are multiple clinical definitions for MetS used worldwide, but MetS is predominantly characterized by increased risk for cardiometabolic diseases such as type 2 diabetes, atherosclerosis and subsequent CVD and infarction. The risk factors used in the various MetS definitions include obesity, high levels of blood glucose (hyperglycemia), abnormal levels of blood lipids (dyslipidemia), increased inflammation and high blood pressure. The utility of the diagnosis MetS is debated, as the MetS definition does not predict cardiovascular disease development any different from the sum of the individual risk factors [16]. Nonetheless, the co-occurrence of the metabolic risk factors indicates a common underlying cause or causes, most likely a combination of genetically determined susceptibility and a change in environmental factors affecting energy metabolism at large. The different risk factors and their known genetic and environmental interactions will be reviewed.

Obesity

In obesity, the adipose tissue mass expansion can be due to increased triglyceride storage in the lipid droplet of the adipocyte (hypertrophy), and/or increased formation of new adipocytes (hyperplasia). The relative importance of hypertrophy and hyperplasia in obesity has been estimated and although total adipose tissue mass predictions were highly correlated to adipocyte size, the correlation failed for morbidly obese individuals. When adipocyte number was also taken into account [17] the majority of the variability in adipose tissue mass could be explained. Therefore both hypertrophy and hyperplasia contribute to (morbid) obesity. In obesity, the absolute adipocyte number is often higher than normal weight controls, as determined by an increased hyperplasia rate before adulthood [17]. Regulation of both hypertrophy and hyperplasia occurs, most likely via negative feedback. A homeostatic set-point of adipocyte size was found in studies conducting short term food restriction or overfeeding studies and a set point of adipocyte number was found in studies towards the effects of liposuction [18, 19].

The expansion of the adipose tissue mass can occur at different adipose tissue depots. Adipose tissue surrounding the internal organs (visceral white adipose tissue, vWAT) has been shown to produce relatively more fatty acids and inflammatory compounds [20] compared to fat stored under the skin (subcutaneous, sWAT). Therefore, expanded vWAT has been associated with an increased risk of the obesity-related complications of the MetS compared to expanded sWAT [21]. Although vWAT is an important risk factor, the abdominal fat in the belly of obese men is mostly sWAT and not vWAT. Why abdominal sWAT is riskier than

sWAT located around the hips remains largely unsolved [22].

The evolutionary mechanisms that have shaped our energy balance seem to favor mechanisms which create a positive energy balance in preparation of periods of shortage. It drives our behavior to eat energy rich foods used for energy storage in order to overcome these periods. Intriguingly, a large part of the known genetic contributors to obesity are polymorphisms in genes involved in eating behavior, regulating the neuronal satiety balance between orexic and anorexic appetite signals [23, 24]. It was estimated that between 40-80% of the variation in body mass index (BMI) can be explained by heritable factors such as genetic variants involved in appetite regulation and pre-adipocyte differentiation regulation [24, 25]. The non-heritable variation is also strongly affected by variation in socio-economic status (SES), as a lower SES is generally associated with a higher body mass [26] or in the variation of individual economic insecurity and related uncertainty stress [27]. These non-heritable factors could prompt less healthy eating habits.

The prevalence of obesity is rising in a timeframe too short to be explained by changes in heritable factors. Therefore, the increased prevalence must be due to environmental changes (obesogenic environment), such as energy-dense foods becoming more widely available in bigger, cheaper portions. This has led to an increased energy intake, mainly by increased carbohydrate intake compared to the 1970s. At the same time, aerobic fitness and energy expenditure have been diminishing, as a result of a more sedentary lifestyle, by for example increased car usage and screen entertainment [28, 29]. What the relative contribution is of the two factors, energy intake and energy expenditure, to the obesity epidemic is difficult to estimate [30].

In obesity, adipocytes are chronically relaying their hypertrophic stressed state by for example high leptin secretion. Therefore, resistance to chronically high adipokine levels occurs during obesity, both in the brain and in peripheral tissues. For example obese subjects suffer from leptin resistance, where leptin can no longer efficiently inhibit hunger signaling nor can it stimulate energy expenditure [31]. Therefore, leptin resistance contributes to a vicious cycle in obesity development. Resistance to other adipokines has been observed, but their role in obesity-related diseases is not as clear as for leptin at the moment [32].

Insulin resistance

Insulin resistance is a decreased responsiveness of the body to insulin signaling. The amount of insulin secreted from the pancreatic β-cells is based on sensing the levels of nutrients, primarily blood glucose levels and secondarily NEFA and amino acid levels, such as branched chain amino acids [33]. Insulin resistance is associated with a decreased number of insulin receptors on the insulin-sensitive cell membranes. Also, the downstream signaling efficiency of the activated insulin receptor is diminished by a decreased number of (active) signal transduction proteins in the insulin pathway [33]. Once insulin resistance develops, the pancreas secretes more insulin to maintain normal blood glucose levels (~5 mM). The insulin

resistant state can deteriorate further, leading to hyperglycemia despite increased levels of insulin. This state is called type 2 diabetes mellitus (T2DM). Finally, the chronically elevated insulin production will lead to a failure of the β-cells, which will cease to produce endogenous insulin. These patients are subsequently dependent on exogenous insulin injections [33].

Insulin resistance may be due to a number of possible causes, their contribution differing widely per individual. As the risk of T2DM is strongly related to increasing BMI, obesity is an important risk factor. Therefore many explanations for T2DM and insulin resistance involve consequences of obesity [34].

Due to an overabundance of digested nutrients entering the bloodstream, adipocytes will take up more NEFAs. It is well known that acute lipid infusion and NEFA uptake in cells will cause insulin resistance on the short term [35], by an acute accumulation of the intermediates of NEFA β-oxidation in mitochondria [36]. Therefore an important early contributor to adipose tissue insulin resistance could be increased NEFA uptake and subsequent mitochondrial processing. Adipocyte-specific knockout of genes involved in mitochondrial functioning resulted in a less burdened mitochondrial membrane potential. Upon feeding a high fat diet, these adipocyte-specific knockout mice showed decreased mitochondrial stress, enhanced adipose insulin sensitivity and enhanced whole-body insulin sensitivity [37, 38].

A later stage contributor to insulin resistance originating from adipose tissue could be the increasing lipid load of adipocytes becoming hypertrophic. Lipid load is correlated to lipid hydrolysis and NEFA release, but also to the release of certain adipokines, such as leptin. Increased adipocyte lipolysis would lead to increased intracellular adipocyte NEFA concentrations, but also to increased circulating NEFA concentrations. NEFAs could become lipotoxic by affecting mitochondrial functioning in adipose tissue, but also in peripheral tissues taking up increased amounts of NEFAs [39]. Furthermore, adipocyte hypertrophy also leads to hyperleptinenemia and leptin resistance. As leptin inhibits β-cell insulin release, leptin resistance can cause systemic hyperinsulinemia [36].

Another late stage contributor to obesity related insulin resistance might be the fact that advanced adipocyte hypertrophy can induce intracellular stress [34], possibly due to: 1) reaching the maximal mechanical expandability of the adipocytes and adipose tissue within the body, 2) intracellular hindrance of the expanding lipid droplet with organelles such as mitochondria and the endoplasmic reticulum, and/or 3) reaching the maximal oxygen diffusion limit of the enlarged cells. As a consequence of adipocyte intracellular stress, serine protein kinases will be activated and will phosphorylate serine residues of insulin receptor substrate 1 (IRS1) [34]. Serine phosphorylation of IRS1 will directly interfere with the kinase activity of the activated insulin receptor on IRS1 tyrosine residues. Insulin resistant adipocytes will respond less to insulin-inhibition of lipolysis and will therefore have a higher rate of basal lipolysis and NEFA release, which then forms a vicious cycle for increased NEFAs.

The intracellular stress of hypertrophic adipocytes can become too great, leading to the secretion of immune modulating stress factors and eventually to adipocyte death. Dying adipocytes attract immune cells, which will start secreting their own immune modulating

factors [34]. This also leads to a vicious cycle of inflammation. These immune cells and immune factors will decrease insulin sensitivity locally, but will eventually spread via the circulation to peripheral tissues, thereby inducing whole-body insulin resistance. Although many important associations have been found between insulin resistance and adipose tissue related changes, the causal sequence and the relative contributions of the adipose tissue changes to adipose and whole-body insulin resistance have not been completely elucidated.

Although T2DM is strongly associated with obesity, the association does not have to be directly causative. Other causative associations exist with T2DM, unrelated to or indirectly related to obesity. For example, 38% of the variation in HOMA-insulin resistance can be explained by heritable factors in Caucasian families [40]. Genome wide association studies on T2DM have been done to identify which molecular mechanisms could be involved. These GWAS have found that most genetic variants associated to T2DM are related to pancreatic β-cell functioning, not to obesity [41, 42]. An unstable pancreatic β-cell functioning might become problematic under certain conditions, such as obesity. If the β-cell functioning of metabolically healthy obese patients is more robust, these obese patients might be more resilient to developing T2DM and will merely develop hyperinsulinemia [43]. As with many complex diseases, the discovered genetic variants are capable of explaining only a small portion of the theoretical heritability of insulin resistance. Therefore, the search for the "missing heritability" of insulin resistance will continue [25].

Dyslipidemia

Dyslipidemia is characterized by abnormal blood lipid levels, such as triglycerides (TG), phospholipids (PL), cholesterol esters (CE) and total cholesterol (TC) levels. Not only is the absolute concentration of blood lipids an important risk factor for CVD, the distribution of blood lipids over lipoprotein particles also contributes [44]. For example, cholesterol is present in both VLDL and LDL (built around apoB100) as well as in HDL (built around apoAI). The VLDL/LDL particles deliver cholesterol and the HDL particles are thought to remove cholesterol from peripheral tissues. If the relative balance between LDL-cholesterol and HDL-cholesterol has shifted towards the LDL side, reverse cholesterol transport would be lowered [45] leading to peripheral and vascular cholesterol accumulation as a potential risk factor for CVD [44]. This view has led to an interest in drugs which shift the LDL/HDL-cholesterol ratio towards the HDL side. One of these drugs is niacin [46].

Another dyslipidemic balance that has gained interest is the omega-3 over omega-6 poly unsaturated fatty acid ratio (n-3/n-6 PUFA ratio) [47]. Similar to total plasma cholesterol the absolute PUFA quantity is the most important determinant of CVD risk [48], and similar to LDL/HDL cholesterol the relative distribution of n-3/n-6 PUFA has been associated with CVD risk [49]. The quantitative intake of PUFAs is easily met in our present-day Western type diet. However, the Western dietary n-3/n-6 PUFA ratio is about 1:16. This low dietary n-3/n-6 PUFA ratio also resulted in a low n-3/n-6 PUFA ratio of the PUFAs incorporated the body's

cell membranes. A shift in the blood n-3/n-6 PUFA ratio away from n-3 PUFAs has been shown to enhance dyslipidemia and increase LDL-cholesterol levels [48]. Epidemiological studies have repeatedly found that people with a higher n-3/n-6 PUFA ratio in their blood have a reduced risk of dying from CVD [50, 51]. Also, the addition of the n-3/n-6 PUFA ratio improves CVD risk estimations on top of the classical dyslipidemia criteria [47, 52].

Susceptibility to dyslipidemia can be inherited. Variation in TG and HDL-C levels can be explained for 31% and 43% respectively by heritable factors in a Dutch population [53]. The known genetic contributors are mostly directly associated with lipid metabolism in the liver. For example, via genetic variants affecting apolipoproteins (such as apolipoprotein A5), lipoprotein particle synthesis enzymes or adaptor proteins involved in the synthesis, transport and binding of lipoprotein particles [54].

Heritable factors also explain some 24% of the biological variation in n-3/n-6 PUFA ratio [55]. Interestingly, genome wide association studies have found an association between plasma cholesterol levels and genetic variants affecting *FADS1* and *FADS2*. These genes encode for the rate-limiting enzymes in the synthesis of n-3 and n-6 PUFAs [56]. This genetic association between PUFA synthesis genes and cholesterol levels is interesting, as PUFAs can inhibit cholesterol biosynthesis [57]. This hints towards a mechanistic link between decreased (endogenously synthesized) PUFAs and the development of dyslipidemia.

The mechanisms underlying the non-heritable causes of dyslipidemia are less clear. Diet quality and increased carbohydrate intake have been associated with dyslipidemia [58]. Obesity and insulin resistance have also been implicated in the development of dyslipidemia. Obesity induces increased blood NEFA levels which are substrates for liver VLDL-TG thereby increasing VLDL production and circulating levels of these atherogenic particles. In the hepatic insulin resistant state, the liver is less responsive to insulin-mediated inhibition of VLDL production. Therefore both obesity and insulin resistance could lead to VLDL overproduction and hyperlipidemia.

Mortality of the Metabolic Syndrome

The majority of severe complications associated with the MetS are due to cardiovascular disease, although MetS also increases the risk of other complications, such as cancer. Cardiovascular diseases are mostly a consequence of atherosclerosis. Atherosclerosis is the process of the narrowing of arteries by accumulation of calcium, (modified) lipids and inflammatory cells in the arterial wall. If the narrowed artery becomes blocked, the downstream tissue becomes ischemic. If the atherosclerotic wall ruptures, the accumulated debris will initiate blood coagulation and the resulting blood clot will travel through the bloodstream. The blood clot can occlude a downstream narrower artery. Depending on the location of the occluded artery, this can result in for example a heart attack or a stroke.

Dyslipidemia is an important prerequisite for atherosclerosis development in most cases.

Dyslipidemia can shift the balance between cholesterol delivery and cholesterol removal by LDL and HDL respectively [45]. Increased levels of LDL particles will bind to proteoglycans on the arterial endothelial cells resulting in increased LDL particle transport across the arterial wall. If these lipids become oxidized and modified, this stimulates phagocytosis by macrophages [59]. and will attract more inflammatory cells to the site of early inflammation. These cells will accumulate in the arterial wall, causing atherosclerosis. If the total cholesterol over HDL-cholesterol doubles in a person between 40-65 years old from 4 to 8 this also doubles the risk to dying from a CVD [60].

The complications of insulin resistance and T2DM are characterized by glucose-induced damage to the retina, kidneys, neurons and the extremities, as specifically endothelial cells and nerve cells cannot efficiently down-regulate glucose influx during hyperglycemia [61]. The increased intracellular glucose level has been suggested to increase mitochondrial production of radical oxygen species and advanced glycosylated end-products [61]. At high concentrations, glucose will react with amino acid residues of proteins, thereby glycosylating proteins, which are an inflammatory trigger [62]. The inflamed capillary endothelial cells become damaged, which can initiate atherosclerosis [63]. About 5% of the Dutch population suffered from type 2 diabetes in 2011 and this percentage is increasing [64]. A person diagnosed with T2DM has an increased risk of dying from CVD within 10 years that is equivalent to that person aging 15 years [60].

Obesity is not lethal as such, however it significantly increases the risk for other co-morbidities which can lead to death. Increased adipose tissue mass is strongly associated with increased blood pressure [21], which can damage the arteries and the heart. In the Netherlands, 42% of the population was overweight in 2013 and 10% was obese [65]. Obese subjects have about a 1.5 time higher risk of dying than normal weight subjects [66].

Predicting the risk of dying from CVD is most effective by measuring factors closely associated to death. For example, atherosclerosis is a better risk marker then dyslipidemia, which is a better risk marker then obesity. The further away from death, the worse the factor will be at predicting the risk of death. But the further away from death, the more time there might be to intervene with the risk of dying.

Outline of this thesis

The research described in this thesis focuses on factors that modulate energy metabolism, leading to obesity and insulin resistance, with a specific focus on fatty acid metabolism. An introductory overview of this topic is presented in Chapter 1. In the subsequent chapters, we examine the role of specific genes in disturbing energy metabolism and reversely, we examine the effects of disturbed energy metabolism on adipose tissue characteristics, in the context of diet-induced obesity and insulin resistance.

GWAS have revealed numerous single nucleotide polymorphisms (SNPs) in genes associated with obesity and related metabolic disorders. However, translating this genetic

information to a mechanism by which the disease could arise has proven difficult. In order to assist scientists in reviewing possible mechanisms by which a SNP could be associated to a disease or disease-marker, we describe in Chapter 2 the application of a newly developed knowledge-based workflow for assisting users in mapping SNPs to genes. We applied this new workflow to a statistically strong, but mechanistically weak association of a SNP mapped to the *HPS5* gene, which associated with branched chain amino acid (BCAA) degradation products [67]. We found that another gene (*LDHA*) is mechanistically a more plausible candidate gene than *HPS5* and we verified this functional association experimentally. Previous research from our laboratory has shown that BCAA metabolism is affected in obese and diabetic individuals, indicating the possible relevance of the SNP mapped to *LDHA* in metabolic diseases.

In Chapter 3, we investigated the mechanism by which the *APOA5* gene, which has been shown to affect plasma triglyceride levels [68], affects energy metabolism using mice deficient for *Apoa5*. APOA5 has been proposed to function as an anchor protein on lipoprotein particles and to play a role in lipoprotein lipase mediated lipolysis [69]. Since *Apoa5* deficient mice eat more food and develop severe obesity, we investigated the mechanism underlying the hyperphagic phenotype. Our results indicate that APOA5 may play a role in the central regulation of satiety.

In the second part of this thesis, we studied the impact of a disturbed energy metabolism on adipose tissue characteristics. Niacin is a drug that has been used to treat dyslipidemia in humans. Although niacin acutely inhibits fatty acid release from adipocytes, prolonged treatment is associated with adipocyte insulin resistance. In Chapter 4, using a transgenic mouse model with a human-like lipoprotein metabolism, the underlying mechanism of prolonged niacin treatment leading to insulin resistance was investigated. Our results show that niacin induced insulin resistance is due to an adaptation of PDE3B; a central regulator of cAMP signaling.

Chapter 5 focuses on changes in PUFA metabolism in mouse adipose tissue after niacin treatment, which might play a role in the effects of niacin on CVD risk. We found that niacin increases PUFA synthesis and n-3 PUFA secretion into the circulation. These n-3 PUFAs were converted to increased levels of anti-inflammatory oxylipins, which might contribute to niacin's beneficial effects on CVD.

In Chapter 6, we examined adipose tissue from extremely obese women with and without T2DM. In previous research from our laboratory we have found that adipose tissue from obese women with T2DM is in a more pro-inflammatory state both at the cellular and at the gene expression level. In Chapter 6 the adipose tissue was analyzed for fatty acid composition. We found that obese women with T2DM have more n-3 and n-6 PUFAs in their adipose tissue and seem to have an increased conversion of PUFAs towards pro-inflammatory leukotrienes. Finally, we will discuss the results obtained from these studies in Chapter 7 and their implications in the regulation of energy and fatty acid metabolism and how they relate to the development of obesity and insulin resistance.

References

1 Hammond RA, Levine R. **2010**; The economic impact of obesity in the United States. *Diabetes, metabolic syndrome and obesity: targets and therapy* 3:285.

2 Last AR, Wilson SA. **2006**; Low-carbohydrate diets. *American family physician* 73:1942.

3 de Jong FM. **2014**; Varkensvlees, spier, algemeen. *www.voedingswaardetabel.nl*.

4 Heymsfield SB, Waki M *et al.* **1991**; Chemical and elemental analysis of humans in vivo using improved body composition models. *American journal of cardiology* 261:E190.

5 Westerterp K. **1993**; Food quotient, respiratory quotient, and energy balance. *American journal of clinical nutrition* 57:759S.

6 Kang J. **2008**. Measurements of Energy Metabolism. In: Bioenergetics Primer for Exercise Science. 1. Human Kinetics; pp. 49.

7 Alon U. **2006**. An introduction to systems biology: design principles of biological circuits. CRC press.

8 Matschinsky FM. **1990**; Glucokinase as Glucose Sensor and Metabolic Signal Generator in Pancreatic β-Cells and Hepatocytes. *Diabetes* 39:647.

9 Habegger KM, Hoffman NJ *et al.* **2012**; AMPK enhances insulin-stimulated GLUT4 regulation via lowering membrane cholesterol. *Endocrinology* 153:2130.

10 Izumida Y, Yahagi N *et al.* **2013**; Glycogen shortage during fasting triggers liver–brain–adipose neurocircuitry to facilitate fat utilization. *Nature communications* 4.

11 Lu B, Bridges D *et al.* **2014**; Metabolic Crosstalk: molecular links between glycogen and lipid metabolism in obesity. *Diabetes*.

12 Friedman JM, Halaas JL. **1998**; Leptin and the regulation of body weight in mammals. *Nature* 395:763.

13 Ahima RS, Antwi DA. **2008**; Brain regulation of appetite and satiety. *Endocrinology and metabolism clinics of North America* 37:811.

14 Martinez de Morentin PB, Varela L *et al.* **2010**; Hypothalamic lipotoxicity and the metabolic syndrome. *Biochimica et biophysica acta* 1801:350.

15 Nilsson S. **2001**; Research contributions of Eskil Kylin. *Svensk medicinhistorisk tidskrift* 5:15.

16 Sattar N, McConnachie A *et al.* Can metabolic syndrome usefully predict cardiovascular disease and diabetes? Outcome data from two prospective studies. *The Lancet* 371:1927.

17 Spalding KL, Arner E *et al.* **2008**; Dynamics of fat cell turnover in humans. *Nature* 453:783.

18 Faust I, Johnson P *et al.* **1977**; Adipose tissue regeneration following lipectomy. *Science* 197:391.

19 Hernandez TL, Kittelson JM *et al.* **2011**; Fat Redistribution Following Suction Lipectomy: Defense of Body Fat and Patterns of Restoration. *Obesity* 19:1388.

20 Lee M-J, Wu Y *et al.* **2013**; Adipose tissue heterogeneity: Implication of depot differences in adipose tissue for obesity complications. *Molecular aspects of medicine* 34:1.

21 Fox CS, Massaro JM *et al.* **2007**; Abdominal Visceral and Subcutaneous Adipose Tissue Compartments: Association With Metabolic Risk Factors in the Framingham Heart Study. *Circulation* 116:39.

22 Frayn KN, Karpe F *et al.* **2003**; Integrative physiology of human adipose tissue. *International journal of obesity and related metabolic disorders* 27:875.

23 Schneeberger M, Gomis R *et al.* **2014**; Hypothalamic and brainstem neuronal circuits controlling homeostatic energy balance. *Journal of endocrinology* 220:T25.

24 Yang W, Kelly T *et al.* **2007**; Genetic Epidemiology of Obesity. *Epidemiologic reviews* 29:49.

25 Llewellyn CH, Trzaskowski M *et al.* **2013**; Finding the missing heritability in pediatric obesity: the contribution of genome-wide complex trait analysis. *International journal of obesity* 37:1506.

26 McLaren L. **2007**; Socioeconomic Status and Obesity. *Epidemiologic reviews* 29:29.

27 Offer A, Pechey R *et al.* **2010**; Obesity under affluence varies by welfare regimes: The effect of fast food, insecurity, and inequality. *Economics & human biology* 8:297.

28 Tomkinson GR, Léger LA *et al.* **2003**; Secular trends in the performance of children and adolescents (1980–2000). *Sports medicine* 33:285.

29 Stubbs CO, Lee AJ. **2004**; The obesity epidemic: both energy intake and physical activity contribute. *Medical journal of Australia* 181:489.

30 Bleich SN, Ku R *et al.* **2011**; Relative contribution of energy intake and energy expenditure to childhood obesity: a review of the literature and directions for future research. *International journal of obesity* 35:1.

31 Myers Martin G, Jr., Heymsfield Steven B *et al.* **2012**; Challenges and Opportunities of Defining Clinical Leptin Resistance. *Cell metabolism* 15:150.

32 Rabe K, Lehrke M *et al.* **2008**; Adipokines and insulin resistance. *Molecular medicine* 14:741.

33 Wilcox G. **2005**; Insulin and Insulin Resistance. *Clinical biochemist reviews* 26:19.

34 Ye J. **2013**; Mechanisms of insulin resistance in obesity. *Frontiers of medicine* 7:14.

35 Shi H, Kokoeva MV *et al.* **2006**; TLR4 links innate immunity and fatty acid-induced insulin resistance. *Journal of clinical investigation* 116:3015.

36 Koves TR, Ussher JR *et al.* **2008**; Mitochondrial overload and incomplete fatty acid oxidation contribute to skeletal muscle insulin resistance. *Cell metabolism* 7:45.

37 Kusminski CM, Holland WL *et al.* **2012**; MitoNEET-driven alterations in adipocyte mitochondrial activity reveal a crucial adaptive process that preserves insulin sensitivity in obesity. *Nature medicine* 18:1539.

38 Vernochet C, Mourier A *et al.* **2012**; Adipose-specific deletion of TFAM increases mitochondrial oxidation and protects mice against obesity and insulin resistance. *Cell metabolism* 16:765.

39 van Herpen NA, Schrauwen-Hinderling VB. **2008**; Lipid accumulation in non-adipose tissue and lipotoxicity. *Physiology & behavior* 94:231.

40 Rasmussen-Torvik LJ, Pankow JS *et al.* **2007**; Heritability and genetic correlations of insulin sensitivity measured by the euglycaemic clamp. *Diabetic medicine* 24:1286.

41 Ali O. **2013**; Genetics of type 2 diabetes. *World journal of diabetes* 4:114.

42 Sun X, Yu W *et al.* **2014**; Genetics of Type 2 Diabetes: Insights into the Pathogenesis and Its Clinical Application. *BioMed research international* 2014:926713. Epub 2014 Apr 17.

43 Lips MA, de Groot GH *et al.* **2014**; Calorie Restriction is a Major Determinant of the Short-Term Metabolic Effects of Gastric Bypass Surgery in Obese Type 2 Diabetic Patients. *Clinical endocrinology* 80:834.

44 Reiner Ž, Catapano AL *et al.* **2011**; ESC/EAS Guidelines for the management of dyslipidaemias: The Task Force for the management of dyslipidaemias of the European Society of Cardiology (ESC) and the European Atherosclerosis Society (EAS). *European heart journal*.

45 Khera AV, Cuchel M *et al.* **2011**; Cholesterol Efflux Capacity, High-Density Lipoprotein Function, and Atherosclerosis. *New England Journal of Medicine* 364:127.

46 Li X, Millar JS *et al.* **2010**; Modulation of HDL Metabolism by the Niacin Receptor GPR109A in Mouse Hepatocytes. *Biochemical pharmacology* In Press, Accepted Manuscript.

47 von Schacky C. **2014**; Omega-3 Index and Cardiovascular Health. *Nutrients* 6:799.

48 Wijendran V, Hayes KC. **2004**; Dietary n-6 and n-3 fatty acid balance and cardiovascular health. *Annual review of nutrition* 24:597.

49 Simopoulos AP. **2002**; The importance of the ratio of omega-6/omega-3 essential fatty acids. *Biomedicine & pharmacotherapy* 56:365.

50 Siscovick DS, Raghunathan TE *et al.* **1995**; Dietary intake and cell membrane levels of long-chain n-3 polyunsaturated fatty acids and the risk of primary cardiac arrest. *JAMA* 274:1363.

51 Albert CM, Campos H *et al.* **2002**; Blood Levels of Long-Chain n–3 Fatty Acids and the Risk of Sudden Death. *New England Journal of Medicine* 346:1113.

52 Harris WS, Kennedy KF *et al.* **2013**; Red blood cell fatty acid levels improve GRACE score prediction of 2-yr mortality in patients with myocardial infarction. *International journal of cardiology* 168:53.

53 Henneman P, Aulchenko YS *et al.* **2008**; Prevalence and heritability of the metabolic syndrome and its individual components in a Dutch isolate: the Erasmus Rucphen Family study. *Journal of medical genetics* 45:572.

54 Kathiresan S, Willer CJ *et al.* **2009**; Common variants at 30 loci contribute to polygenic dyslipidemia. *Nature genetics* 41:56.

55 Harris WS, Pottala JV *et al.* **2012**; Clinical correlates and heritability of erythrocyte eicosapentaenoic and docosahexaenoic acid content in the Framingham Heart Study. *Atherosclerosis* 225:425.

56 Lemaitre RN, Tanaka T *et al.* **2011**; Genetic Loci Associated with Plasma Phospholipid n-3 Fatty Acids: A Meta-Analysis of Genome-Wide Association Studies from the CHARGE Consortium. *PLoS genetics* 7:e1002193.

57 Karanth S, Tran VM *et al.* **2013**; Polyunsaturated fatty acyl-coenzyme As are inhibitors of cholesterol biosynthesis in zebrafish and mice. *Disease models & mechanisms* 6:1365.

58 Musunuru K. **2010**; Atherogenic dyslipidemia: cardiovascular risk and dietary intervention. *Lipids* 45:907.

59 Williams KJ, Tabas I. **1995**; The Response-to-Retention Hypothesis of Early Atherogenesis. *Arteriosclerosis, Thrombosis, and Vascular Biology* 15:551.

60 NHG. **2012**; Cardiovasculair risicomanagement M84 (januari 2012).

61 Brownlee M. **2005**; The Pathobiology of Diabetic Complications: A Unifying Mechanism. *Diabetes* 54:1615.

62 Aronson D. **2008**. Hyperglycemia and the Pathobiology of Diabetic Complications. In: Cardiovascular diabetology: Clinical, metabolic and inflammatory facets. Edited by: Fisman, Tenenbaum. *Basel:* Karger; pp. 1.

63 Schmidt AM, Yan SD *et al.* **2001**; The multiligand receptor RAGE as a progression factor amplifying immune and inflammatory responses. *Journal of clinical investigation* 108:949.

64 RIVM. **2013**; Meer dan 800.000 mensen met diabetes in Nederland; toename fors.

65 CBS. Rapport Gezondheid en Welzijn 2013.

66 Zheng W, McLerran DF *et al.* **2011**; Association between Body-Mass Index and Risk of Death in More Than 1 Million Asians. *New England Journal of Medicine* 364:719.

67 Suhre K, Shin SY *et al.* **2011**; Human metabolic individuality in biomedical and pharmaceutical research. *Nature* 477:54.

68 Pennacchio LA, Olivier M *et al.* **2001**; An apolipoprotein influencing triglycerides in humans and mice revealed by comparative sequencing. *Science* 294:169.

69) Grosskopf I, Baroukh N *et al.* **2005**; Apolipoprotein A-V deficiency results in marked hypertriglyceridemia attributable to decreased lipolysis of triglyceride-rich lipoproteins and removal of their remnants. *ATVB* 25:2573.

2

Reanalysis of mGWAS results and in vitro validation show that lactate dehydrogenase interacts with branched-chain amino acid metabolism

Mattijs M. Heemskerk, Vanessa J.A. van Harmelen, Ko Willems van Dijk, Jan Bert van Klinken

European Journal of Human Genetics **2015**

Abstract

The assignment of causative genes to noncoding variants identified in Genome Wide Association Studies (GWASs) is challenging. We show how combination of knowledge from gene and pathway databases and chromatin interaction data leads to reinterpretation of published quantitative trait loci for blood metabolites. We describe a previously unidentified link between the rs2403254 locus, which is associated with the ratio of 3-methyl-2-oxobutanoate and alpha-hydroxyisovalerate levels, and the distal *LDHA* gene. We confirmed that lactate dehydrogenase can catalyze the conversion between these metabolites *in vitro*, suggesting that it plays a role in branched-chain amino acid metabolism. Examining datasets from the ENCODE project we found evidence that the locus and *LDHA* promoter physically interact, showing that *LDHA* expression is likely under control of distal regulatory elements. Importantly, this discovery demonstrates that bioinformatic workflows for data integration can play a vital role in the interpretation of GWAS results.

Introduction

Due to recent advances in metabolomics technology and decreasing costs, Genome Wide Association Studies have now been performed on a wide range of metabolites [1–4]. These studies have provided new insights into how biochemical pathways are affected by genetic polymorphisms and have increased our understanding of the pathogenesis of metabolic disease [3,5]. Since variation in metabolite levels is often linked to changes in enzyme or transporter activity, functional annotation of the loci that are located in or close to enzyme coding genes has been straightforward. However, for a substantial part of the loci identified in mGWAS no obvious link between the metabolite and proximal enzyme coding genes exists, and the association with the phenotype is much harder to explain.

We developed an automated workflow for mapping the results of GWASs on pathway databases to assist in their interpretation. We applied the workflow on the 37 loci that have been reported by Suhre *et al.* [3] and were able to provide a new functional annotation of the rs2403254 (chr11.hg19:g.18325146C>T) single nucleotide polymorphism (SNP) which associates with the ratio of 3-methyl-2-oxobutanoate and alpha-hydroxyisovalerate levels in the blood. Reanalysis of this locus uncovered a functional link to the gene coding for the lactate dehydrogenase (LDH) A enzyme and *in vitro* analysis confirmed that LDH could convert 3-methyl-2-oxobutanoate into alpha-hydroxyisovalerate. In addition, we found a physical association between the rs2403254 locus and the *LDHA* promoter region in the chromatin interaction data from the ENCODE project [6–8]. Combined, our data suggest that LDH interacts with branched-chain amino acid metabolism and is affected by genetic variation at a distal locus.

Materials and methods

Automated annotation of GWAS results

In order to facilitate the manual process of assigning a gene to each locus, we developed an automated workflow *in house* to generate reports containing the associated protein, enzyme, metabolic reaction, pathway, and disease phenotypes of each gene within a distance of 500 kb of the locus. In detail, the reports created by our workflow were based on the dbSNP[9], NCBI-Gene (http://www.ncbi.nlm.nih.gov/gene), ConsensusPathDB[10], UniProtKB[11], OMIM[12], Gene Ontology[13], TCDB[14], ExPASy[15] and KEGG database[16]. The databases had been downloaded earlier from the respective ftp servers and have been integrated offline using MATLAB (R2010a, The Mathworks Inc., Natick, MA, USA).

Characterization of rs2403254 locus

Chromatin accessibility and interactions were initially evaluated in the UCSC genome browser (http://genome.ucsc.edu). Subsequently cell-type specific DHS correlations and ChIA-PET (K562 Pol II) data were imported in MATLAB and superimposed on the regional LD data of the rs2403254 locus based on the 1000 Genomes Pilot 1 data of the CEU population (calculated using SNAP[17]). Since the ChIA-PET K562 Pol II data comprised two replicates, we only considered interactions for which the interacting regions overlapped between both replicates. Finally, eQTLs associated with *LDHA* expression as reported in the GTEx (http://www.ncbi.nlm.nih.gov/gtex/GTEX2) and gEUVADIS[18] database were imported and added to the regional LD plot.

Lactate dehydrogenase activity

Enzyme kinetic measurements were done in a 96 well plate in quadruple, based on the protocol of Vassault *et al.* [19]. Briefly, substrates were dissolved in buffer solution (80 mM TrisHCl, 0.20 mM NADH, pH 7.2 at 30°C) to the final concentrations mentioned in figure 2 in 180 µl. Lactate dehydrogenase was added (20 µl) containing $2.03 \bullet 10^{-5}$ mg LDH per well for pyruvate, $9.27 \bullet 10^{-3}$ mg for 3-methyl-2-oxobutanoate, $9.27 \bullet 10^{-2}$ mg for 3-methyl-2-oxopentanoate and $1.63 \bullet 10^{-2}$ mg for 4-methyl-2-oxopentanoate reactions. The decrease of A_{340} nm for NADH was measured every 8 sec for 6 min after which the slope was taken and using a calibration curve for NADH was recalculated as specific activity (U) in µmol NADH min^{-1} mg^{-1} LDH.

Data availability

We have submitted our finding of the link between rs2403254 and *LDHA* to the ClinVar database (http://www.ncbi.nlm.nih.gov/clinvar; accession number SCV000211950).

Results

Automated annotation of GWAS results

The automated workflow we developed was used to generate reports for each of the 37 SNPs published by Suhre *et al.* [3], containing the associated protein, enzyme, metabolic reaction, pathway, and disease phenotypes of each gene within a distance of 500 kb of the locus. Inspection of the results showed that for one of the 37 SNPs, rs2403254, there was an alternative candidate gene that provided a more likely explanation of the association. The rs2403254 SNP was associated with alpha-hydroxyisovalerate levels in the blood ($p=1.0 \cdot 10^{-20}$) and showed an even stronger correlation with the ratio of 3-methyl-2-oxobutanoate and alpha-hydroxyisovalerate levels ($p=7.9 \cdot 10^{-28}$). The rs2403254 SNP lies inside the *HPS5* gene and had therefore been assigned to *HPS5* by Suhre and colleagues. However, from inspection of the results from our workflow it followed that a plausible alternative candidate gene in the vicinity of the locus was *LDHA*, which codes for the A-isoform of the lactate dehydrogenase (LDH) enzyme. In addition, from information retrieved from the KEGG database [16] it followed that LDH has a broad substrate specificity and can catalyze the conversion of several keto and hydroxy acids, even though 3-methyl-2-oxobutanoate or alpha-hydroxyisovalerate were not listed as substrates (Supplemental Text S1).

The rs2403254 locus

Closer examination of the locus showed that rs2403254 is located in a large linkage disequilibrium (LD) block, which lies approximately 20kb upstream of *LDHA* (Fig. 1). To investigate the presence of potential long-distance regulatory mechanisms, we first looked at expression Quantitative Trait Loci (eQTLs) in lymphoblastoid cell lines that were associated with *LDHA*. These eQTLs were all located downstream of the LD block and were not in strong LD with rs2403254. In contrast, we found that rs2403254 is an eQTL for *HPS5* ($p=4.4 \cdot 10^{-9}$) and *GTF2H1* ($p=8.4 \cdot 10^{-15}$), most likely because it is in strong LD ($R^2 > 0.8$) with several SNPs that lie close to the transcription start sites of these genes.

Subsequently we explored chromatin interactions and the presence of regulatory elements in the LD block by looking at the DNase I signal data from the ENCODE project [6–8]. Interestingly, several regulatory regions were present within the LD block whose DNase I signal had a strong cross-cell-type correlation with the *LDHA* promoter (Fig. 1; bottom). These potential distal interactions were supported by the Chromatin Interaction Analysis with Paired-End-Tag (ChIA-PET) sequencing data, which showed that there were significant chromatin interactions between the central region of the LD block and the region containing the *LDHA* promoter. Collectively, these data show that long-range regulation of *LDHA* by enhancers that are located more than 20 kbp upstream of its transcription start site is indeed plausible.

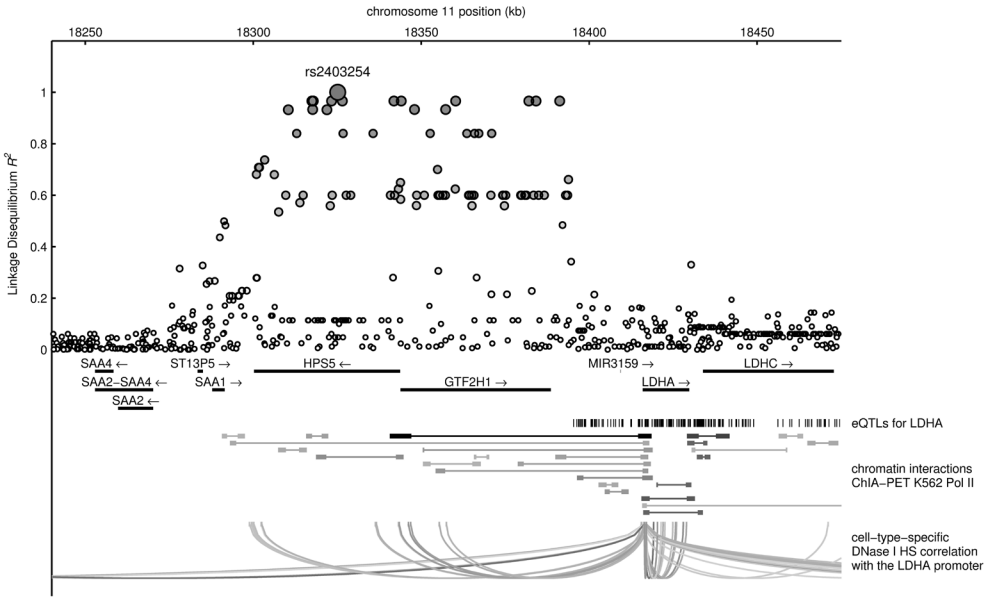

Figure 1: Regional Linkage Disequilibrium (LD) plot of the rs2403254 locus. The rs2403254 locus is located in a region of strong LD spanning over approximately 100kb. Several eQTLs have been identified that associate with LDHA expression, but none lie in LD with rs2403254. In contrast, chromatin interaction ChIA-PET data and cell type specific DNase I hypersensitive site correlations show that there are several chromatin interactions between the LDHA promoter and regulatory elements within the LD block.

Experimental validation

Subsequently, we investigated whether LDH could catalyze the conversion between branched-chain alpha-keto and hydroxy acids. In previous studies LDH had already been shown to catalyze a broad range of substrates [20, 21], but because of the extremely low rates with which branched-chain alpha-keto and hydroxy acids were converted it was unclear whether this reaction was mediated by LDH or another dehydrogenase [22, 23]. We therefore validated our finding by assaying the activity of LDH in the presence of NADH and the transaminated branched-chain keto acid products 3-methyl-2-oxobutanoate (valine), 4-methyl-2-oxopentanoate (leucine), 3-methyl-2-oxopentanoate (isoleucine) and pyruvate for a range of different substrate concentrations (Fig. 2). Results show that LDH was indeed able to convert 3-methyl-2-oxobutanoate, but it had a specificity constant k_{cat}/K_m that was approximately 3000 times lower than with pyruvate as substrate (Table 1). In comparison, the k_{cat}/K_m of the other two branched-chain alpha-keto acids was around 10 times lower than with 3-methyl-2-oxobutanoate as substrate. Most probably 3-methyl-2-oxobutanoate is converted more efficiently by LDH because it is a smaller molecule, having a carbon chain of 4 atoms, whereas 3- and 4-methyl-2-oxopentanoate have a carbon chain of 5 atoms. Interestingly, the K_m value for pyruvate and 3-methyl-2-oxopentanoate were very similar, while for the other two branched-chain alpha-keto acids it was 3 to 4 times larger.

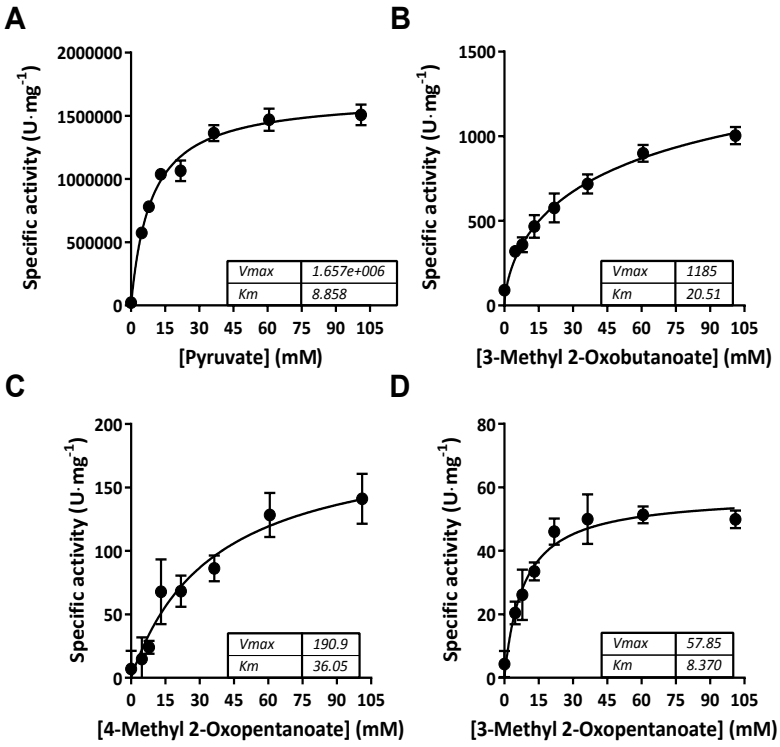

Figure 2: Enzyme kinetics of rabbit muscle lactate dehydrogenase. Specific activity in µmol NADH min^{-1} mg^{-1} LDH of rabbit muscle lactate dehydrogenase for A) pyruvate, B) 3-methyl-2-oxobutanoate, C) 4-methyl-2-oxopentanoate and D) 3-methyl-2-oxopentanoate. Assay conditions were 30°C, pH 7.2, initial [NADH]=0.20 mM.

*Table 1: Kinetic parameters of rabbit muscle lactate dehydrogenase. K_m and k_{cat} are Michaelis-Menten parameters ($v = k_{cat}[E][S] / (K_m+[S])$), while h, $K_{1/2}$ and k_{cat}' are allosteric sigmoidal parameters ($v = k_{cat}'[E][S]^h / (K_{1/2}{}^h+[S]^h)$). *p<0,05 for allosteric sigmoidal kinetics compared to Michaelis-Menten kinetics.*

Substrate	**k_{cat}** [µmol min^{-1} mg^{-1}]	**k_{cat}/K_m** [ml^{-1} min^{-1} mg^{-1}]	**h**	**$K_{1/2}$** [mM]	**k_{cat}'** [µmol min^{-1} mg^{-1}]
pyruvate	$1.66 \cdot 10^6$	$1.87 \cdot 10^5$			
3-methyl-2-oxobutanoate	$1.19 \cdot 10^3$(*)	58.0	0.65	66.6	$1.80 \cdot 10^3$
3-methyl-2-oxopentanoate	57.9	6.9			
4-methyl-2-oxopentanoate	190.9	5.3			

Discussion

The discovery of the functional link between the rs2403254 locus and the *LDHA* gene has been made possible by the automated workflow we developed for annotating GWAS results, which allowed us to examine the set of loci reported by Suhre *et al.* [3] in both a quick and thorough manner. In recent years there has been an increasing interest in bioinformatics tools for the analysis, interpretation and integration of results from GWASs [24, 25]. Suhre and colleagues have employed the tool GRAIL from the Broad Institute [26] in their study, which uses textual relationships between genes to prioritize candidate genes for a given locus. Nonetheless, using this method the authors did not identify *LDHA* as a plausible candidate for the rs2403254 locus, most likely because alpha-hydroxyisovalerate is currently not present in pathway databases and its link to LDH has only been scarcely described in the literature. In fact, the locus was replicated in a recent meta-analysis on the same metabolomics platform [27], but *HPS5* was still proposed as candidate gene.

In contrast, with our approach we focused on integrating the knowledge present in several databases in order to produce succinct SNP reports containing relevant information about all neighboring genes. In the case of the rs2403254 locus the SNP report showed that *LDHA* was the closest gene with a metabolic function and that LDH was documented in the KEGG pathway database as an enzyme that can catalyze multiple reactions. Subsequent investigation of the chemical structure of alpha-hydroxyisovalerate suggested that - in principle - its conversion could be catalyzed by LDH. This hypothesis was further reinforced by the observation that the same locus had a stronger association with the ratio of alpha-hydroxyisovalerate and 3-methyl-2-oxobutanoate levels and that alpha-hydroxyisovalerate is the product of 3-methyl-2-oxobutanoate after reduction of the alpha-carbonyl group.

Our results suggest that there is a functional link between *LDHA* and alpha-hydroxyisovalerate levels and, more specifically, that LDH can compensate for large build-ups of branched-chain alpha-keto acids under hypoxic conditions. In fact, the first step of branched-chain amino acid catabolism involves the transamination of the amino group, which changes the oxidation level of the adjacent carbon atom. Under anaerobic conditions the redox balance needs to be restored, which can be achieved through LDH by converting the alpha-keto acid into an alpha-hydroxycarboxylic acid (Fig. 2). This process has been observed in babies who suffered from asphyxia during birth, where elevated levels of alpha-hydroxyisovalerate were found in the urine [28]. Interestingly, also infants that suffer from Maple syrup urine disease, which is a defect in any of the genes coding for the components of the BCKDH enzyme complex, have elevated levels of alpha-hydroxyisovalerate in the urine [29]. This can be explained by the fact that a blockage in the second step of the branched-chain amino acid degradation pathway causes a build-up of keto acid intermediates, which are then partly converted to hydroxycarboxylic acids via LDH (Fig. 3).

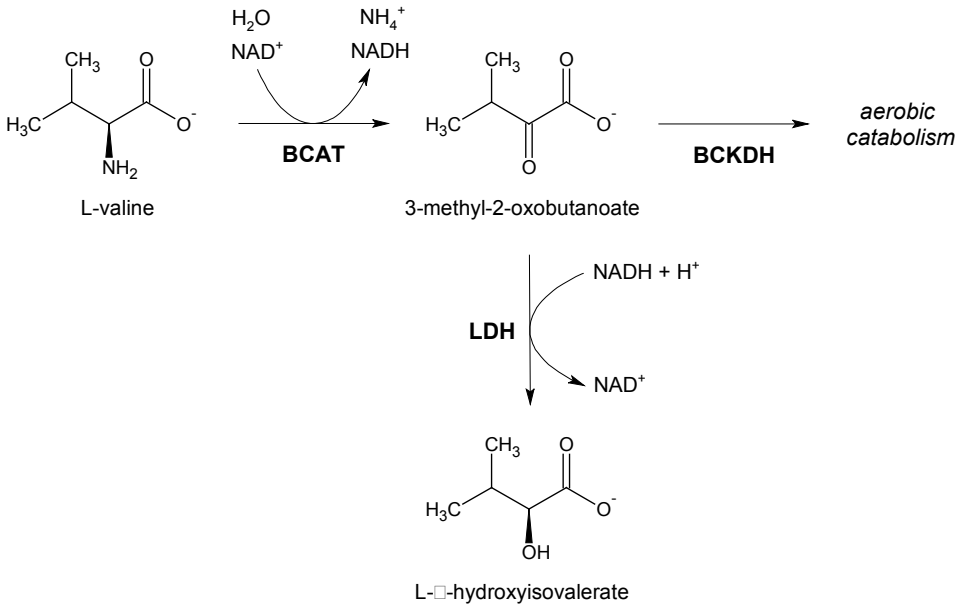

Figure 3: Visualization of the valine degradation pathway and the interaction with lactate dehydrogenase. Abbreviations of enzyme names are shown in boldface (BCAT: branched-chain aminotransferase; BCKDH: branched-chain alpha-keto acid dehydrogenase; LDH: lactate dehydrogenase). LDH can convert 3-methyl-2-oxobutanoate, which is the product of valine after transamination, into alpha-hydroxyisovalerate to balance the redox potential under hypoxic conditions. Under aerobic conditions 3-methyl-2-oxobutanoate can be further degraded by the enzymes of branched-chain amino acid catabolism. In contrast, alpha-hydroxyisovalerate cannot be metabolized any further and is excreted in urine.

Interestingly, in the meta-analysis of Shin *et al.* [27] rs2403254 was found to have the strongest association with the ratio of 3-(4-hydroxyphenyl)lactate and alpha-hydroxyisovalerate levels. 3-(4-hydroxyphenyl)lactate is the product of 4-hydroxyphenylpyruvate after reduction of the alpha-carbonyl group, which is the product of tyrosine after transamination. Given their structural differences it is unlikely that 3-(4-hydroxyphenyl)lactate and alpha-hydroxyisovalerate can be converted into one another in one or two enzymatic steps. The association with rs2403254 is therefore probably due to other mechanisms, such as co-regulation of aromatic and branched-chain amino acid metabolism.

Importantly, our finding does not preclude effects of rs2403254 on *HPS5* or other genes. In fact, in our analysis we found that rs2403254 is an expression QTL for *HPS5* and *GTF2H1*, which shows that multiple genes can be affected by a single SNP. However, neither of these genes provide a biochemical explanation of the phenotype, namely, why rs2403254 is associated with the ratio of 3-methyl-2-oxobutanoate and alpha-hydroxyisovalerate levels. The absence of eQTLs for *LDHA* in the databases that we enquired seems to confirm that distal eQTLs are more difficult to identify and demonstrates the additional value of chromatin interaction data to establish SNP-gene interactions.

In conclusion, we have uncovered a novel functional link between lactate dehydrogenase and the branched-chain keto acid intermediate of valine metabolism by reanalyzing published mGWAS results using automated workflows for integrating information from pathway databases.

Acknowledgements

We would like to thank Peter-Bram 't Hoen for critically reviewing the manuscript and Thomas Hankemeier for providing stock solutions of the branched-chain alpha-keto acids. This study has been funded by the European Network for Genetic and Genomic Epidemiology (ENGAGE) and by the Centre for Medical Systems Biology (CMSB) and Netherlands Consortium for Systems Biology (NCSB), both within the framework of the Netherlands Genomics Initiative (NGI)/Netherlands Organisation for Scientific Research (NWO).

References

1 Gieger C, Geistlinger L *et al.* **2008**; Genetics meets metabolomics: a genome-wide association study of metabolite profiles in human serum. *PLoS genetics* 4:e1000282.

2 Illig T, Gieger C *et al.* **2010**; A genome-wide perspective of genetic variation in human metabolism. *Nature genetics* 42:137.

3 Suhre K, Shin SY *et al.* **2011**; Human metabolic individuality in biomedical and pharmaceutical research. *Nature* 477:54.

4 Demirkan A, van Duijn CM *et al.* **2012**; Genome-wide association study identifies novel loci associated with circulating phospho- and sphingolipid concentrations. *PLoS genetics* 8:e1002490.

5 Kettunen J, Tukiainen T *et al.* **2012**; Genome-wide association study identifies multiple loci influencing human serum metabolite levels. *Nature genetics* 44:269.

6 ENCODE Project Consortium, Bernstein BE *et al.* **2012**; An integrated encyclopedia of DNA elements in the human genome. *Nature* 489:57.

7 Li G, Ruan X *et al.* **2012**; Extensive promoter-centered chromatin interactions provide a topological basis for transcription regulation. *Cell* 148:84.

8 Thurman RE, Rynes E *et al.* **2012**; The accessible chromatin landscape of the human genome. *Nature* 489:75.

9 Sherry ST, Ward MH *et al.* **2001**; dbSNP: the NCBI database of genetic variation. *Nucleic acids research* 29:308.

10 Kamburov A, Pentchev K *et al.* **2011**; ConsensusPathDB: toward a more complete picture of cell biology. *Nucleic acids research* 39:D712.

11 Magrane M, UniProt Consortium. **2011**; UniProt Knowledgebase: a hub of integrated protein data. *Database (Oxford)* 2011.

12 McKusick VA. **1998**. Mendelian Inheritance in Man. A Catalog of Human Genes and Genetic Disorders. *Baltimore, MD:* Johns Hopkins University Press.

13 Ashburner M, Ball CA *et al.* **2000**; Gene ontology: tool for the unification of biology. *Nature genetics* 25:25.

14 Saier J, M.H., Tran CV *et al.* **2006**; TCDB: the Transporter Classification Database for membrane transport protein analyses and information. *Nucleic acids research* 34:D181.

15 Gasteiger E, Gattiker A *et al.* **2003**; ExPASy: The proteomics server for in-depth protein knowledge and analysis. *Nucleic acids research* 31:3784.

16 Kanehisa M, Goto S. **2000**; KEGG: Kyoto Encyclopedia of Genes and Genomes. *Nucleic acids research* 28:27.

17 Johnson AD, Handsaker RE *et al.* **2008**; SNAP: A web-based tool for identification and annotation of proxy SNPs using HapMap. *Bioinformatics* 24:2938.

18 Lappalainen T, Sammeth M *et al.* **2013**;

19 Vassault A. **1983.**Lactate dehydrogenase. In: Methods of enzymatic analysis. Edited by: Bergmeyer, Bergmeyer, Grassl. *Weinheim:* Verlag Chemie; pp. 118.

20 Steinbüchel A, Schlegel HG. **1983**; NAD-linked L(+)-lactate dehydrogenase from the strict aerobe Alcaligenes eutrophus. 1. Purification and properties. *European journal of biochemistry* 130:321.

21 Kim MJ, Whitesides GM. **1988**; L-Lactate dehydrogenase: substrate specificity and use as a catalyst in the synthesis of homochiral 2-hydroxy acids. *Journal of the American Chemical Society* 110:2959.

22 Mamer OA, Reimer ML. **1992**; On the mechanisms of the formation of L-alloisoleucine and the 2-hydroxy-3-methylvaleric acid stereoisomers from L-isoleucine in maple syrup urine disease patients and in normal humans. *Journal of biological chemistry* 267:22141.

23 Hoffer LJ, Taveroff A *et al.* **1993**; Alpha-keto and alpha-hydroxy branched-chain acid interrelationships in normal humans. *Journal of nutrition* 123:1513.

24 Franke L, van Bakel H *et al.* **2006**; Reconstruction of a functional human gene network, with an application for prioritizing positional candidate genes. *American journal of human genetics* 78:1011.

25 Dharuri H, Henneman P *et al.* **2013**; Automated workflow-based exploitation of pathway databases provides new insights into genetic associations of metabolite profiles. *BMC Genomics* 14:865.

26 Raychaudhuri S, Plenge RM *et al.* **2009**; Identifying Relationships Among Genomic Disease Regions: Predicting Genes at Pathogenic SNP Associations and Rare Deletions. *PLoS genetics* 5:e1000534.

27 Shin SY, Fauman EB *et al.* **2014**; An atlas of genetic influences on human blood metabolites. *Nature genetics* 46:543.

28 Walker V, Mills GA. **1992**; Effects of birth asphyxia on urinary organic acid excretion. *Biology of the neonate* 61:162.

29 Chuang DT, Shih VE. **2001**. Maple syrup urine disease (branched-chain ketoaciduria). In: The Metabolic and Molecular Bases of Inherited Disease. Edited by: Scriver, Beaudet, Sly *et al. New York, NY:* McGraw-Hill; pp. 1971.

Supplemental data

Text S1: SNP report of the rs2403254 locus for LDHA. Similar gene-reports were generated for all genes within a 500 kbp distance of rs2403254, as retrieved from NCBI-Gene, ConsensusPathDB, UniProtKB, OMIM, Gene Ontology, TCDB, ExPASy and KEGG database.

SNP rs2403254 Chr 11 18325146

Distance to locus: -90790 LD R2 of rs2403254 with intragenic SNP rs3758683: 0.11936
Gene: **3939** (LDHA) Chr 11 18415936-18429765 (+)

23516535 the role played by ERRalpha in the regulation of lactate dehydrogenases A and B

23404405 Lactate dehydrogenase A is overexpressed in pancreatic cancer.

23266049 Data indicate that serum lactic dehydrogenase (S-LDH) appears to be a significant independent prognostic index in patients with metastatic nasopharyngeal carcinoma (NPC).

23184277 Increased LDH5 expression is associated with lymph node metastasis in oral squamous cell carcinoma.

23166385 Elevated lactate dehydrogenase level is associated with recurrent or refractory aggressive lymphoma.

22961700 LDHA plays an important role in the progression of esophageal squamous cell carcinoma by modulating cell growth

22948140 Cells expressing either PDK1 or LDHA maintained a lower mitochondrial membrane potential and decreased reactive oxygen species production with or without exposure to toxins.

22923663 Lactic acid induces myofibroblast differentiation via pH-dependent activation of transforming growth factor beta.

22897481 Studies indicate the mechanisms by which lactate dehydrogenase A (LDHA) promotes tumor growth and metastasis.

22593701 Data suggest that serum lactate dehydrogenase (LDH) kinetics might reflect disease behaviour in extracranial metastatic and primary sites without need for comprehensive imaging studies and is a quite inexpensive diagnostic test.

22429998 We demonstrate that LDH-A reduction can suppress the tumorigenicity of intestinal-type gastric cancer (ITGC) cells by downregulating Oct4 both in vitro and in vivo.

22360420 A protein encoded by this locus was found to be differentially expressed in postmortem brains from patients with atypical frontotemporal lobar degeneration.

22127970 Case Report: describe an elderly patient with physical therapy-induced rhabdomyolysis complicated by acute kidney injury associated with reduced skeletal muscle LDH-A activity.

21969607 LDH-A is tyrosine phosphorylated and activated by FGFR1 in cancer cells.

21858537 Results show that S-100B, MIA and LDH levels were significantly higher in patients with advanced melanoma than in disease-free patients or healthy controls.

21632858 Serum LDH and tissue LDH5 levels are complementary features that help to characterize the activity of LDH in colorectal cancer and have a potent value in predicting response to chemotherapy.

21452021 LDH-A reduction resulted in an inhibited cancer cell proliferation, elevated intracellular oxidative stress, and induction of mitochondrial pathway apoptosis.

21249322 High LDH is associated with M1b prostate cancer.

20951115 Presented are QM/MM calculations that show differences in geometries of active sites of M(4) and H(4) isoforms of human LDH ligated with oxamate, pyruvate or L-lactate.

20828817 High lactate dehydrogenase is associated with acute adult T-cell leukemia/ lymphoma.

20385008 LDH5 is overexpressed in non-small cell lung cancer and could serve as a marker for malignancy. LDH5 correlates positively with the prognostic marker transketolase like 1 protein.

19923867 LDH5 is highly expressed in squamous cell head and neck cancer and is linked with local relapse, survival and distant metastasis.

19847924 Observational study and genome-wide association study of gene-disease association. (HuGE Navigator)

19838163 Correlation of LDH-5 expression with clinicopathological factors and with the expression of Bcl-2, Bcl-XL, Mcl-1 and GRP78 was examined in pigmented lesions, including nevi and melanoma at different stages of progression

19668225 ErbB2 promotes glycolysis at least partially through the HSF1-mediated upregulation of LDH-A.

19276158 LDH-A knockdown in the background of FH knockdown results in significant reduction in tumor growth in a xenograft mouse model.

19021062 LDH5 is highly upregulated in B-cell non-Hodgkin lymphomas and is in direct relation to factor HIF1alpha and HIF2alpha expression. LDH5 expression is linked with activated VEGFR2/KDR expression in both lymphoid lesions.

18821170 The expression of LDH and its isoenzymes in pleural effusions reflects the host reaction in pleural space and, in non-small-cell lung cancer, may also feature the anaerobic phenotype of cancer cells.

18814027 Modulation of LDH expression involves alpha6beta4 integrin-FAK-p38MAPK pathway.

18534967 LDL-M is released into blood fo patients exposed to myocardial ischemia reperfusion.

18521687 The results of the current study show that LDH-5 expression may be a useful

prognostic factor for patients with gastric carcinoma.
17483170 biophysical study of ligand binding and protein dynamics in lactate dehydrogenase
17178662 LDH1 was decreased in essential thrombocythemia. This isoenzymatic pattern could be expression of a metabolic adaptation.
17178662 LDH5 was reduced in idiopathic myelofibrosis. This isoenzymatic pattern could be expression of a metabolic adaptation [LDH5]
16766262 Reduction in LDH-A activity resulted in stimulation of mitochondrial respiration and decrease of mitochondrial membrane potential.The tumorigenicity of the LDH-A-deficient cells was severely diminished.
16132575 Lactate dehydrogenase 5 content in tumor cells is directly related to an up-regulated hypoxia inducible factor pathway and is linked with an aggressive phenotype in colorectal adenocarcinomas.
15240094 These data indicate that LDH-A is induced through a non-genomic pathway of estrogen action.
12712614 The activity of this enzyme was studied in tissues, erythrocytes, and blood plasma of patients with peptic ulcer both in its uncomplicated course and in the development of complications.
12629811 The study of this protein in a sportsman is significant for assessment of training efficiency.
12555229 an LDHA exon5 haplotype confers increased risk for paradoxically decreased minute volume respiratory response to CO2 challenge but not to panic disorder
Pathway: Pyruvate metabolism - Homo sapiens (human) (database: KEGG)
Pathway: Glycolysis / Gluconeogenesis - Homo sapiens (human) (database: KEGG)
Pathway: Propanoate metabolism - Homo sapiens (human) (database: KEGG)
Pathway: HIF-1 signaling pathway - Homo sapiens (human) (database: KEGG)
Pathway: Cysteine and methionine metabolism - Homo sapiens (human) (database: KEGG)
Pathway: Cori Cycle (database: Wikipathways)
Pathway: Glycolysis and Gluconeogenesis (database: Wikipathways)
Pathway: hypoxia-inducible factor in the cardivascular system (database: BioCarta)
Pathway: TCR (database: NetPath)
Pathway: Pyruvate metabolism (database: Reactome)
Pathway: Validated targets of C-MYC transcriptional activation (database: PID)
Pathway: Pyruvate metabolism and Citric Acid (TCA) cycle (database: Reactome)
Pathway: The citric acid (TCA) cycle and respiratory electron transport (database: Reactome)
Pathway: Methionine Cysteine metabolism (database: INOH)
Pathway: Propanoate metabolism (database: INOH)
Pathway: Glycolysis Gluconeogenesis (database: INOH)
Pathway: EGFR1 (database: NetPath)
Pathway: Pyruvate metabolism (database: INOH)
Pathway: pyruvate fermentation to lactate (database: HumanCyc)
Pathway: HIF-1-alpha transcription factor network (database: PID)
Pathway: hypoxia-inducible factor in the cardivascular system (database: PID)
Protein: **LDHA** (P00338) L-lactate dehydrogenase A chain;
EC: **1.1.1.27** L-lactate dehydrogenase. (S)-lactate + NAD(+) = pyruvate + NADH.
GO: 0004459 L-lactate dehydrogenase activity
GO: 0005515 protein binding
GO: 0005634 nucleus
GO: 0005739 mitochondrion
GO: 0005829 cytosol
GO: 0005929 cilium
GO: 0006090 pyruvate metabolic process
GO: 0006096 glycolytic process
GO: 0021762 substantia nigra development
GO: 0031668 cellular response to extracellular stimulus
GO: 0044237 cellular metabolic process
GO: 0044281 small molecule metabolic process
GO: 0070062 extracellular vesicular exosome
KO: **K00016** L-lactate dehydrogenase [EC:1.1.1.27]
ReactionKEGG: **R00703** (S)-Lactate + NAD+ <=> Pyruvate + NADH + H+
ReactionKEGG: **R01000** 2-Hydroxybutanoic acid + NAD+ <=> 2-Oxobutanoate + NADH + H+
ReactionKEGG: **R03104** 3-Mercaptolactate + NAD+ <=> Mercaptopyruvate + NADH + H+
OMIM: **150000** LACTATE DEHYDROGENASE A; LDHA
OMIM: **612933** GLYCOGEN STORAGE DISEASE XI; GSD11

footnotes:
- Linkage disequilibrium R2 is based on founders in HapMap r27 CEU population

3

Apolipoprotein A5 deficiency aggravates high fat diet induced obesity due to impaired central regulation of food intake

Mattijs M. Heemskerk*, Sjoerd A.A. van den Berg*, Janine J. Geerling, Jan-Bert van Klinken, Frank G. Schaap, Silvia Bijland, Jimmy F.P. Berbée, Vanessa J.A van Harmelen, Amanda C.M Pronk, Marijke Schreurs, Louis M. Havekes, Patrick C.N Rensen, Ko Willems van Dijk

*Both authors contributed equally to this work.

FASEB journal **2013**, 27(8): 3354-3362

Abstract

Mutations in apolipoprotein A5 (APOA5) have been associated with hypertriglyceridemia in humans and mice. This has been attributed to a stimulating role for APOA5 in lipoprotein lipase-mediated triglyceride hydrolysis and hepatic clearance of lipoprotein remnant particles. However, due to the low APOA5 plasma abundance, we investigated an additional signaling role for APOA5 in high fat diet (HFD) induced obesity.

Wildtype (WT) and *Apoa5*$^{-/-}$ mice on chow diet showed no difference in bodyweight or 24h food intake (*Apoa5*$^{-/-}$, 4.5±0.6g, WT, 4.2±0.5g), while on HFD *Apoa5*$^{-/-}$ mice ate more in 24h (*Apoa5*$^{-/-}$, 2.8±0.4g, WT, 2.5±0.3g, $p<0.05$) and became more obese than WT mice. Also, intravenous injection of APOA5-loaded VLDL-like particles lowered food intake (VLDL-control, 0.26±0.04g, VLDL+APOA5, 0.11±0.07g, $p<0.01$). In addition, the HFD induced hyperphagia of *Apoa5*$^{-/-}$ mice was prevented by adenovirus-mediated hepatic overexpression of *APOA5*. Finally, intracerebroventricular injection of APOA5 reduced food intake compared to injection of the same mouse with artificial cerebral spinal fluid (aCSF, 0.40±0.11g, APOA5, 0.23±0.08g, $p<0.01$).

Introduction

Elevated plasma triglyceride (TG) levels and prolonged circulation of lipoprotein remnants are independent risk factors for cardiovascular disease [1-5]. In the post absorptive state, hypertriglyceridemia is a consequence of aberrant kinetics of VLDL, including hepatic overproduction and/or delayed clearance [6]. Apolipoprotein A5 (APOA5) has classically been described to be involved in the regulation of TG-rich lipoprotein metabolism [7]. APOA5 is a potent stimulator of lipoprotein lipase (LPL) [8, 9] and facilitates lipoprotein remnant clearance in a LDL-receptor dependent manner [10]. The function of APOA5 in lipid metabolism is supported by the fact that non-obese carriers of the *APOA5* -1131T>C polymorphism have a disturbed postprandial lipidemic response after a high fat meal [11, 12]. However, even though *in vitro* and animal studies suggest that APOA5 accelerates LPL mediated TG metabolism and the fact that APOA5 levels are positively associated with plasma TG levels, APOA5 does not directly affect postprandial VLDL kinetics in mild dyslipidemics or type 2 diabetics [13, 14].

In humans, the plasma concentration of APOA5 is low (114 to 258ng·ml^{-1} in normolipidemic subjects [15, 16]), possibly due to its low excretion rate [17, 18]. On a molar basis, APOA5 plasma levels are 1,000 and 10,000 fold lower when compared to Apolipoprotein B (APOB) and APOA1, respectively. Because of the low plasma concentration [19] and in light of the low secretion rate, APOA5 has been suggested to play a role in intracellular lipid metabolism. Intracellular APOA5 is associated with lipid droplets in liver [20] and adipocytes [21]. Interestingly, APOA5 shows a high protein similarity to perilipin-1 (PLIN1), a well-studied inhibitor of hormone sensitive lipase (HSL) activity [22]. Recently, intracellular APOA5 has been shown to co-localize with perilipin-1 in adipose tissue, and to actively regulate TG uptake, and thus may be involved in the development of obesity [21].

In addition to dyslipidemia, and in support of a role of APOA5 in the development of obesity, *APOA5* gene variants have been associated with a greater degree of obesity in a number of epidemiological studies involving Caribbean Hispanics [23], pediatric patients [24] and Brazilian elderly [25]. In part, this could be due to the proposed role of APOA5 in circulating lipid metabolism. Interestingly, it may also be due to altered food intake patterns, as the *APOA5* -1131T>C gene variant has been shown to be associated with higher fat intake [26] and to modulate the effects of dietary fat intake on body mass index and obesity risk [27, 28] and dyslipidemia [29].

The aim of this study was to assess the role of APOA5 in the regulation of food intake. First, we confirmed that *Apoa5*$^{-/-}$ mice are dyslipidemic and have an impaired lipid clearance. In addition, we further demonstrate that *Apoa5*$^{-/-}$ mice become more obese, and develop hepatic steatosis and become more insulin resistant on a high fat diet (HFD) than WT mice, due to a hyperphagic phenotype. Furthermore, the hyperphagic phenotype of *Apoa5*$^{-/-}$ mice is reduced upon adenoviral vector mediated overexpression of *APOA5*. Moreover, systemic (intravenous) as well as central (lateral ventricle) administration of APOA5 reduced food

intake by 60% and 45%, respectively, suggesting that APOA5 inhibits food intake, at least partly, via a central mechanism.

Materials and Methods

Animals and diets

Male wild type (WT) C57Bl/6Jico mice were obtained from Charles River laboratories (Charles River, Maastricht, The Netherlands) at an age of 10 weeks. After at least 2 weeks of acclimatization, mice were fed a HFD (45% energy as fat, 4.73kcal·g^{-1}, D12451, Research Diet Services, Wijk bij Duurstede, The Netherlands). *Apoa5*$^{-/-}$ mice [30] were bred in-house at the Leiden University Medical Center and back-crossed on the C57Bl/6Jico background for at least 8 generations prior to homozygous breeding. Absence of the *Apoa5*$^{-/-}$ gene was confirmed by isolated tail DNA PCR (forward; TGGAGGGTCAAAGAAGGATG, reverse; GGTTGCTGGTCACAGGATTT). Animals were housed in a controlled environment (21°C, 40-50% humidity) under a 12h photoperiod (07:00–19:00). Food and tap water was available *ad libitum* during the whole experiment, unless otherwise indicated. In all experiments, male mice were used. All animals were weighed at least once every week. All animal experiments were performed in accordance with the regulations of Dutch law on animal welfare and the institutional ethics committee for animal procedures from the Leiden University Medical Center, Leiden, The Netherlands approved the protocol.

Plasma and liver lipid analysis

Plasma was obtained via tail vein bleeding and assayed for TC and TG, using the commercially available enzymatic kits 236691 and 11488872 (Roche Molecular Biochemicals, Indianapolis, IN, USA), respectively. Free fatty acids (FA) were measured using NEFA-C kit from Wako Diagnostics (Instruchemie, Delfzijl, the Netherlands). Human APOA5 levels were determined using a previously described ELISA [31].

Lipids were extracted from livers according to a protocol modified from Bligh and Dyer [32]. In short, a small piece of liver was homogenized in ice-cold methanol. After centrifugation, lipids were extracted by addition of 1,800µl of CH_3OH-$CHCl_3$ (3:1 vol/vol) to 45µl of homogenate. The organic phase was dried and dissolved in 2% Triton X-100. Hepatic TG and TC concentrations were measured using commercial kits, as described above. Liver lipids were expressed per milligram of protein, which was determined using the Pierce BCA protein assay kit (Thermo Scientific, Rockford, IL, USA).

Lipid clearance analysis

Glycerol tri(9,10(n)[^{3}H]oleate ([^{3}H]TO) and [1α,2α(n)-^{14}C]cholesteryl oleate ([^{14}C]CO) double radiolabeled VLDL-like emulsion particles (mean diameter 80nm) were prepared as described before [33]. Mice were anesthetized with 6.25mg·kg^{-1} Acepromazine (Alfasan, Woerden, The Netherlands), 6.25mg·kg^{-1} Midazolam (Roche, Mijdrecht, The Netherlands) and 0.31mg·kg^{-1} Fentanyl (Janssen-Cilag, Tilburg, The Netherlands) prior to particle injection via the tail vein. At time points 2, 5, 10 and 15min post-injection, blood was taken to determine clearance rates. After 15 minutes mice were sacrificed and organs were harvested to determine [^{3}H]TO and [^{14}C]CO uptake.

Determination of adipocyte differentiation capacity

Adipose tissue from the reproductive and subcutaneous region were harvested and kept in PBS. The tissue was minced and digested in 0.5g·l^{-1} collagenase in HEPES buffer (pH 7.4) with 20g·l^{-1} of dialyzed bovine serum albumin (BSA, fraction V, Sigma, ST Louis, USA) for 1h at 37°C. The disaggregated adipose tissue was filtered through a nylon mesh with a pore size of 236μm and the stromal vascular cells were isolated. Preadipocytes were differentiated in an adipogenic medium and differentiation capacity was determined as previously described [34].

Indirect calorimetry/metabolic cage analysis

WT and *Apoa5*$^{-/-}$ mice were subjected to indirect calorimetry/metabolic cage analysis (Phenomaster, TSE Systems, Bad Homburg, Germany). A period of 48 hours of acclimatization was included prior to the start of the experiment. Oxygen consumption (VO_2) and carbon dioxide production (VCO_2) were determined at 9 minute intervals. Respiratory exchange ratio (RER) was calculated as the ratio between VCO_2 and VO_2. Energy expenditure (EE), fat oxidation (FAox) rate and carbohydrate oxidation (CHox) rate were calculated as previously described [35]. Food intake was monitored in real time. Data from the light and dark phase were averaged and tested separately to distinguish periods of high and low physical activity. In total the measurement period lasted 7.5 days (chow≈3 days and HFD≈4.5 days). The switch to the HFD was performed inside the metabolic cage system at 14:00 for all animals. For the long term experiment, mice were fed a HFD for a period of 4 weeks prior to analysis.

Adenovirus vector mediated overexpression of human APOA5 in Apoa5$^{-/-}$ mice

A separate group of *Apoa5*$^{-/-}$ mice were used for adenoviral vector gene transfer, and subjected to indirect calorimetry/metabolic cage analysis during the initial week of high fat feeding. A period of 24 hours of acclimatization was included prior to the start of the experiment and baseline measurements were performed for each individual animal. Subsequently, animals were randomized based on body mass and injected intravenously (*vena caudalis*) with mock LacZ or human *APOA5* expressing adenovirus vectors (≈2·10^{9}pfu). Calorimetric analysis was continued for 4 days after injection until the expected peak in transgenic expression [36, 37]. Since adenovirus vector mediated gene expression in itself may affect energy balance [38-40] data were analyzed per animal separately in a paired comparison setting (i.e. pre-injection vs. post-injection). Differences in the change in food intake over the 4 days were compared between groups.

Intravenous APOA5 injection and food intake test

WT mice were fed a high fat diet for a period of 1 week prior to analysis to ascertain habituation to the high fat diet. All mice were food restricted for 6 hours prior to injection, starting at 12:00, to induce the drive for food intake. To assess the effect of elevated circulating APOA5 levels on food intake, VLDL emulsion particles [41] were loaded with human APOA5 (100ng·µl^{-1}, Abnova, Jhongli, Taiwan). Human APOA5 protein was produced in an *in vitro* wheat germ expression system, which generally results in negligible endotoxin levels (Personal communication, V. Yu, Abnova, Jhongli, Taiwan). Analysis of the Sepharose purified preparation by SDS-PAGE and Coomassie staining revealed a single band. Non-loaded control and APOA5 loaded emulsion particles were intravenously injected in the tail vein at a dose of 6µg per mouse and injected 6h after food restriction. After injection, food intake was recorded up to 120 minutes post injection and expressed as gram food consumed per unit of 60 minutes.

Lateral ventricle cannulation and ICV APOA5 injection and food intake test

WT mice were fed a high fat diet for a period of 1 week prior to analysis to ascertain habituation to the high fat diet. To assess the effect of central administration of APOA5 on food intake, a 25 gauge guide cannula was implanted into the left lateral ventricle as previously described [42, 43]. Similar to the IV injection experiment, mice were food restricted to induce the drive for food intake. All animals received a successive 1µl bolus injection of artificial cerebrospinal fluid (aCSF, Harvard Apparatus, Holliston, MA, USA) (7d post-surgery), APOA5 (10d post-surgery, 8ng/mouse) and neuropeptide Y (NPY, 14d post-surgery, 5µg/mouse) under light

isoflurane anesthesia. After injection, food intake was recorded during the first 120 minutes post injection and expressed as gram food eaten per unit of 60 minutes. Correct placement of the cannula was assessed in all mice in the fed state at 14d post-surgery by a bolus injection of neuropeptide Y at 0900 a.m. Cannulation was assumed to be correct if the animal consumed more than 300mg of food within 1 hour post NPY injection. One animal did not meet this criterion and was excluded from the experiment.

Hyperinsulinemic-euglycemic clamp in conscious mice

WT and *Apoa5*$^{-/-}$ mice were subjected to hyperinsulinemic-euglycemic clamp analysis as previously described [44]. In short, all mice were equipped with a single catheter in the right jugular vein for infusion. After surgery, mice recovered for a period of 8 days prior to the clamp analysis, in individual cages. Food intake and body weight returned to preoperative levels within 2-3 days. Food was removed 9 hours before the start of the experiment, but the animals had free access to water. Clamp quality control was determined by calculating the coefficient of variation (COV) of the glucose infusion rate (GIR) and plasma glucose levels over the last 30 minutes of the clamp. COV of the GIR and glucose levels were determined to be below 2% for both genotypes.

Statistics

All data are represented as mean ± standard deviation. Energy intake data was tested by unpaired t-test for normally distributed data or paired t test in case of the adenoviral and icv experiment. Threshold for statistical significance was set at 5%. Tests were performed using PASW (SPSS) Statistics, version 18.

Results

High fat fed Apoa5$^{-/-}$ mice are hyperlipidemic and have severely impaired lipid clearance

Plasma was isolated from food restricted *Apoa5*$^{-/-}$ and WT mice fed a HFD for 10 weeks, after which plasma cholesterol, TG, phospholipid and free fatty acid levels were determined. *Apoa5*$^{-/-}$ mice were hyperlipidemic (Table 1) and in line with these data, *Apoa5*$^{-/-}$ mice showed severely impaired lipid clearance. The plasma decay of injected [^{3}H]TO and [^{14}C]CO-labeled emulsion particles was slower in *Apoa5*$^{-/-}$ mice for the TO label (Figure 1 A, B) as well as the CO label (Figure 1 C, D), due to a significantly lower uptake in organs with a high metabolic activity (liver, heart, muscle, brown adipose tissue). In addition, CO label uptake was also lower in liver and brown adipose tissue, but not in heart and muscle. These data confirm previously published data (10;30) and demonstrate that the hyperlipidemic phenotype of *Apoa5*$^{-/-}$ mice is associated with an impaired lipid partitioning.

*Table 1: Plasma lipid levels of HFD fed Apoa5$^{-/-}$ and WT control mice. Data represent mean values ± SD, **=p<0.01.*

	Apoa5-/-	**WT**
Triglyceride(mmol/L)	5.7±2.8	1.1 ± 0.2**
Cholesterol (mmol/L)	6.8 ± 1.1	4.0 ± 0.6**
Phospholipids (mmol/L)	7.1 ± 1.0	4.3 ± 0.5**
Free fatty acids (mmol/L)	1.9 ± 0.9	1.0 ± 0.3**

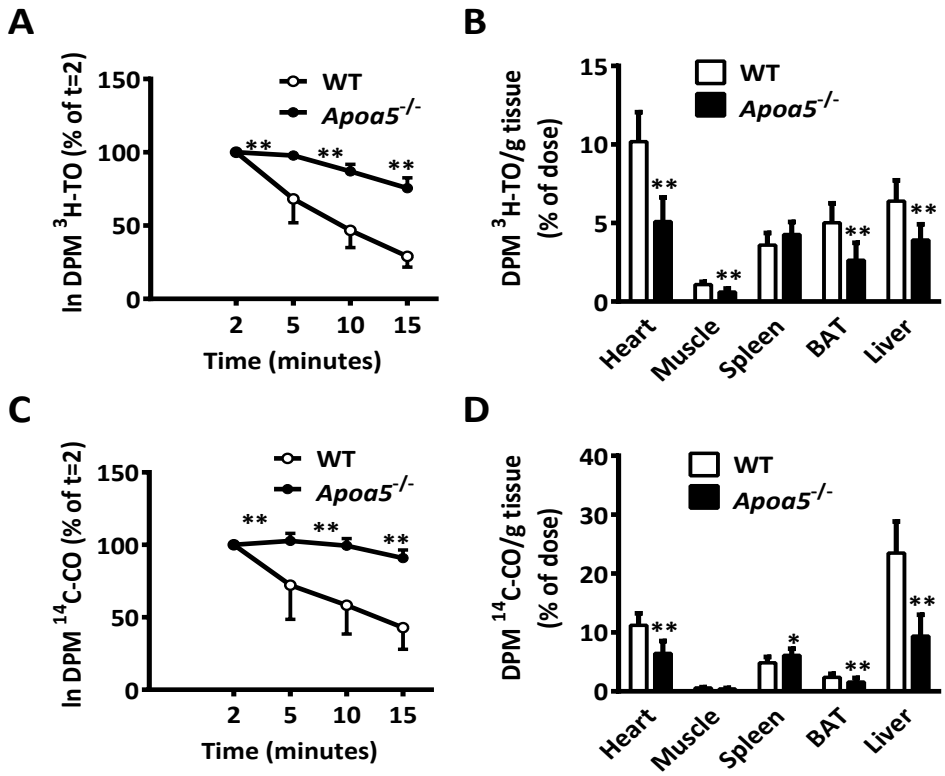

*Figure 1: Plasma decay curve (A) and tissue specific retention (B) of the ^{3}H-TO label and the decay curve (C) and tissue specific retention (D) label of the ^{14}C-CO label after mass lipid injection in Apoa5$^{-/-}$ and WT mice. Data represent mean values ± SD, *=p<0.05, **=p<0.01.*

High fat diet feeding aggravated obesity development in Apoa5$^{-/-}$ mice

Bodyweight was monitored in WT and *Apoa5*$^{-/-}$ mice fed a HFD. Diet induced weight gain was more pronounced in *Apoa5*$^{-/-}$ mice, which thereby became more obese compared to WT (Figure 2). White adipose tissue mass was significantly higher in *Apoa5*$^{-/-}$ mice in both the reproductive (*Apoa5*$^{-/-}$, 2.4±0.3g, WT, 1.7±0.5g, p<0.01) and subcutaneous (*Apoa5*$^{-/-}$, 1.7±0.6g, WT, 1.1±0.3g, p<0.01) white adipose tissue depot. Due to the large infiltration of pancreatic tissue, the mesenteric fat depot could not be isolated in a reproducible manner [45]. Heart, liver, spleen, lung, or kidney mass did not differ between genotype (data not shown). Since APOA5 has been described to regulate fatty acid uptake in adipocytes [21] and thus possibly affect adipogenesis, the differentiation capacity of pre-adipocytes isolated from the reproductive and subcutaneous fat pads of HFD fed *Apoa5*$^{-/-}$ and WT mice was studied by Nile red assay. Differentiation capacity did not differ between genotypes for either of the

isolated fat pads (p=0.70 and p=0.69 for reproductive and subcutaneous fat, respectively (Supplemental Figure S1). Together, these data demonstrate that HFD fed *Apoa5*$^{-/-}$ mice become more obese than WT mice and that this is not due to an intrinsic difference in the adipogenic capacity of the white adipose tissue.

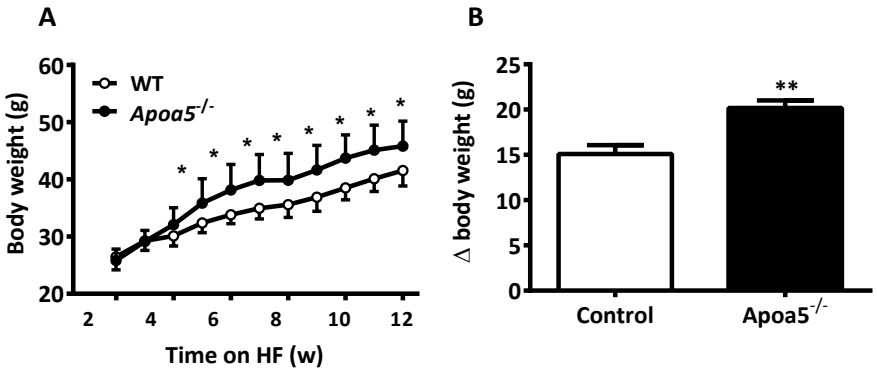

Figure 2: Weight development of Apoa5$^{-/-}$ *mice and WT controls during high fat diet intervention. Data represent mean values ± SD, *=p<0.05, **=p<0.01.*

Apoa5$^{-/-}$ *develop aggravated hepatic steatosis and insulin resistance upon HFD feeding*

Ectopic fat accumulation in the liver of *Apoa5*$^{-/-}$ and WT control mice was assessed. Although total hepatic mass did not differ between groups, hepatic TG content was 50% higher in HFD fed *Apoa5*$^{-/-}$ mice (*Apoa5*$^{-/-}$, 0.47±0.16μmol·mg^{-1} protein, WT, 0.31±0.17μmol·mg^{-1} protein, p=0.056). Hepatic cholesterol and phospholipid accumulation did not differ between groups (data not shown).

Since HFD fed *Apoa5*$^{-/-}$ mice become more obese and develop hepatic steatosis upon HFD feeding, tissue specific insulin sensitivity was determined by hyperinsulinemic-euglycemic clamp analysis in conscious mice (Supplemental Figure S2). GIR was lower in *Apoa5*$^{-/-}$ mice (*Apoa5*$^{-/-}$, 335±64μmol· (kg·min)$^{-1}$, WT, 408±60μmol·(kg·min)$^{-1}$, p<0.05, (Supplemental Figure S2a)), indicating a reduction in insulin sensitivity. In addition, the hyperinsulinemic circulating glucose level at stable GIR was significantly higher in *Apoa5*$^{-/-}$ mice (*Apoa5*$^{-/-}$, 6.6±1.2mmol·l^{-1}, WT, 5.5±0.7mmol·l^{-1}, p<0.05 (Supplemental Figure S2b)). To correct for this difference in circulating glucose pool, metabolic clearance rates (MCR) were determined. MCR was significantly reduced in *Apoa5*$^{-/-}$ mice (*Apoa5*$^{-/-}$, 77.0±15.4ml·(kg·min)$^{-1}$WT, 101.0±18.1ml·(kg·min)$^{-1}$, p<0.05 (Supplemental Figure S2c)). Collectively, these data show that *Apoa5*$^{-/-}$ mice, in addition to obesity, develop hepatic steatosis and insulin resistance when fed a HFD.

Apoa5$^{-/-}$ mice are hyperphagic when fed a high fat diet

Given the association of APOA5 with fat intake (27;28), we determined whether the change in energy balance in *Apoa5$^{-/-}$* mice was due to a defect in oxidative metabolism (which may arise from the reduced lipid clearance capacity) or food intake (FI). At the start of the experiment, when animals were fed a chow diet, bodyweight did not differ significantly between groups (*Apoa5$^{-/-}$*, 25.3±0.8g, WT, 26.2±1.4g, p=0.2). Furthermore, FI measured over a period of 24 hours did not differ between groups when animals were fed a chow diet (*Apoa5$^{-/-}$*, 4.5±0.6g, WT, 4.2±0.5g). In addition, respiratory exchange ratio (RER) and energy expenditure (EE) were similar between groups (Data not shown).

After the chow period, all animals were switched to the HFD (Figure 3). During the first 24 hrs after the switch to the HFD, FI was significantly higher when compared to the chow diet in both groups (*Apoa5$^{-/-}$*, 4.7±0.3g, WT, 4.7±0.1g, p<0.01 for both groups vs. chow), but did not differ between groups (p=0.20). After that, FI declined in both groups, but remained higher in the *Apoa5$^{-/-}$* group. Food intake during the last 24 hours was significantly higher in *Apoa5$^{-/-}$* mice during the dark period (*Apoa5$^{-/-}$*, 2.1±0.3g, WT, 1.9±0.7g, p<0.05) but did not differ between groups during the light period (*Apoa5$^{-/-}$*, 1.2±0.5g, WT, 1.1±0.4g). Total FI during the first 96 hours of HFD intervention was higher in the *Apoa5$^{-/-}$* group (*Apoa5$^{-/-}$*, 16.5±1.2g, WT, 14.2±0.7g, p<0.01). The HFD induced a gradual shift from carbohydrate to fat metabolism in both groups. RER and absolute carbohydrate oxidation declined and absolute fat oxidation increased, but this switch was less pronounced in *Apoa5$^{-/-}$* mice (Figure 3).

Similar results were found after 4 weeks of HFD intervention, where food intake was significantly higher in *Apoa5$^{-/-}$* mice during a period of 24 h (*Apoa5$^{-/-}$*, 2.8±0.4g, WT, 2.5±0.3g, p<0.05). Oxidative fat metabolism was still reduced in *Apoa5$^{-/-}$* mice compared to controls (Supplemental Table S1). These data show that HFD fed *Apoa5$^{-/-}$* mice remain hyperphagic, and have reduced relative and absolute fat oxidation rates after prolonged high fat feeding.

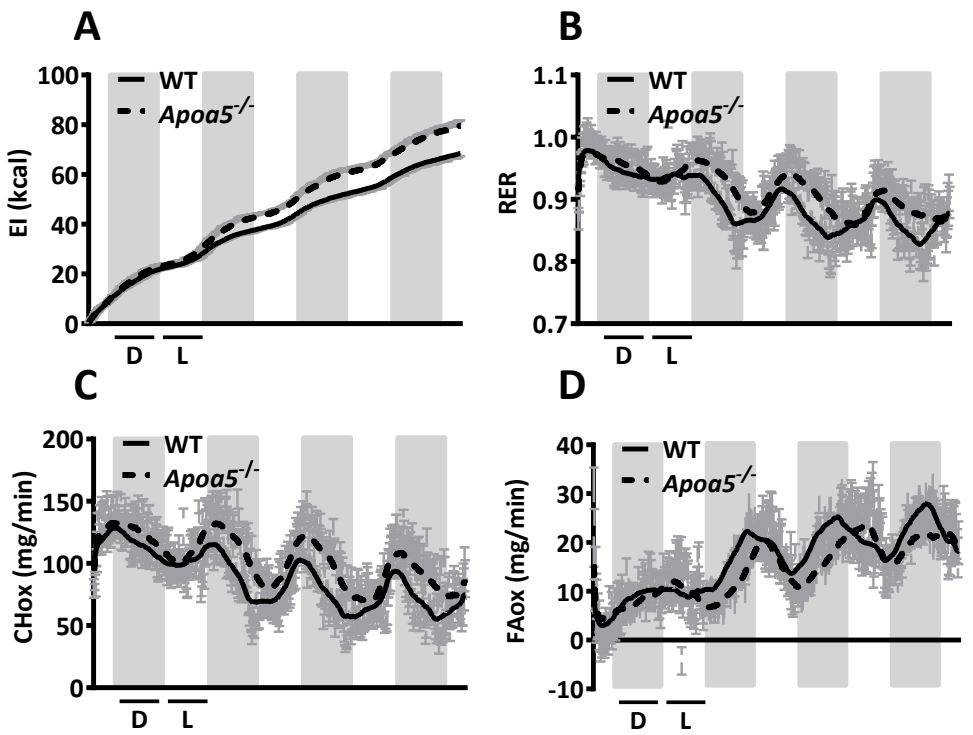

Figure 3: Indirect calorimetry data from Apoa5$^{-/-}$ (dashed line) and WT (solid line) mice during the first week of high fat diet intervention in the light (L) and dark (D) periods of the day. A) Energy intake (EI),B) Respiratory exchange ratio (RER), C) Carbohydrate oxidation (CHox) and D) Fat oxidation (FAox). All graphs depict the smoothed average ± SEM.

Adenovirus mediated gene transfer of APOA5 to Apoa5$^{-/-}$ mice reduces food intake

To assess whether hepatic expression of *APOA5* rescues the hyperphagic phenotype, *Apoa5*$^{-/-}$ mice were injected with adenovirus vectors expressing either LacZ or human *APOA5*. At the time of injection, body mass did not differ significantly between the groups (*APOA5*, 22.7±1.8g, LacZ, 24.2±3.0g, p=0.3). Basal FI, determined at day 0, did not differ between groups during the light (*APOA5*, 0.66±0.23g, LacZ, 0.53±0.16g, p=0.2) or dark period (*APOA5*, 1.43±0.50g, LacZ, 1.54±0.23g, p=0.6). At the fourth day after virus injection, FI was compared to basal levels in both groups. In LacZ mice, FI was significantly higher compared to basal levels during the light (0.80±0.23g, p<0.01) as well as the dark period (2.01±0.72g, p<0.01), whereas in *APOA5* injected animals, FI during the light and dark period was similar to basal values (Light, 0.85±0.39g, p=0.08 and dark period 1.41±0.59g, p=0.46, respectively). Hepatic overexpression of *APOA5* resulted in human APOA5 plasma levels of 57.6±16.6µl·ml^{-1}. These data show that *APOA5* overexpression is sufficient to reduce food intake.

Peripheral and central APOA5 protein administration reduce food intake

To determine whether hepatic *Apoa5* expression, or increased circulating APOA5 protein levels mediates reduction in food intake (FI), APOA5 protein was loaded onto VLDL like emulsion particles and injected intravenously in WT mice. Injection of APOA5-loaded emulsion particles significantly reduced food intake (-60%) during the first 60 minutes post injection as compared to unloaded (control) emulsion particles (control, 0.26±0.04g, APOA5, 0.11±0.07g, p<0.01, Figure 4A). During the second hour after the injection, APOA5-loaded emulsion particles did not lower food intake compared to control particles (control, 0.18±0.11g, APOA5, 0.13±0.08g). These data show that increased circulating APOA5 protein levels are capable of reducing food intake.

A peripheral increase of circulating APOA5 protein may affect FI via upregulation of LPL mediated lipolysis (45) or a direct peripheral to central signaling pathway. To determine whether APOA5 protein is capable to reduce FI directly via a central mechanism, aCSF (as a negative control) or aCSF+APOA5 protein was injected into the lateral ventricle of food deprived WT mice (Figure 4B). APOA5 injection significantly lowered FI during the first 60 minutes post injection (40-50%) compared to aCSF (aCSF, 0.40±0.11g, APOA5, 0.23±0.08g, p<0.01) (Figure 4B). FI tended to be reduced during the second hour after APOA5 injection (aCSF, 0.17±0.06g, ApoA5, 0.11±0.10g, p=0.1). These data show that central APOA5 protein administration directly reduces food intake, even at nano-molar concentrations and suggest that the food intake-reducing effect of APOA5 may be regulated, in part, via a central mechanism.

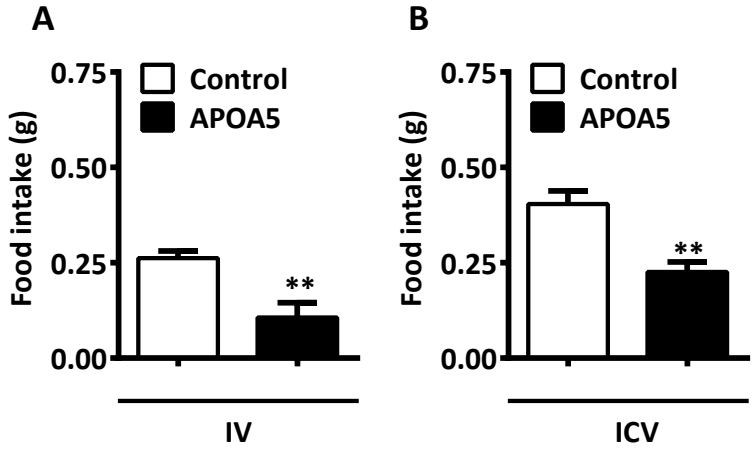

*Figure 4: Food intake during the first 60 min. after (A) intravenous injection of unloaded VLDL-like emulsion particles (white bars) or APOA5 loaded VLDL-like emulsion carrier particles (black bars) and (B) intracerebroventricular injection of aCSF with (black bars) or without (white bars) APOA5 injection. Data represent mean values +/- SD, **=p<0.01.*

Discussion

Here, we confirm previous reports that APOA5 plays a central role in lipid metabolism and energy balance. *Apoa5*$^{-/-}$ mice are hypertriglyceridemic and hypercholesterolemic and display impaired lipid partitioning. Furthermore, *Apoa5*$^{-/-}$ mice develop obesity, hepatic steatosis and insulin resistance when fed a HFD. In addition, we show that *Apoa5*$^{-/-}$ mice are hyperphagic, and that adenoviral overexpression of *APOA5* reverses this phenotype. Furthermore, intravenous as well as central injection of purified APOA5 protein reduced food intake in WT mice (60% and 45%, respectively), suggesting a central effect of APOA5 on the regulation of food intake. Collectively, we confirm that APOA5 plays a crucial role in lipid clearance but we also demonstrate a novel role of APOA5 in the regulation of food intake. Therefore, we speculate that peripheral to central translocation of APOA5 is a satiety signal acting perhaps independently of the effects of APOA5 on LPL-mediated lipolysis.

Food intake is known to be variable and time dependent in C57Bl/6 mice switched to a HFD [46]. After an initial phase of hyper caloric intake, food intake decreases and hypothalamic expression of pro- opiomelanocortin (POMC) is up regulated, possibly as a defensive mechanism against the development of obesity [46]. Here, we confirm that food intake upon high fat feeding was only transiently elevated in control C57Bl/6 mice. In contrast, food intake was significantly higher in *Apoa5*$^{-/-}$ mice upon HFD intervention when compared to controls, and, interestingly, the decline in food intake was largely absent in *Apoa5*$^{-/-}$ mice. Food intake of *Apoa5*$^{-/-}$ mice remained higher compared to both WT mice and baseline values for a period of at least 5 weeks. In addition to hyperphagia, the oxidative metabolism of *Apoa5*$^{-/-}$ mice was characterized by a low rate of fat oxidation. It is, however, unlikely that the increased obesity grade in the *Apoa5*$^{-/-}$ mice is due to a reduced fat oxidation, as peak oxidation rates (during the light period, after 4 weeks of HFD feeding) did not differ from controls. Together, these data clearly show that, compared to controls, *Apoa5*$^{-/-}$ mice have a higher caloric intake when fed a HFD, but do not match fat oxidation to this excess, ultimately leading to a more positive fat balance, and thus obesity.

To assess the hyperphagic phenotype in more detail, human *APOA5* was overexpressed in the liver via an adenovirus. Four days after *APOA5* virus injection, the hyperphagic phenotype of *Apoa5*$^{-/-}$ mice was prevented compared to LacZ virus injected animals. The established human APOA5 plasma concentration was substantially higher (100-300 fold) than the endogenous mouse APOA5 concentration, which is in the same range as earlier experiments [8, 47]. Thus, supraphysiological APOA5 levels reduced food intake. Subsequently, we investigated whether low plasma levels of APOA5 could also reduce food intake. Therefore protein free VLDL like emulsion particles were loaded with 6µg purified APOA5 and injected intravenously to mimic the postprandial hypertriglyceridemic situation. Addition of APOA5 to the VLDL particles resulted in a large, but transient reduction in food intake, which is in line with a putative function of APOA5 as a satiation signal. These data show that APOA5 is involved in the regulation of food intake, either directly via a central mechanism and/or

indirectly by its known effect on peripheral lipolysis. The liberation of free fatty acids at the vessel wall during peripheral lipolysis may in itself induce meal termination, as hypothalamic sensors monitor energy status and adjust food intake [48]. Recent studies showed that central administration of oleic acid results in a reduction of food intake [45] in a melanocortin-4-receptor (MC4R) dependent manner, and that this is dependent on nutritional status [49]. Therefore, it could be that the effect of APOA5 on food intake is indirect and involves the stimulation of peripheral lipolysis, and subsequent transport of fatty acids to the brain. In previous studies, however, it has been shown that although APOA5 levels rise concomitantly with TG levels in the postprandial period, this does not affect postprandial VLDL kinetics [13, 14], arguing that the satiating effect of APOA5 may be independent of its effect on lipolysis.

Human cerebrospinal fluid (CSF) contains spherical lipoproteins that resemble HDL in plasma [50, 51]. Furthermore, it has been described that active endocytosis of lipoproteins occurs at the blood brain barrier [52]. A number of apolipoproteins have been identified in human CSF. APOE and APOA1 are the major apolipoproteins; with APOA2, A4, C1, D, C2, C3, C4, J and H present as well [50, 51, 53]. Interestingly, it has been shown that the concentration of APOA4 in CSF increases as a result of lipid feeding [54]. To be able to act as a nutritional sensor, the peripheral-to-central transition of the signal must be rapid. The transcytosis time of lipoprotein particles at the blood brain barrier has been shown to be short (≈15 minutes). Thus, if lipoprotein bound APOA5 acts as a satiety signal, the transition time is likely not rate limiting in the potential of APOA5 to mediate satiation.

Interestingly, central APOE is involved in food intake in rats via a melanocortin 3/4 receptor dependent mechanism [55]. Furthermore, APOA4, the closest structural homolog of APOA5, has also been shown to be expressed in the hypothalamus [56] and to decrease food intake in a cholecystokinin dependent manner [57], also partly via a melanocortin regulated central mechanism [54, 58]. These findings indicate that the effect of APOA4 and APOE on food intake may share a common signaling route. APOA5 is often described as being exclusively expressed in the liver [59, 60]. However, a recent report demonstrated that *APOA5* is expressed in the duodenum and colon in mice and human subjects, and that this expression can be modulated by fatty acids as well as fibrates [61]. Furthermore, active transcription of *Apoa5* in the brain has been shown in birds [62] and mice [63]. More specifically, in mice, central transcription of *Apoa5* was determined to be located at the hypothalamus [64]. In humans, microarray analysis of post mortem brain material revealed that *APOA5* is expressed in the brainstem and near the paraventricular nuclei of the hypothalamus [65]. To assess whether the hyperphagic food intake of *Apoa5*$^{-/-}$ mice could be a direct consequence of the loss of central APOA5 signaling rather than a consequence of impaired peripheral lipolysis, purified APOA5 was injected in the lateral ventricle of HFD fed mice. Central administration of purified APOA5 also largely reduced food intake. Although we cannot formally exclude the presence of contaminants in the commercially produced APOA5, the endotoxin-free production of the protein and the further 12-fold dilution in aCSF, make it unlikely that the

observed effect of ICV administered APOA5 on food intake is non-specific. Possibly, APOA5 mediates energy balance by its association with lipid particles, some of which are able to be transported across the blood brain barrier. It has been shown that in particular LDL and HDL can cross the blood brain barrier via receptor mediated transport [66, 67]. A possible site of peripheral to central translocation of APOA5 containing lipoproteins could be the median eminence of the basal hypothalamus, adjacent to the arcuate nucleus [68]. The arcuate nucleus is crucially involved in the regulation of energy balance and is subject to plastic remodeling when dietary fat content is modulated [69]. Interestingly, low, but significant, APOA5 protein levels have been detected at the lateral ventricle wall in humans [70], which is directly adjacent to the arcuate nucleus.

Interestingly, the inhibiting effect of APOA5 on food intake after intracerebroventricular injection was already achieved at a dose of 8ng/mouse. This dose was approximately 500 fold lower compared to the doses of APOE [55] and APOA4 [54] that are able to reduce food intake. As mentioned before, APOE and APOA4 decrease food intake in a dose dependent manner, which is mediated by the melanocortin system [55, 56]. Since the anorexigenic effects of central oleic acid injection are also mediated via the melanocortin system [45], it is possible that the effect of APOE, APOA4 and APOA5 on food intake are mediated by a regulation of brain lipid metabolism rather than by a direct effect of the individual apolipoproteins themselves. This is further strengthened by the observation that LDL receptor knock out (*Ldlr*$^{-/-}$) mice become more obese compared to controls when fed a 60% HFD [71] and that the LDL receptor mediates, at least in part, the effect of APOE on obesity [72]. Interestingly, similar to *Apoa5*$^{-/-}$ mice, *Ldlr*$^{-/-}$ mice do not reduce their caloric intake when switched from a chow to a HFD [71].

In summary, we demonstrate that *Apoa5*$^{-/-}$ mice are hyperphagic and become more obese and insulin resistant on a HFD when compared to WT mice. Furthermore, we show that APOA5 reduces food intake after central administration. Peripheral injected APOA5 reduces food intake by 60% while ICV injection reduced food intake by 40%, suggesting that the effect of APOA5 on food intake may, at least in part, be mediated via a central mechanism. We propose that the low circulating levels of APOA5 seen in rodents and humans signify a satiety-related signaling function, possibly in addition to an effect of APOA5 on triglyceride hydrolysis.

Acknowledgments

This work was supported by grants from the Center of Medical Systems Biology (CMSB), the Netherlands Consortium for Systems Biology (NCSB) established by The Netherlands Genomics Initiative/Netherlands Organization for Scientific Research (NGI/NWO), and the Netherlands Diabetes Foundation (DFN2007.00.010 to PCN Rensen). PCN Rensen is Established Investigator of the Netherlands Heart Foundation (grant 2009T038). Furthermore, we would like to thank Rick Havinga (University Medical Center Groningen) for surgical and analytical assistance.

References

1 Hokanson JE, Austin MA. **1996**; Plasma triglyceride level is a risk factor for cardiovascular disease independent of high-density lipoprotein cholesterol level: a meta-analysis of population-based prospective studies. *Journal of cardiovascular risk* 3:213.

2 Austin MA, McKnight B *et al.* **2000**; Cardiovascular disease mortality in familial forms of hypertriglyceridemia: A 20-year prospective study. *Circulation* 101:2777.

3 Cullen P. **2000**; Evidence that triglycerides are an independent coronary heart disease risk factor. *American journal of cardiology* 86:943.

4 Ginsberg HN. **2000**; Insulin resistance and cardiovascular disease. *Journal of clinical investigation* 106:453.

5 Mooradian AD. **2009**; Dyslipidemia in type 2 diabetes mellitus. *Nature clinical practice endocrinology & metabolism* 5:150.

6 Chan DC, Barrett PH *et al.* **2004**; Lipoprotein transport in the metabolic syndrome: pathophysiological and interventional studies employing stable isotopy and modelling methods. *Clinical science* 107:233.

7 Forte TM, Shu X *et al.* **2009**; The ins (cell) and outs (plasma) of apolipoprotein A-V. *Journal of Lipid Research* 50 Suppl:S150.

8 Schaap FG, Rensen PC *et al.* **2004**; ApoAV reduces plasma triglycerides by inhibiting very low density lipoprotein-triglyceride (VLDL-TG) production and stimulating lipoprotein lipase-mediated VLDL-TG hydrolysis. *Journal of biological chemistry* 279:27941.

9 Merkel M, Loeffler B *et al.* **2005**; Apolipoprotein AV accelerates plasma hydrolysis of triglyceride-rich lipoproteins by interaction with proteoglycan-bound lipoprotein lipase. *Journal of biological chemistry* 280:21553.

10 Grosskopf I, Baroukh N *et al.* **2005**; Apolipoprotein A-V deficiency results in marked hypertriglyceridemia attributable to decreased lipolysis of triglyceride-rich lipoproteins and removal of their remnants. *Arteriosclerosis, Thrombosis, and Vascular Biology* 25:2573.

11 Kim JY, Kim OY *et al.* **2006**; Comparison of low-fat meal and high-fat meal on postprandial lipemic response in non-obese men according to the -1131T>C polymorphism of the apolipoprotein A5 (APOA5) gene (randomized cross-over design). *Journal of the American College of Nutrition* 25:340.

12 Moreno-Luna R, Perez-Jimenez F *et al.* **2007**; Two independent apolipoprotein A5 haplotypes modulate postprandial lipoprotein metabolism in a healthy Caucasian population. *Journal of clinical endocrinology and metabolism* 92:2280.

13 Pruneta-Deloche V, Ponsin G *et al.* **2005**; Postprandial increase of plasma apoAV concentrations in Type 2 diabetic patients. *Atherosclerosis* 181:403.

14 Chan DC, Watts GF *et al.* **2006**;

15 Ishihara M, Kujiraoka T *et al.* **2005**; A sandwich enzyme-linked immunosorbent assay for human plasma apolipoprotein A-V concentration. *Journal of Lipid Research* 46:2015.

16 O'Brien PJ, Alborn WE *et al.* **2005**; The novel apolipoprotein A5 is present in human serum, is associated with VLDL, HDL, and chylomicrons, and circulates at very low concentrations compared with other apolipoproteins. *Clinical chemistry* 51:351.

17 Weinberg RB, Cook VR *et al.* **2003**; Structure and interfacial properties of human apolipoprotein A-V. *Journal of biological chemistry* 278:34438.

18 Shu X, Ryan RO *et al.* **2008**; Intracellular lipid droplet targeting by apolipoprotein A-V requires the carboxyl-terminal segment. *Journal of Lipid Research* 49:1670.

19 Merkel M, Heeren J. **2005**; Give me A5 for lipoprotein hydrolysis! *Journal of clinical investigation* 115:2694.

20 Shu X, Nelbach L *et al.* **2010**; Apolipoprotein A-V associates with intrahepatic lipid droplets and influences triglyceride accumulation. *Biochimica et biophysica acta* 1801:605.

21 Zheng XY, Zhao SP *et al.* **2012**; Apolipoprotein A5 internalized by human adipocytes modulates cellular triglyceride content. *Biological chemistry* 393:161.

22 Yang L, Ding Y *et al.* **2012**; The proteomics of lipid droplets: structure, dynamics, and functions of the organelle conserved from bacteria to humans. *Journal of Lipid Research* 53:1245.

23 Smith CE, Tucker KL *et al.* **2010**; Apolipoprotein A5 and lipoprotein lipase interact to modulate anthropometric measures in Hispanics of Caribbean origin. *Obesity* 18:327.

24 Horvatovich K, Bokor S *et al.* **2011**; Haplotype analysis of the apolipoprotein A5 gene in obese pediatric patients. *International journal of pediatric obesity* 6:e318.

25 Chen ES, Furuya TK *et al.* **2010**; APOA1/A5 variants and haplotypes as a risk factor for obesity and better lipid profiles in a Brazilian Elderly Cohort. *Lipids* 45:511.

26 Hedley AA, Ogden CL *et al.* **2004**; Prevalence of overweight and obesity among US children, adolescents, and adults, 1999-2002. *JAMA* 291:2847.

27 Corella D, Lai CQ *et al.* **2007**; APOA5 gene variation modulates the effects of dietary fat intake on body mass index and obesity risk in the Framingham Heart Study. *Journal of molecular medicine* 85:119.

28 Sanchez-Moreno C, Ordovas JM *et al.* **2011**; APOA5 gene variation interacts with dietary fat intake to modulate obesity and circulating triglycerides in a Mediterranean population. *Journal of nutrition* 141:380.

29 Hishida A, Morita E *et al.* **2012**; Associations of apolipoprotein A5 (APOA5), glucokinase (GCK) and glucokinase regulatory protein (GCKR) polymorphisms and lifestyle factors with the risk of dyslipidemia and dysglycemia in Japanese - a cross-sectional data from the J-MICC Study. *Endocrine journal* 59:589.

30 Pennacchio LA, Olivier M *et al.* **2001**; An apolipoprotein influencing triglycerides in humans and mice revealed by comparative sequencing. *Science* 294:169.

31 Parker HM, Johnson NA *et al.* **2012**; Omega-3 supplementation and non-alcoholic fatty liver disease: A systematic review and meta-analysis. *Journal of hepatology* 56:944.

32 Bligh EG, Dyer WJ. **1959**; A rapid method of total lipid extraction and purification. *Canadian journal of biochemistry and physiology* 37:911.

33 Lichtenstein L, Berbee JF *et al.* **2007**; Angptl4 upregulates cholesterol synthesis in liver via inhibition of LPL- and HL-dependent hepatic cholesterol uptake. *Arteriosclerosis, Thrombosis, and Vascular Biology* 27:2420.

34 Tiller G, Fischer-Posovszky P *et al.* **2009**; Effects of TWEAK (TNF superfamily member 12) on differentiation, metabolism, and secretory function of human primary preadipocytes and adipocytes. *Endocrinology* 150:5373.

35 Peronnet F, Massicotte D. **1991**; Table of nonprotein respiratory quotient: an update. *Canadian journal of sport sciences* 16:23.

36 Gerritsen G, Rensen PC *et al.* **2005**; ApoC-III deficiency prevents hyperlipidemia induced by apoE overexpression. *Journal of Lipid Research* 46:1466.

37 van der Hoogt CC, Berbee JF *et al.* **2006**; Apolipoprotein CI causes hypertriglyceridemia independent of the very-low-density lipoprotein receptor and apolipoprotein CIII in mice. *Biochimica et biophysica acta* 1761:213.

38 Dhurandhar NV, Whigham LD *et al.* **2002**; Human adenovirus Ad-36 promotes weight gain in male rhesus and marmoset monkeys. *Journal of nutrition* 132:3155.

39 So PW, Herlihy AH *et al.* **2005**; Adiposity induced by adenovirus 5 inoculation. *International journal of obesity* 29:603.

40 Whigham LD, Israel BA *et al.* **2006**; Adipogenic potential of multiple human adenoviruses in vivo and in vitro in animals. *American journal of physiology. Regulatory, integrative and comparative physiology* 290:R190.

41 Rensen PC, Herijgers N *et al.* **1997**; Particle size determines the specificity of apolipoprotein E-containing triglyceride-rich emulsions for the LDL receptor versus hepatic remnant receptor in vivo. *Journal of Lipid Research* 38:1070.

42 Coomans CP, Biermasz NR *et al.* **2011**; Stimulatory effect of insulin on glucose uptake by muscle involves the central nervous system in insulin-sensitive mice. *Diabetes* 60:3132.

43 Coomans CP, Geerling JJ *et al.* **2011**; Circulating insulin stimulates fatty acid retention in white adipose tissue via KATP channel activation in the central nervous system only in insulin-sensitive mice. *Journal of Lipid Research* 52:1712.

44 van Dijk TH, Boer TS *et al.* **2003**; Quantification of hepatic carbohydrate metabolism in conscious mice using serial blood and urine spots. *Analytical biochemistry* 322:1.

45 Schwinkendorf DR, Tsatsos NG *et al.* **2011**; Effects of central administration of distinct fatty acids on hypothalamic neuropeptide expression and energy metabolism. *International journal of obesity* 35:336.

46 Ziotopoulou M, Mantzoros CS *et al.* **2000**; Differential expression of hypothalamic neuropeptides in the early phase of diet-induced obesity in mice. *American journal of physiology. Endocrinology and metabolism* 279:E838.

47 Wilcox G. **2005**; Insulin and Insulin Resistance. *Clinical biochemist reviews* 26:19.

48 Wolfgang MJ, Lane MD. **2006**; The role of hypothalamic malonyl-CoA in energy homeostasis. *Journal of biological chemistry* 281:37265.

49 Morgan K, Obici S *et al.* **2004**; Hypothalamic responses to long-chain fatty acids are nutritionally regulated. *Journal of biological chemistry* 279:31139.

50 Demeester N, Castro G *et al.* **2000**; Characterization and functional studies of lipoproteins, lipid transfer proteins, and lecithin:cholesterol acyltransferase in CSF of normal individuals and patients with Alzheimer's disease. *Journal of Lipid Research* 41:963.

51 Koch S, Donarski N *et al.* **2001**; Characterization of four lipoprotein classes in human cerebrospinal fluid. *Journal of Lipid Research* 42:1143.

52 Dehouck B, Fenart L *et al.* **1997**; A new function for the LDL receptor: transcytosis of LDL across the blood-brain barrier. *Journal of cell biology* 138:877.

53 Schutzer SE, Liu T *et al.* **2010**; Establishing the proteome of normal human cerebrospinal fluid. *PLoS ONE* 5:e10980.

54 Fujimoto K, Fukagawa K *et al.* **1993**; Suppression of food intake by apolipoprotein A-IV is mediated through the central nervous system in rats. *Journal of clinical investigation* 91:1830.

55 Shen L, Tso P *et al.* **2008**; Brain apolipoprotein E: an important regulator of food intake in rats. *Diabetes* 57:2092.

56 Gotoh K, Liu M *et al.* **2006**; Apolipoprotein A-IV interacts synergistically with melanocortins to reduce food intake. *American journal of physiology. Regulatory, integrative and comparative physiology* 290:R202.

57 Glatzle J, Darcel N *et al.* **2004**; Apolipoprotein A-IV stimulates duodenal vagal afferent activity to inhibit gastric motility via a CCK1 pathway. *AJP. Regulatory, integrative and comparative physiology* 287:R354.

58 Okumura T, Fukagawa K *et al.* **1994**; Intracisternal injection of apolipoprotein A-IV inhibits gastric secretion in pylorus-ligated conscious rats. *Gastroenterology* 107:1861.

59 van der Vliet HN, Sammels MG *et al.* **2001**; Apolipoprotein A-V: a novel apolipoprotein associated with an early phase of liver regeneration. *Journal of biological chemistry* 276:44512.

60 Genoux A, Dehondt H *et al.* **2005**; Transcriptional regulation of apolipoprotein A5 gene expression by the nuclear receptor RORalpha. *Arteriosclerosis, Thrombosis, and Vascular Biology* 25:1186.

61 Guardiola M, Alvaro A *et al.* **2012**; APOA5 gene expression in the human intestinal tissue and its response to in vitro exposure to fatty acid and fibrate. *Nutrition, metabolism, and cardiovascular diseases* 22:756.

62 Dichlberger A, Cogburn LA *et al.* **2007**; Avian apolipoprotein A-V binds to LDL receptor gene family members. *Journal of Lipid Research* 48:1451.

63 Mortazavi A, Williams BA *et al.* **2008**; Mapping and quantifying mammalian transcriptomes by RNA-Seq. *Nature methods* 5:621.

64 Shimogori T, Lee DA *et al.* **2010**; A genomic atlas of mouse hypothalamic development. *Nature neuroscience* 13:767.

65 Fox PT, Lancaster JL. **2002**; Opinion: Mapping context and content: the BrainMap model. *Nature reviews. Neuroscience* 3:319.

66 Candela P, Gosselet F *et al.* **2008**; Physiological pathway for low-density lipoproteins across the blood-brain barrier: transcytosis through brain capillary endothelial cells in vitro. *Endothelium* 15:254.

67 von EA, Rohrer L. **2009**; Transendothelial lipoprotein transport and regulation of endothelial permeability and integrity by lipoproteins. *Current opinion in lipidology* 20:197.

68 Mullier A, Bouret SG *et al.* **2010**; Differential distribution of tight junction proteins suggests a role for tanycytes in blood-hypothalamus barrier regulation in the adult mouse brain. *Journal of comparative neurology* 518:943.

69 McNay DE, Briancon N *et al.* **2012**; Remodeling of the arcuate nucleus energy-balance circuit is inhibited in obese mice. *Journal of clinical investigation* 122:142.

70 Ponten F, Schwenk JM *et al.* **2011**; The Human Protein Atlas as a proteomic resource for biomarker discovery. *Journal of internal medicine* 270:428.

71 Schreyer SA, Vick C *et al.* **2002**; LDL receptor but not apolipoprotein E deficiency increases diet-induced obesity and diabetes in mice. *American journal of physiology. Endocrinology and metabolism* 282:E207.

72 Karagiannides I, Abdou R *et al.* **2008**; Apolipoprotein E predisposes to obesity and related metabolic dysfunctions in mice. *FEBS journal* 275:4796.

Supplemental data

*Table S1: Indirect calorimetry data from long term HFD fed Apoa5$^{-/-}$ and WT controls. Data represent mean ± SD, *p < 0.05*

	Light period		Dark period	
	Apoa5$^{-/-}$	**WT**	**Apoa5$^{-/-}$**	**WT**
Respiratory exchange rate	0.798 ± 0.011	0.793 ± 0.011	0.847 ± 0.010	0.830 ± 0.010*
Energy expenditure (kcal/h)	0.583 ± 0.052	0.554 ± 0.031	0.657 ± 0.045	0.656 ± 0.026
Carbohydrate oxidation rate (mg/h)	54.3 ± 11.2	47.1 ± 5.7	88.7 ± 8.8	79.0 ± 8.3
Fat oxidation rate (mg/h)	40.0 ± 1.9	39.8 ± 3.6	34.2 ± 4.2	37.9 ± 2.2*
Activity (beam breaks)	118 ± 26	130 ± 36	284 ± 90	476 ± 140*

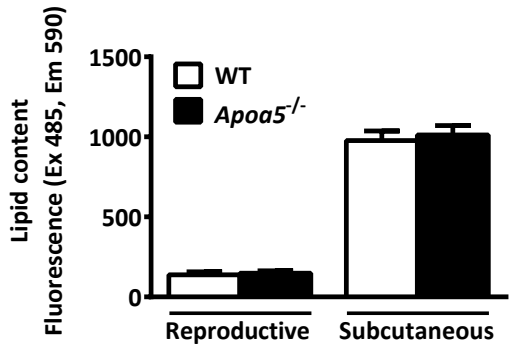

Figure S1: Data representing the differentiation capacity of adipocytes from reproductive and subcutaneous fat depots. Data represent mean ± SD.

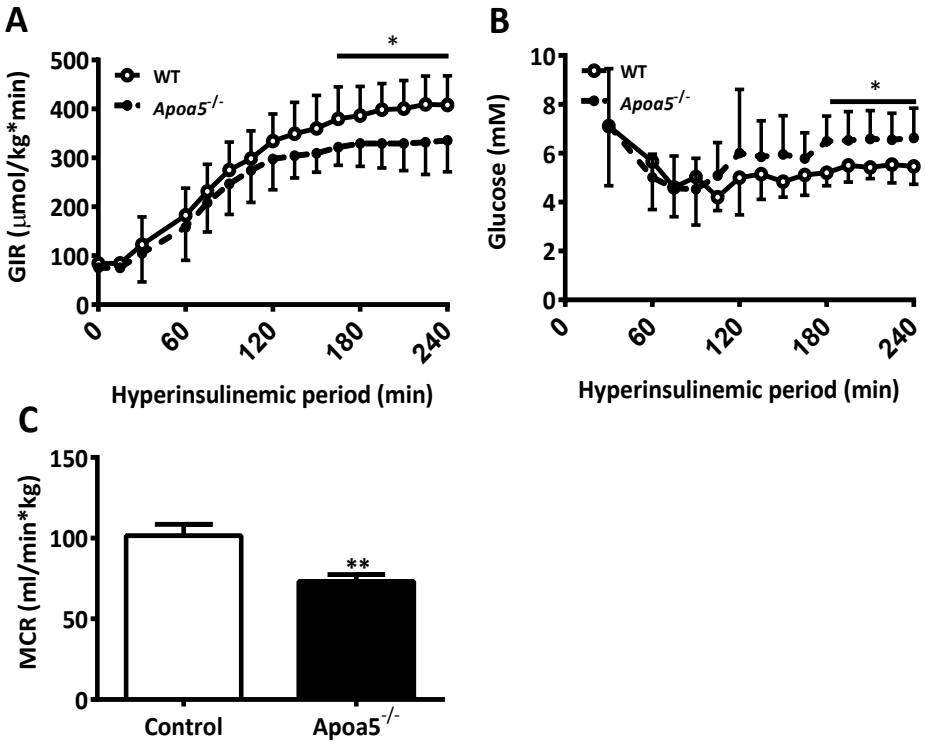

*Figure S2: Glucose infusion rates (A), plasma glucose levels (B) and hyperinsulinemic metabolic clearance rate (C) during the hyperinsulinemic-euglycemic clamp analysis of Apoa5$^{-/-}$ and WT represent mean ± SD, *p < 0.05, **p < 0.01.*

4

Long term niacin treatment induces insulin resistance and adrenergic responsiveness in adipocytes by adaptive down-regulation of phosphodiesterase 3B

Mattijs M. Heemskerk*, Sjoerd A.A. van den Berg*, Amanda C.M. Pronk, Jan-Bert van Klinken, Mariëtte R. Boon, Louis M. Havekes, Patrick C.N. Rensen, Ko Willems van Dijk, Vanessa van Harmelen

[1]Both authors contributed equally

AJP Endocrinology & Metabolism **2014**, 306(7): 808-813

Abstract

The lipid lowering effect of niacin has been attributed to the inhibition of cAMP production in adipocytes, thereby inhibiting intracellular lipolysis and release of non-esterified fatty acids (NEFA) to the circulation. However, long term niacin treatment leads to a normalization of plasma NEFA levels and induces insulin resistance, for which the underlying mechanisms are poorly understood. The current study addressed the effects of long term niacin treatment on insulin-mediated inhibition of adipocyte lipolysis and focused on the regulation of cAMP levels. APOE*3-Leiden.CETP transgenic mice treated with niacin for 15 weeks were subjected to an insulin tolerance test and showed whole body insulin resistance. Similarly, adipocytes isolated from niacin treated mice were insulin resistant and, interestingly, exhibited an increased response to cAMP stimulation by 8Br-cAMP, β_1 and β_2-adrenergic stimulation. Gene expression analysis of the insulin and β-adrenergic pathways in adipose tissue indicated that all genes were down-regulated, including the gene encoding the cAMP degrading enzyme phosphodiesterase 3B (PDE3B). In line with this, we showed that insulin induced a lower PDE3B response in adipocytes isolated from niacin treated mice. Inhibiting PDE3B with cilostazol increased lipolytic responsiveness to cAMP stimulation in adipocytes. These data show that long term niacin treatment leads to a down-regulation of PDE3B in adipocytes which could explain part of the observed insulin resistance and the increased responsiveness to cAMP stimulation.

Introduction

Niacin, also known as vitamin B_3, is required for the synthesis of the co-factor nicotinamide adenine dinucleotide (NAD^+) and is therefore essential for oxidative phosphorylation in energy metabolism [1]. It has been used for more than 50 years for the treatment of dyslipidemias, as it decreases plasma triglycerides, LDL-cholesterol and hepatic VLDL triglyceride production [2], in addition to increasing HDL-cholesterol. Supplementation with niacin was shown to decrease risk of cardiovascular disease and atherosclerosis in dyslipidemic humans [3] and in dyslipidemic mouse models [4], using the APOE*3-Leiden.cholesteryl ester transfer protein (CETP) transgenic female mouse.

The molecular mechanism by which niacin conveys its lipid-lowering effects is mostly unknown. The receptor for niacin, HCA_2 (formerly known as GPR109A) has been shown to play an important role in acute anti-lipolytic effects [5, 6], but is not required for the long term lipid-lowering effects [6]. This receptor is expressed mostly in spleen, immune cells and adipose tissue [7] where binding of niacin leads to the release of a Gα-inhibitory subunit that inhibits production of the secondary messenger cyclic AMP by adenyl cyclase (AC). Niacin is known to inhibit lipolysis in adipocytes via this reduction of cAMP [8], which leads to a reduced protein kinase A (PKA) activation and thus less phosphorylation and activation of the lipolytic enzyme hormone sensitive lipase (HSL) [9]. By inhibiting lipolysis, less NEFAs are released by adipocytes thus making less substrate available for VLDL-Triglyceride (TG) production in the liver. Niacin may therefore lower lipid levels via its anti-lipolytic effect. However, during niacin administration the initial drop in NEFA and glycerol is followed within hours by a rebound and normalization of NEFA and glycerol levels and adipose tissue lipolysis rates [2, 6, 10-12].

In addition, long term niacin administration leads to insulin resistance in liver, adipose and muscle tissue [13, 14] for which the underlying mechanisms are poorly understood. In adipocytes, binding of insulin to its receptor leads to phosphorylation and activation of protein kinase B (PKB/Akt) and phosphodiesterase 3B, breaking down cAMP which in turn reduces NEFA release from the cells.

We hypothesized that long term niacin treatment modulates insulin signaling by acting at the level of PDE3B. Oh *et al.* [10] have previously shown that 24h treatment with niacin induces insulin resistance and reduces expression of PDE3B in adipose tissue, hinting towards a possible role for PDE3B. In this study we functionally tested in APOE*3-Leiden.CETP transgenic female mice whether long term niacin-induced down regulation of the enzyme PDE3B would lead to less PDE3B activity when stimulated by insulin, which would explain (part of) the observed insulin resistance in adipose tissue.

Materials and Methods

Animal model

In contrast to wildtype mice, female APOE*3-Leiden.CETP mice [15] have a human-like lipoprotein profile, which makes them exquisitely suited to test hypolipidemic drugs, such as niacin [4]. This mouse model was bred at the Leiden University Medical Center. At age 15 ± 1 week, mice were fed a western type diet (Diet T with 0.1% cholesterol, which consisted of 17 kcal% protein, 43 kcal% carbohydrate and 41 kcal% fat; AB Diets, Woerden, the Netherlands) with or without niacin (0.3% w/w, Sigma Aldrich, St Louis, MO, USA). Body weight was registered weekly. Animals were housed in a controlled environment (21°C, 40-50% humidity) with a daily 12h photoperiod (07h00-19h00). Food and tap water were available *ad libitum* during the whole experiment. All experiments were performed after a 15 week dietary intervention period. All animal experiments were performed in accordance with the regulations of Dutch law on animal welfare. The institutional ethics committee for animal procedures from the Leiden University Medical Center, Leiden, The Netherlands approved the protocols.

Intraperitoneal insulin tolerance test

Food was withdrawn from all animals at 08h00 for a period of 6.5 hours. Subsequently, all animals received a single intra-peritoneal (*ip*) injection with insulin (0.2 U/kg, Novo-Nordisk, Bagsværd, Denmark) and blood samples were taken every 30 min for a period of 2 hours. Blood samples were taken from the tail tip into chilled paraoxon-coated capillaries and placed on ice to prevent *ex vivo* lipolysis.

Organ collection

All animals were sacrificed and organs were collected in the fed state between 08h00 and 9h30 unless otherwise indicated. Blood was collected by cardiac punction and plasma was collected after centrifugation. Fresh subcutaneous (sWAT), gonadal (gWAT) and visceral (vWAT) white adipose tissue were harvested and used for determination of morphometry and lipolysis experiments as described below. In addition, a portion of the gWAT was frozen for qPCR and cAMP measurement. Liver and adrenal glands were harvested quantitatively and weighed prior to freezing. All tissues were stored at -80°C prior to further analysis.

Plasma and liver parameters

Commercially available kits were used to determine plasma levels of triglycerides (1488872, Roche Molecular Biochemicals, Indianapolis, IL, USA), total cholesterol (236691 Roche

Molecular Biochemicals), phospholipids (Instruchemie, Delftzijl, The Netherlands), NEFAs (Wako Chemicals, Neuss, Germany), glucose (Accucheck, Roche, The Netherlands) and insulin (Crystal Chem Inc., Downers Grove, IL, USA), according to the manufacturer's instructions.

Adipocyte morphometry

Adipose tissue from the gWAT, sWAT and vWAT were minced and digested in 0.5 g/l collagenase in HEPES buffer (pH 7.4) with 20 g/l of dialyzed bovine serum albumin (BSA, fraction V, Sigma Aldrich) for 1 h at 37°C. The disaggregated WAT was filtered through a nylon mesh with a pore size of 236 µm. For the isolation of mature adipocytes, cells were obtained from the surface of the filtrate and washed several times. Cell size and volume of mature adipocytes was determined from micrographs (± 1000 cells/WAT sample) using image analysis software that was developed in-house in MATLAB (MathWorks, Natick, MA, USA).

Lipolysis experiments in isolated adipocytes

Adipocytes were incubated in DMEM/F12 with 2% (w/w) BSA in 96 well plates with ~10,000 adipocytes in 200 µl per well in the presence of #1) No additional reagents, #2) 10^{-3} M of the PDE3B sensitive cAMP analogue 8Bromo-cAMP, #3) 10^{-3} M 8Br-cAMP + 10^{-10} M insulin (Novo-Nordisk), #4) 10^{-6} M of the selective β_2-adrenergic agonist terbutaline, #5) 10^{-6} M of the selective β_1-adrenergic agonist dobutamine. The wells of the adipocytes from niacin treated mice contained 10^{-6} M niacin, while control adipocyte medium did not contain niacin. Basal lipolysis rates were determined in incubations without these reagents. PDE3B responsiveness in adipocytes from control and niacin treated mice was assayed by lipolysis assay using the selective PDE3 inhibitor cilostazol (all obtained from Sigma Aldrich). under the following additional conditions: #6-8) 10^{-6} or 10^{-5} or 10^{-4} M cilostazol, #9-11) 10^{-3} M 8Br-cAMP + 10^{-6} or 10^{-5} or 10^{-4} M cilostazol. The adipocytes were incubated for two hours at 37°C, after which 100 µl of lipolysis assay medium was frozen at -20°C. At the day of analysis, 10 µl of lipolysis assay medium was mixed with 100 µl of Free Glycerol Reagent (F6428, Sigma Aldrich) and 0.5µl Amplex UltraRed Reagent (A36006, Invitrogen, Carlsbad, CA, USA). After 10 min of incubation in the dark, the fluorescence was excited at 530 nm and measured at 590 nm on a Fluorometer (SpectraMAX Gemini, Molecular Devices, CA, USA).

Adipose tissue cAMP measurement

cAMP concentrations were measured in 50 mg of gWAT, using the cAMP direct immunoassay kit (Biovision, Inc, Milpitas, CA, USA).

Quantitative PCR

RNA was isolated from gWAT using the Nucleospin RNA/Protein kit (MACHEREY-NAGEL GmbH & Co. KG, Düren, Germany). Subsequently, 1µg of RNA was used for cDNA synthesis by iScript (BioRad, Hercules, CA, USA), which was purified by the Nucleospin Gel and PCR clean-up kit (Machery Nagel). Real-Time PCR was carried out on the IQ5 PCR machine (BioRad) using the Sensimix SYBR Green RT-PCR mix (Quantace, London, UK) and QuantiTect SYBR Green RT-PCR mix (Qiagen, Venlo, the Netherlands). Target mRNA levels were normalized to glyceraldehyde-3-phosphate dehydrogenase (*Gapdh*) mRNA levels. Primer sequences are listed in table 1.

Table 1: Mouse qPCR primer sequences all with an optimal temperature at 60°C.

Gene	Forward primers	Reverse primers
Hsl	AGACACCAGCCAACGGATAC	ATCACCCTCGAAGAAGAGCA
Insr	ATGGGCTTCGGGAGAGGAT	GGATGTCCATACCAGGGCAC
Irs1	CGATGGCTTCTCAGACGTG	CAGCCCGCTTGTTGATGTTG
Pde3b	AAAGCGCAGCCGGTTACTAT	CACCACTGCTTCAAGTCCCAG
Adrb1	TCGCTACCAGAGTTTGCT	GGCACGTAGAAGGAGACGAC
Adrb2	AACGACAGCGACTTCTTGCT	GCACACGCCAAGGAGATTAT
Adrb3	TGAAACAGCAGACAGGGACA	AGTCTGTCAGCTTCCCTCCA
Arrb1	CCCGCTTTCCCAGGTAGAC	AAGGGACACGAGTGTTCAAGA
Gapdh	GGGGCTGGCATTGCTCTCAA	TTGCTCAGTGTCCTTGCTGGGG

Statistics

All data in figures are represented as mean ± standard error of the mean. The mean of all data was tested between groups for differences by unpaired T-Test for normally distributed data. A repeated measures ANOVA was used when indicated. Threshold for significance was set at 5%. Tests were performed using GraphPad Prism version 5.00 for Windows, GraphPad Software, San Diego, CA, USA).

Results

Niacin does not alter body composition

We have applied a humanized mouse model, which has previously been shown [4] to react to niacin on plasma lipid parameters, atherosclerosis and body weight in a similar manner as dyslipidemic humans. After fifteen weeks of niacin treatment body weight (Table 2) and weight gain (not shown) did not differ between the niacin treated and control mice. Adipose tissue depots were similar in weight, whereas the adrenal glands were heavier after niacin treatment (Table 2). Liver cholesterol content was significantly lower in niacin treated mice (Table 2).

Niacin lowers plasma lipids, but increases fasting glucose and insulin

Long term niacin treatment resulted in the expected decrease of non-fasting plasma total cholesterol, triglycerides and phospholipids (Table 2). In contrast to short term niacin treatment, long term niacin treatment did not lower NEFA levels [2], but slightly lowered glycerol levels as compared to control mice (Table 2). Glucose and insulin concentrations were significantly higher after niacin treatment (Table 2), suggesting insulin resistance.

*Table 2: Body composition, liver and plasma metabolic parameters and adipocyte sizes of mice treated 15 weeks with or without 0.3% niacin in the diet. Fasting values were determined after 6.5h without feeding from 08h00 until 14h30. *p≤0.05, **p≤0.01.*

	Control	Niacin		
	Mean±SD	Mean±SD	N	p-value
Body composition				
Body weight (g)	28.9±2.6	29.3±5.3	13	NS
Gonadal adipose tissue (g)	0.48±0.19	0.54±0.34	13	NS
Visceral adipose tissue (g)	0.40±0.11	0.48±0.28	13	NS
Subcutaneous adipose tissue (g)	0.32±0.09	0.39±0.23	13	NS
Adrenal glands (mg)	3.9±1.2	5.1±1.0	13	*
Liver (g)	1.44±0.34	1.28±0.24	13	NS
Liver lipids				
Cholesterol (nmol/mg protein)	163±67	96±29	13	**
Triglycerides (nmol/mg protein)	851±382	651±213	13	0.11
Phospholipids (nmol/mg protein)	165±42	148±23	13	NS
Plasma lipids, glucose and insulin				
Fed state cholesterol (mM)	13.0±4.9	5.1±1.4	13	**
Fed state triglycerides (mM)	4.11±2.66	0.94±0.19	13	**
Fed state phospholipids (mM)	4.02±0.88	2.94±0.53	13	**
Fasting NEFA (mM)	1.1±0.3	1.0±0.2	12	NS
Fasting glycerol (mM)	0.92±0.29	0.74±0.14	12	0.08
Fasting glucose (mM)	9.1+0.9	10.6+0.9	12	*
Fasting insulin (ng/ml)	0.49±0.21	0.82±0.39	12	*
Adipocyte mean volume				
Gonadal (pl)	342±98	334±140	13	NS
Visceral (pl)	152±39	190±97	13	NS
Subcutaneous (pl)	167±43	158±60	13	NS

Niacin induces insulin resistance in vivo

To verify the development of *in vivo* insulin resistance upon long term niacin treatment we performed an insulin tolerance test. Insulin stimulates glucose uptake in muscle and adipose tissue and suppresses WAT glycerol release. After an *ip* injection of insulin, blood was drawn and at indicated times glucose (Fig. 1A), glycerol (Fig. 1B) and insulin (Fig. 1C) were measured. Glucose levels dropped and insulin levels rose in both groups. As glucose levels were already higher due to niacin treatment at t=0, the percentage change in glucose, glycerol and insulin levels from the t=0 values were calculated (data not shown). A repeated measures ANOVA of the percentage change in insulin values indicated no significant effect of niacin, while a similar analysis of glucose values showed significant treatment differences. At

60 min, the percentage change in glucose was smaller for niacin treated animals, indicating insulin resistance on a whole body level. Insulin induced a decrease in glycerol levels in the control group, but failed to do so in the niacin treated group, indicating adipose tissue insulin resistance.

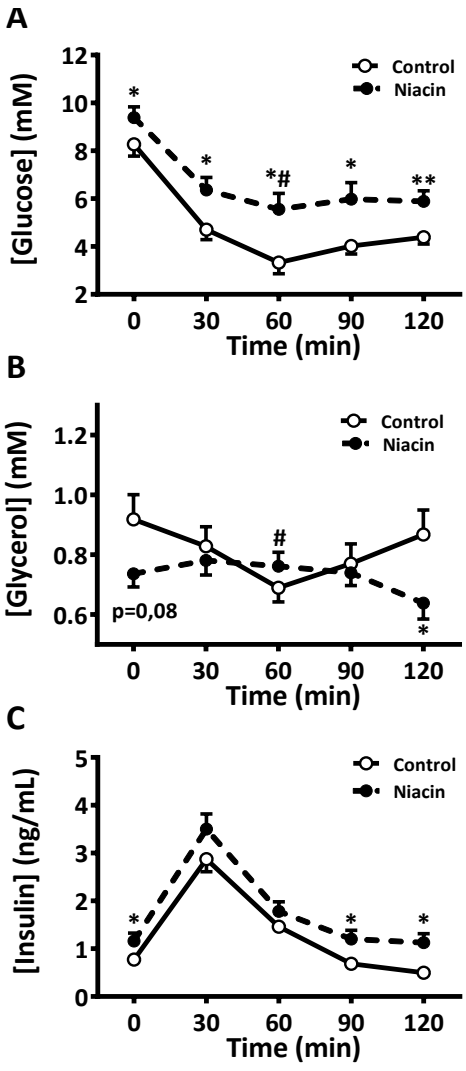

*Figure 1: Intraperitoneal insulin tolerance tests of mice treated with or without niacin. After 0.2U/kg insulin injection A) glucose, B) glycerol and C) insulin concentrations were measured during 2 h. All values are means±SEM. N=12 mice per group, *p≤0.05 compared to control treatment, **p≤0.01 compared to niacin treatment, #p≤0.05 compared to niacin treatment, when calculated as percentage change from t=0 level.*

Niacin reduces the anti-lipolytic effect of insulin in isolated adipocytes

To study whether long term niacin treatment also alters the response to insulin at the level of adipocyte lipolysis, we isolated gWAT adipocytes from control and niacin treated mice and performed an *ex vivo* lipolysis assay. Basal lipolysis (i.e. unstimulated lipolysis) did not differ between the niacin treated and control mice (Fig. 2A). 8Br-cAMP stimulated glycerol release was higher in adipocytes from niacin treated mice compared to control treatment. The anti-lipolytic effect of insulin, reflected by the percentage lipolysis suppression by insulin of 8Br-cAMP stimulated lipolysis, was significantly smaller in the niacin treated adipocytes (Fig. 2B). This implies a reduced insulin response of adipocytes from niacin treated mice.

Niacin increases the lipolytic effect of β-adrenergic stimulation in isolated adipocytes

Similar to testing the response of adipocyte lipolysis to inhibition by insulin, β_1 and β_2-adrenergic stimulation of gonadal adipocyte lipolysis was tested. Gonadal adipocytes from niacin treated mice exhibited a greater response to both the β_1-agonist dobutamine and the β_2-agonist terbutaline, as well as the secondary lipolytic messenger 8Br-cAMP (Fig 2A). These data show that lipolysis in niacin treated adipocytes is more responsive to β-adrenergic and cAMP stimulation.

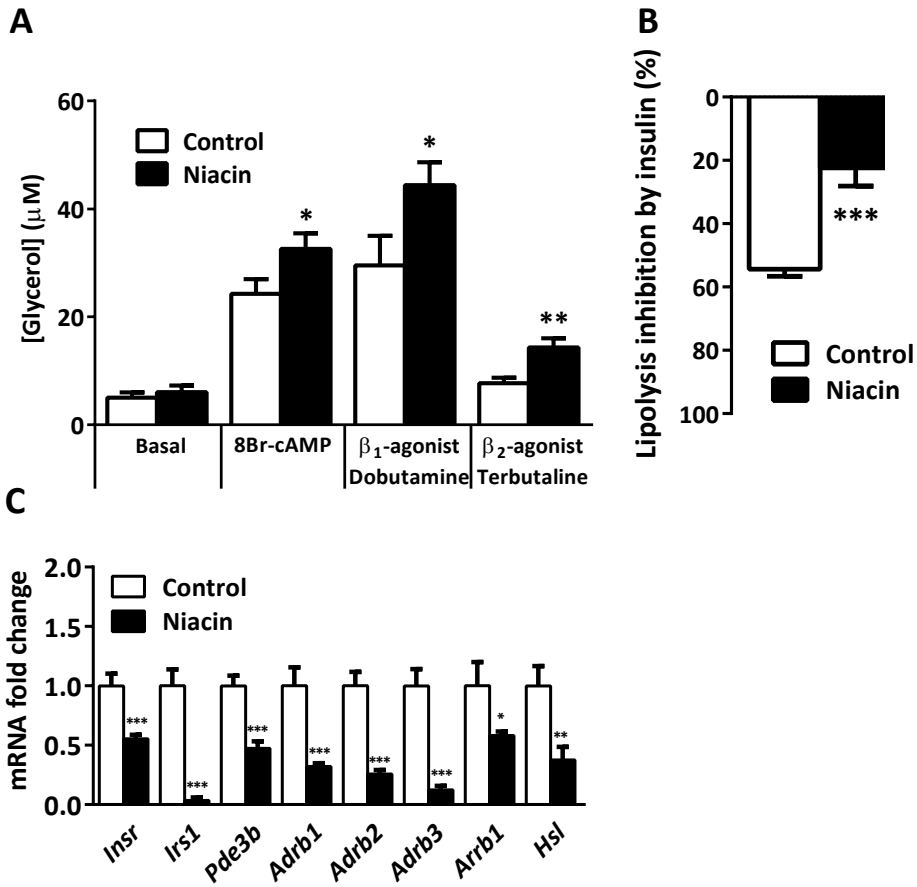

Figure 2: Isolated adipocyte responsiveness to lipolysis stimulation and inhibition. A) Glycerol concentration in ex vivo gonadal adipocyte medium after 2 h incubation with different reagents. B) Suppression of gonadal adipocyte lipolysis by 10^{-10} M insulin (100 – 100(8Br-cAMP+Ins / 8Br-cAMP)). C) gWAT mRNA fold change of niacin treatment compared to control treatment. Insr (Insulin receptor), Irs1 (Insulin receptor substrate 1), Pde3b (Phosphodiesterase 3B), Adrb1,2,3 (β-Adrenoceptor 1,2,3), Arrb1 (β-arrestin 1), Hsl (Hormone sensitive lipase). All values are means±SEM. N=13 mice per group, *p≤0.05, **p≤0.01, ***p≤0.001.*

Niacin down-regulates genes involved in both the insulin and the β-adrenergic signaling pathways that regulate lipolysis

Expression of genes involved in the insulin and/or β-adrenergic pathways, were analyzed by qPCR in gWAT. The niacin treated adipose tissues showed a down-regulation of the insulin signaling cascade: mRNA levels of the insulin receptor (*Insr*), insulin receptor substrate-1 (*Irs1*) and *Pde3b* were down-regulated by 45%, 97% and 53%, respectively, compared to control (Fig. 2C). Also mRNA levels of the lipolytic enzyme hormone sensitive lipase (*Hsl*) were down-regulated (62%) in the niacin treated mice. Furthermore, all β-adrenergic receptor genes were significantly down-regulated. The β_1-adrenoceptor (*Adrb1*) was down-regulated

by 68%, *Adrb2* by 74% and *Adrb3* by 88%. The intracellular adrenergic adaptor β-Arrestin1 (*Arrb1*) was also down-regulated by 42%. These data indicate a decreased gene expression of the insulin and β-adrenergic receptors, and their post-receptor signaling pathways to lipolysis.

Niacin treated adipocytes display less PDE3B capacity

As the down-regulation of the β-adrenoceptors was not consistent with the observed increased β-adrenergic response, we investigated whether the increased β-adrenergic response was the result of post-receptor signaling changes. Therefore we first tested the basal levels of the lipolytic post-receptor mediator cAMP. The cAMP concentration of non-fasted gWAT showed no difference after long term niacin treatment (control: 19.9±6.5, niacin: 21.6±8.2 pmol/g adipose tissue, p=0.63).

We then focused on the post receptor enzyme PDE3B, catalyzing cAMP hydrolysis, whose gene expression was down-regulated after niacin treatment. PDE3B is the most predominant PDE3 isoform in adipose tissue [16] which is activated by insulin. The role of PDE3B in lipolysis was characterized in gWAT adipocytes using the PDE3 selective inhibitor cilostazol (Fig 3). Adding cilostazol to unstimulated adipocytes in basal medium did not increase lipolysis, indicating that under basal conditions PDE3B was not active. However, when 8Br-cAMP stimulated adipocytes were subjected to increasing concentrations of cilostazol, there was a sharp rise in lipolysis. Therefore, inhibiting PDE3B capacity can increase the responsiveness to cAMP stimulation, e.g. by catecholamines. Futhermore, lipolysis of adipocytes from niacin treated mice was stimulated to a lesser degree by 10^{-4} M cilostazol then control treated mice. A repeated measures ANOVA indicated a significant interaction ($p<0.0001$) between the concentration of cilostazol and the 8Br-cAMP stimulated control/niacin adipocytes. This implied a lower responsiveness (slope) of PDE3B to its inhibitor in adipocytes from niacin treated mice, independent of insulin signaling.

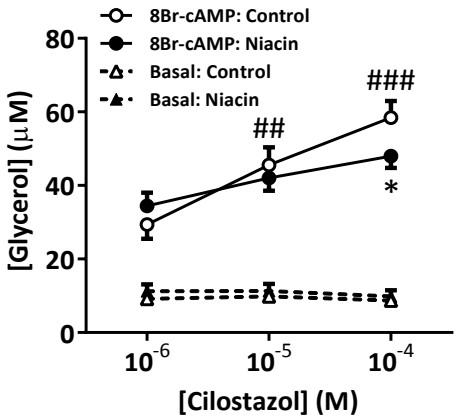

*Figure 3: PDE3B capacity of isolated adipocytes after lipolysis stimulation and inhibition. Glycerol concentration in ex vivo gonadal adipocyte medium after 2 h incubation with PDE3B inhibitor cilostazol. A) Responsiveness of basal and 8Br-cAMP stimulated lipolysis to PDE3B inhibition by different cilostazol concentrations. B) PDE3B capacity as glycerol release after PDE3B activation by 10^{-10} M Insulin compared to PDE3B inhibition by 10^{-4} M cilostazol (Δ = 8Br-cAMP+Ins+Cilo - 8Br-cAMP+Ins) tested in ex vivo adipocytes from control and niacin treated mice. All values are means±SEM. N=10 mice per group, *p≤0.05, **p≤0.01 compared to niacin treatment, ##p≤0.01, ###p≤0.001 compared to Cilo 10^{-6} M level.*

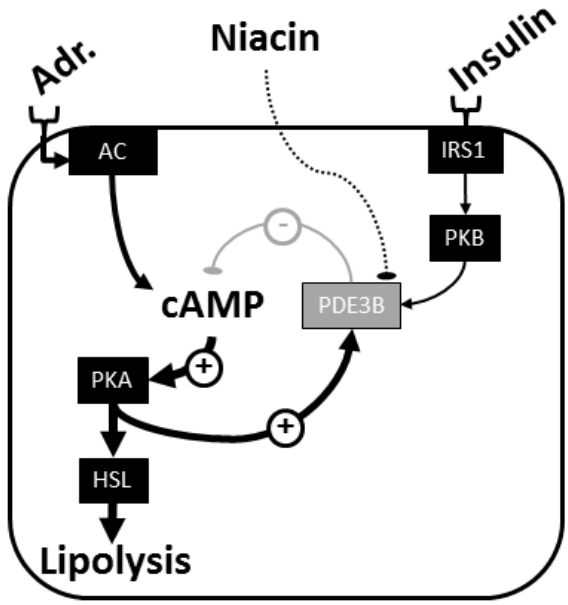

Figure 4: Molecular mechanism of niacin action in adipocytes. Adrenergic stimulation of adipocytes will activate AC to produce cAMP. This rise in cAMP will both activate lipolysis via PKA & HSL and will activate PDE3B leading to a negative feedback loop degrading cAMP. Insulin will activate IRS1 and PKB, also leading to PDE3B activation, thereby inhibiting lipolysis. Prolonged niacin leads to down regulation of the β-adrenergic and insulin pathway, but concomitantly to a down-regulation of PDE3B. Whether this is a direct or indirect effect is unknown. The diminished PDE3B capacity dampens the negative feedback loop, resulting in an increased responsiveness to adrenergic and cAMP stimulation of lipolysis, as well as decreased responsiveness to insulin inhibition of lipolysis.

Discussion

The present paper shows that long term niacin induces insulin resistance in APOE*3-Leiden. CETP female transgenic mice fed a Western type diet. The insulin resistance by niacin has been shown before in dyslipidemic patients and is confirmed in our humanized mouse model, both *in vivo* on glucose and glycerol metabolism and *ex vivo* in isolated adipocytes on lipolysis. The niacin induced insulin resistance was associated with a reduction in the expression of key insulin signaling genes (i.e. *Insr* and *Irs1*) in WAT. This indicates that niacin down-regulates the insulin signaling pathway at the transcriptional level which led to the reduced anti-lipolytic effect of insulin. In contrast, gene expression of all β-adrenergic receptors, as well as *Hsl* and *Arrb1* were down-regulated in white adipose tissue, while an increased adrenergic lipolytic effect was observed. This might be due to desensitization after niacin-induced prolonged stress [10, 17-20]. Prolonged stress leads to increased adrenal gland size [21], also evident in our study. Decreased β-adrenoceptor gene expression combined with an increased β-adrenergic responsiveness suggests that the effects of niacin on β-adrenergic stimulation are due to post-receptor signaling mechanisms that enhance cAMP stimulation and thus lipolysis.

Interestingly, 8Br-cAMP, which acts at the post-receptor level, induced lipolysis to a higher extent in niacin treated mice, which strengthens the hypothesis that a post-receptor signaling mechanism is affected by niacin. The adipocyte lipolysis assays were not confounded by a difference in weight of the gWAT depots, nor in adipocyte mean cell volume (Table 1), which in itself might change responsiveness to reagents. It was shown by Oh *et al.* [10] that 24 h niacin infusion lowered the expression level of *Pde3b* in gWAT to a similar extent (-57%) as compared to our study (-53%). PDE3B regulates intracellular cAMP levels and is the key enzyme involved in the anti-lipolytic action of insulin. Moreover, by modulating cAMP levels PDE3B may interact with β-adrenergic signaling. Oh and co-workers suggested that the reduction in *Pde3b* may be an indirect effect of niacin, that serves as a counter-regulatory mechanism to increase the cellular cAMP/AMP ratio in order to maintain basal lipolytic rate. In the current paper we show that the reduction of expression of *Pde3b* in adipose tissue by niacin is accompanied by a reduced anti-lipolytic effect of insulin. We further show by using the selective PDE3 inhibitor cilostazol in an adipocyte lipolysis assay that the PDE3B responsiveness in adipocytes isolated from long term niacin treated mice was diminished. We also showed that cilostazol increased 8Br-cAMP-stimulated lipolysis in a concentration dependent manner in adipocytes from control mice, whereas it did not have an effect on unstimulated cells.

These data suggest that in adipocytes PDE3B will only degrade cAMP when the lipolytic cascade is stimulated. These observations could explain the increased responsiveness to β-adrenergic or 8Br-cAMP stimulation in niacin treated adipocytes. In the unstimulated basal condition PDE3B was not activated, which corresponds to the unchanged adipocyte lipolysis rate and basal adipose tissue cAMP levels between control and niacin treated mice.

In line with this, plasma NEFA levels did not differ between the groups at the start of the *ip* insulin tolerance test, indicating that *in vivo* adipose lipolysis was also similar between the groups, despite decreased *Pde3b* expression.

We propose a molecular mechanism for long term niacin treatment occurring in adipocytes (Fig. 4): Lipolysis is regulated by hormone sensitive lipase, which is controlled by cAMP levels. Production of cAMP can be stimulated via β-adrenergic pathways or inhibited by PDE3B which is activated by the insulin signaling cascade. PKA is activated by cAMP, which can activate PDE3B creating a negative feedback loop [22–24] (Fig. 4). Long term niacin treatment leads to down-regulation of PDE3B (Fig. 4). This down-regulation of PDE3B is also accompanied by a down-regulation of the rest of the insulin signaling pathway, leading to reduced insulin responsiveness in the adipocyte. In addition, as the PDE3B responsiveness is smaller in adipocytes from niacin treated mice, stimulated cAMP levels in the niacin treated mice -after b-adrenergic stimulation- will be degraded to a lesser extent, leading to a net higher lipolysis.

In this study we have focused on adipocyte insulin response after long term niacin treatment. But the sequence of events leading up to adipocyte insulin resistance and decreased *Pde3b* expression remain unclear, as does the possible role of adipocyte insulin resistance in the development of whole body insulin resistance. Moreover niacin has been shown to increase plasma adiponectin, an important insulin sensitizing hormone. The increase in adiponectin plasma levels after niacin treatment were shown to correlate to the decrease in insulin resistance [25], indicating a possible compensatory insulin sensitizing effect. We however did not detect an increase of adiponectin gene expression in gWAT after niacin treatment (data not shown). Whether niacin acutely interferes with the insulin receptor cascade remains to be investigated, although PDE3B capacity was not affected in control adipocytes exposed to niacin for two hours (data not shown). Choi *et al.* have shown a reduced phosphorylation of PKB/Akt in adipose tissue after 1.5h infusion of niacin [26], which leads to a lower insulin response. Niacin thus seems to induce decreased adipocyte insulin responsiveness via more than one mechanism.

In conclusion, long term niacin treatment resulted in insulin resistance and increased β-adrenergic responsiveness which may in part be explained by a niacin induced down-regulation of PDE3B.

Acknowledgements

We thank S.J.M. van der Tuin for discussions on gene expression analysis. This work was supported by grants from the Center of Medical Systems Biology (CMSB), the Netherlands Consortium for Systems Biology (NCSB) established by The Netherlands Genomics Initiative/ Netherlands Organization for Scientific Research (NGI/NWO). MRB is supported by the Board of Directors of the Leiden University Medical Center (LUMC). PCNR is Established Investigator of the Netherlands Heart Foundation (NHS2009T038).

References

1 Jacobson EL, Kim H *et al.* **2012**; Niacin: vitamin and antidyslipidemic drug. *Sub-cellular biochemistry* 56:37.

2 Wang W, Basinger A *et al.* **2001**; Effect of nicotinic acid administration on hepatic very low density lipoprotein-triglyceride production. *American journal of physiology. Endocrinology and metabolism* 280:E540.

3 Bruckert E, Labreuche J *et al.* **2010**; Meta-analysis of the effect of nicotinic acid alone or in combination on cardiovascular events and atherosclerosis. *Atherosclerosis* 210:353.

4 van der Hoorn JWA, de Haan W *et al.* **2008**; Niacin Increases HDL by Reducing Hepatic Expression and Plasma Levels of Cholesteryl Ester Transfer Protein in APOE*3Leiden. CETP Mice. *Arteriosclerosis, Thrombosis, and Vascular Biology* 28:2016.

5 Tunaru S, Kero J *et al.* **2003**; PUMA-G and HM74 are receptors for nicotinic acid and mediate its anti-lipolytic effect. *Nature medicine* 9:352.

6 Lauring B, Taggart AKP *et al.* **2012**; Niacin Lipid Efficacy Is Independent of Both the Niacin Receptor GPR109A and Free Fatty Acid Suppression. *Science translational medicine* 4:148ra115.

7 Soga T, Kamohara M *et al.* **2003**; Molecular identification of nicotinic acid receptor. *Biochemical and biophysical research communications* 303:364.

8 Carlson LA, Orë L. **1965**; Inhibition of the mobilization of free fatty acids from adipose tissue*. *Annals of the New York Academy of Sciences* 131:119.

9 Holm C. **2003**; Molecular mechanisms regulating hormone-sensitive lipase and lipolysis. *Biochemical Society transactions* 31:1120.

10 Oh YT, Oh K-S *et al.* **2011**; Continuous 24-h Nicotinic Acid Infusion in Rats Causes FFA Rebound and Insulin Resistance by Altering Gene Expression and Basal Lipolysis in Adipose Tissue. *American journal of physiology. Endocrinology and metabolism* 300:1012.

11 Wang W, Basinger A *et al.* **2000**; Effects of nicotinic acid on fatty acid kinetics, fuel selection, and pathways of glucose production in women. *American journal of physiology. Endocrinology and metabolism* 279:E50.

12 Chen X, Iqbal N *et al.* **1999**; The effects of free fatty acids on gluconeogenesis and glycogenolysis in normal subjects. *Journal of clinical investigation* 103:365.

13 Fabbrini E, Mohammed BS *et al.* **2010**; Effect of Fenofibrate and Niacin on Intrahepatic Triglyceride Content, Very Low-Density Lipoprotein Kinetics, and Insulin Action in Obese Subjects with Nonalcoholic Fatty Liver Disease. *Journal of clinical endocrinology and metabolism* 95:2727.

14 Poynten AM, Khee Gan S *et al.* **2003**; Nicotinic acid-induced insulin resistance is related to increased circulating fatty acids and fat oxidation but not muscle lipid content. *Metabolism* 52:699.

15 Westerterp M, van der Hoogt CC *et al.* **2006**; Cholesteryl ester transfer protein decreases high-density lipoprotein and severely aggravates atherosclerosis in APOE*3-Leiden mice. *Arterioscler Thromb Vasc Biol* 26:2552.

16 Liu H, Maurice DH. **1998**; Expression of cyclic GMP-inhibited phosphodiesterases 3A and 3B (PDE3A and PDE3B) in rat tissues: Differential subcellular localization and regulated expression by cyclic AMP. *British journal of pharmacology* 125:1501.

17 Quabbe H-J, Luyckx AS *et al.* **1983**; Growth Hormone, Cortisol, and Glucagon Concentrations during Plasma Free Fatty Acid Depression: Different Effects of Nicotinic Acid and an Adenosine Derivative (BM 11.189). *Journal of clinical endocrinology and metabolism* 57:410.

18 Watt MJ, Holmes AG *et al.* **2004**; Reduced plasma FFA availability increases net triacylglycerol degradation, but not GPAT or HSL activity, in human skeletal muscle. *American journal of physiology. Endocrinology and metabolism* 287:E120.

19 O'Neill M, Watt MJ *et al.* **2004**; Effects of reduced free fatty acid availability on hormone-sensitive lipase activity in human skeletal muscle during aerobic exercise. *Journal of applied physiology* 97:1938.

20 Kaushik SV, Plaisance EP *et al.* **2009**; Extended-release niacin decreases serum fetuin-A concentrations in individuals with metabolic syndrome. *Diabetes/metabolism research and reviews* 25:427.

21 Ulrich-Lai YM, Figueiredo HF *et al.* **2006**; Chronic stress induces adrenal hyperplasia and hypertrophy in a subregion-specific manner. *American journal of physiology. Endocrinology and metabolism* 291:E965.

22 Rahn T, Rönnstrand L *et al.* **1996**; Identification of the Site in the cGMP-inhibited Phosphodiesterase Phosphorylated in Adipocytes in Response to Insulin and Isoproterenol. *Journal of biological chemistry* 271:11575.

23 Omori K, Kotera J. **2007**; Overview of PDEs and Their Regulation. *Circulation research* 100:309.

24 Perino A, Ghigo A *et al.* **2011**; Integrating Cardiac PIP3 and cAMP Signaling through a PKA Anchoring Function of p110γ. *Molecular cell* 42:84.

25 Fraterrigo G, Fabbrini E *et al.* **2012**; Relationship between Changes in Plasma Adiponectin Concentration and Insulin Sensitivity after Niacin Therapy. *Cardiorenal medicine* 2:211.

26 Choi S, Yoon H *et al.* **2011**; Widespread effects of nicotinic acid on gene expression in insulin-sensitive tissues: implications for unwanted effects of nicotinic acid treatment. *Metabolism* 60:134.

5

Prolonged niacin treatment leads to increased adipose tissue PUFA synthesis and an anti-inflammatory lipid and oxylipin plasma profile

Mattijs M. Heemskerk*, Harish K. Dharuri*, Sjoerd A.A. van den Berg, Hulda S. Jónasdóttir, Dick-Paul Kloos, Martin Giera, Ko Willems van Dijk, Vanessa van Harmelen

*Both authors contributed equally

Journal of Lipid Research **2014**, 55(12): 2532-2540

Abstract

Prolonged niacin treatment elicits beneficial effects on the plasma lipid and lipoprotein profile that are associated with a protective cardiovascular disease (CVD) risk profile. Acute niacin treatment inhibits non-esterified fatty acid (NEFA) release from adipocytes and stimulates prostaglandin release from skin Langerhans cells, but the acute effects diminish upon prolonged treatment, while the beneficial effects remain. To gain insight in the prolonged effects of niacin on lipid metabolism in adipocytes, we used a mouse model with a human-like lipoprotein metabolism and drug response (female APOE*3-Leiden. CETP mice) treated with and without niacin for 15 weeks. The gene expression profile of gonadal white adipose tissue (gWAT) from niacin treated mice showed an up-regulation of the "biosynthesis of unsaturated fatty acid (PUFA)" pathway, which was corroborated by qPCR and analysis of the FA ratios in gWAT. Also, adipocytes from niacin treated mice secreted more of the PUFA docosahexaenoic acid (DHA) *ex vivo*. This resulted in an increased DHA/arachidonic acid (AA) ratio in the adipocyte FA secretion profile and in plasma of niacin treated mice. Interestingly, the DHA metabolite 19,20-dihydroxy docosapentaenoic acid (19,20-diHDPA) was increased in plasma of niacin treated mice. Both an increased DHA/AA ratio and increased 19,20-diHDPA are indicative for an anti-inflammatory profile and may indirectly contribute to the atheroprotective lipid and lipoprotein profile associated with prolonged niacin treatment.

Introduction

Niacin (vitamin B3) treatment reduces cardiovascular disease and atherosclerosis development [1]. These beneficial effects are mediated, in part, by lowering circulating levels of LDL-cholesterol, VLDL-TG and lipoprotein(a) [2] as well as by increasing HDL-cholesterol [3]. In addition, prolonged niacin treatment also decreases plasma, adipose tissue and vascular inflammation [4, 5], which might contribute to reducing CVD. The induction of these beneficial effects after prolonged niacin treatment are in striking contrast to the unwanted acute niacin effects.

Acutely, niacin binds to the inhibitory hydroxycarboxylic acid receptor 2 (HCA_2) (previously known as GPR109A). In adipocytes this leads to an inhibition of adipocyte lipolysis followed by an acute reduction of plasma non-esterified fatty acid (NEFA) levels. Lowering NEFA levels causes metabolic stress [6, 7], which increases stress hormone levels [8–12] after niacin treatment. In the skin Langerhans cells and keratinocytes, acute niacin binding to the HCA_2 receptor leads to a release of arachidonic acid (AA) and subsequent cyclooxygenase-mediated oxylipin synthesis (mostly prostaglandins) causing flushing [13] and a decrease in blood pressure [14]. Intriguingly, these acute effects decrease upon prolonged niacin treatment. Adipocyte lipolysis normalizes [15, 16] and flushing diminishes [17].

The fact that certain acute niacin effects decrease over time whereas the beneficial lipid lowering and anti-inflammatory effects remain, suggests differences between the induction of intracellular signaling pathways upon acute and prolonged niacin treatment. In the current study we set out to characterize changes in signaling regulation upon prolonged niacin treatment. We specifically investigated effects of niacin on adipose tissue as adipose tissue has been shown to be the most affected organ at the gene expression level after 7h of niacin treatment [18].

We treated mice with 0.3% niacin mixed through the diet and isolated gonadal white adipose tissue (gWAT) after 15 weeks of intervention. The mice used in this study were female APOE*3-Leiden.CETP mice [19] which-in contrast to wild type mice-have a human like lipoprotein profile and respond similarly to atheroprotective drugs like niacin [20]. A microarray was used to compare gene expression profiles in the adipose tissue. We applied bio-informatic and statistical analyses to the gene expression data and showed that prolonged niacin treatment led to an increase in the pathways unsaturated FA synthesis. To investigate whether PUFA levels and possible derivatives thereof (i.e. oxylipins) were functionally affected we determined the fatty acid (FA) composition in the adipose tissue by gas chromatography mass spectrometry (GC-MS) and measured PUFA and oxylipin profiles in plasma by liquid chromatography tandem mass spectrometry (LC-MS/MS).

Materials and methods

Mouse experiments

Female APOE*3-Leiden.CETP mice were bred at the Leiden University Medical Center. At age 15 ± 1 week, mice were fed a western type diet (Diet T with 0.1 g% cholesterol, which consisted of 16 kcal% protein, 43 kcal% carbohydrate and 41 kcal% fat. AB Diets, Woerden, the Netherlands) with or without niacin (0.3 g%, Sigma Aldrich, St Louis, MO, USA). Supplementary table S2 shows the fatty acid composition of the diet. Body weight was registered weekly. Animals were housed in a controlled environment (21°C, 40-50% humidity) with a daily 12h photoperiod (07h00-19h00). Food and tap water were available ad libitum during the whole experiment. Food intake was determined weekly by weighing the food in the cages at t=0 and at t= 1 days. The difference between these time points was equal to 24h food intake of the mice. The mice in this study are the same as in our previously published study (16). All experiments were performed after a 15 week dietary intervention period. All animals (n=14 per group) were anaesthetized and sacrificed in the fed state between 08h00 and 9h30 by cardiac puncture. Organs and plasma were collected and stored at -80°C. Fresh gonadal white adipose tissue (gWAT) was harvested and kept in PBS with or without niacin. One niacin treated animal did not have sufficient gWAT for the analyses. All animal experiments were performed in accordance with the regulations of Dutch law on animal welfare. The institutional scientific committee and ethics committee for animal procedures from the Leiden University Medical Center, Leiden, The Netherlands approved the protocols.

gWAT gene expression analysis

RNA was isolated from gWAT using the Nucleospin RNA/Protein kit (MACHEREY-NAGEL GmbH & Co. KG, Düren, Germany) after which RNA quality was assessed by NanoDrop (NanoDrop) and 2100 BioAnalyzer (Agilent). All samples had an RNA Integrity Number of >7.5. cRNA was synthesized using the TotalPrep RNA Amplification Kit (Ambion, Illumina). cRNA levels were normalized to 150ng/μL and loaded onto MouseWG-6 v2.0 Expression BeadChips by Service XS (Leiden, The Netherlands). Each BeadChip contains eight arrays. Hybridization and washing were performed according to the Illumina manual. Image analysis and extraction of raw expression data was performed with Illumina GenomeStudio v2011.1 gene expression software with default settings.

Lumi [21] module in the R-based Bioconductor package was used to read in the combined (average) signal intensities per probe. A variance-stabilizing transformation (lumiT) available in the R package was used to stabilize the expression variance based on the bead level expression variance and mean relations. Expression data were normalized using the function lumiN available within the lumi package. We used limma [22] an R-based Bioconductor

package to calculate the level of differential gene expression. In addition to determining significant differentially expressed genes, gene set analysis based on KEGG pathway and Gene Ontology was performed using the Bioconductor package "GlobalTest" [23].

Quantitative PCR

RNA was isolated from gWAT and liver using the Nucleospin RNA/Protein kit (MACHEREY-NAGEL GmbH & Co. KG, Düren, Germany). Subsequently, 1µg of RNA was used for cDNA synthesis by iScript (BioRad, Hercules, CA, USA), which was purified by the Nucleospin Gel and PCR clean-up kit (Machery Nagel). Real-Time PCR was carried out on the IQ5 PCR machine (BioRad) using the Sensimix SYBR Green RT-PCR mix (Quantace, London, UK) and QuantiTect SYBR Green RT-PCR mix (Qiagen, Venlo, the Netherlands). Target mRNA levels were normalized to *Rplp0* & *Ppia* mRNA levels. Primer sequences and PCR conditions can be found in Supplementary table S1.

gWAT, liver and diet fatty acid composition

FA composition analysis of gWAT, liver and diet was carried out as described recently by Kloos *et al.* [24]. Briefly: triplicate samples were weighed of approximately 10 mg diet or organ from niacin treated and control mice. 1 mL of water, 3 mL MeOH and 1 mL 10M NaOH were added, the samples flushed with argon and hydrolyzed for 1 h at 90 °C. After acidification with 2 mL of 6M HCl, 10 µL of an internal standard solution ([$^{2}H_{31}$]palmitic acid and ergosterole 10 µg/mL each) was added. The samples were extracted twice with 3 mL *n*-hexane and the combined organic extracts were dried under a gentle stream of nitrogen. Dried samples were derivatized using 25 µL of *N-tert*.-butyldimethylsilyl-*N*-methyltrifluoroacetamide (Sigma Aldrich, Schnelldorf, Germany) for 10 min at 21 °C, subsequently 25 µL of N,O-bis(trimethylsilyl) trifluoroacetamide containing 1% trimethylchlorosilane (Thermo Scientific, Waltham, MA, USA) and 2.5 µL of pyridine were added and the sample was heated for 15 min to 50 °C. Next, 947.5 µL of n-hexane, containing 10 µg/mL octadecane (C_{18}) as system monitoring component, was added. Samples were analyzed in SIM mode on a Scion TQ GC-MS (Bruker, Bremen, Germany) equipped with a 15 m × 0.25 mm × 0.25 mm BR5MS column (Bruker). The injection volume was 1 µL, the injector was operated in splitless mode at 280 °C and the oven program was as follows: 90 °C kept constant for 0.5 min, then ramped to 180 °C with 30 °C/min then to 250 °C with 10 °C/min then to 266 °C with 2 °C/min and finally to 300 °C with 120 °C/min, kept constant for 2 min. Helium (99.9990%, Air Products, The Netherlands) was used as carrier gas. For data analysis a total area correction was applied and triplicates were averaged.

Gonadal adipocyte PUFA release assay

Fresh gonadal adipose tissue was minced and digested in 0.5 g/L collagenase type I in HEPES buffer (pH 7.4) with 20 g/L of dialyzed bovine serum albumin (BSA, fraction V, Sigma Aldrich) for 1 h at 37°C. The disaggregated WAT was filtered through a nylon mesh with a pore size of 236 µm. For the isolation of mature adipocytes, cells were obtained from the surface of the filtrate and washed several times. Adipocytes (~10,000 cells/mL) were incubated in triplicate in a 96 well plate at 37°C in 200µL per well of DMEM/F12 medium with 2%w/w BSA with or without niacin (10^{-6} M) for 2 hours. The adipocyte conditioned medium (100 µL) was frozen at -20°C until further analysis.

Plasma PUFA and oxylipins measurement

Protein precipitation was performed on adipocyte conditioned medium (80 µL) or plasma (20 µL) by the addition of methanol (233.6 µL for medium and 53.6 µl for plasma) and 6.4 µL of internal standard solution containing ($[^2H_8]$15-HETE, $[^2H_4]PGE_2$, $[^2H_4]LTB_4$ and $[^2H_5]$ DHA, each 50 ng/mL in methanol), which was left to equilibrate for 20 minutes at -20°C. The samples were spun down for 10 min, 16200g at 4°C. Supernatant (240 µL for medium and 30 µL for plasma) was pipetted into a deactivated glass insert (Agilent, CA, USA). Plasma supernatant was diluted in 30 µL of H_2O, while medium supernatant was dried by Speedvac at room temperature. The dried medium sample was dissolved in 60 µL 1:2 methanol/H_2O. For both sample types, 20 µL was injected for LC-MS/MS analysis as described previously [25, 26].

LC-MS/MS analysis is carried out on a QTrap 6500 mass spectrometer (AB Sciex, Nieuwerkerk aan den Ijssel, The Netherlands), coupled to a Dionex Ultimate 3000 LC-system including auto-sampler and column oven (Dionex part of Thermo, Oberschleiβheim, Germany). The employed column was a Kinetex C18 50 × 2.1 mm, 1.7 µm, protected with a C_8 pre-column (Phenomenex, Utrecht, The Netherlands). H_2O (A) and methanol (B) both with 0.01% acetic acid were used. The gradient program started at 40% eluent B and was kept constant for 1 min, then linearly increased to 45% B at 1.1 min, then to 53.5% B at 4 min, to 55% B at 6.5 min, then to 90% B at 12 min and finally to 100% B at 12.1 min, kept constant for 3 min. The flow rate was set to 250.0 µL/min. The MS was operated under the following conditions: the collision gas flow was set to medium, the drying temperature was 400 °C, the needle voltage -4500 V, the curtain gas was 30 psi, ion source gas 1 was 40 psi and the ion source gas 2 was 30 psi (air was used as drying gas and nitrogen as curtain gas). For quantitation, the multiple reaction monitoring (MRM) transitions and collision energies (CE) given in supplementary table S5 were used combined with calibration lines. All substances used as standards were from Cayman Chemicals (Ann Arbor, MI, USA) if not stated otherwise, except RvE1, RvE2 18S-RvE3 and 18R-RvE3 (gifts from Dr. Makoto Arita, Tokyo, Japan). Metabolite identification in plasma was verified by MS/MS spectral comparison with standards, of which leukotriene

E_4, thromboxane B_2 and 19,20-diHDPA are included in the supplements (Supplementary figure S4 until S6).

Statistics

Mean values and standard deviations are reported in all figures. The gene expression data were statistically analyzed by using the multiple test correction method of Benjamin-Hochberg for control of false discovery rate (FDR) for both differentially expressed individual genes and for KEGG pathways. An adjusted p-value < 0.05 was considered significant. Calculations for the lipid measurements were performed in Prism version 6 (GraphPad Software, La Jolla, USA). Multiple T-tests were performed and a 5% FDR value was applied. An F-test was applied to test whether linear regression lines were significantly non-zero. The levels of significance were set at $p < 0.05$.

Results

gWAT gene expression analysis

Female APOE3.Leiden.CETP mice (n=14 per group) were fed a Western type diet (containing 0.1% cholesterol) with and without niacin for 15 weeks. As previously published [16], niacin treatment did not lead to differences in body weight nor gonadal white adipose tissue weight in these mice. However, plasma lipids, i.e. total cholesterol, triglycerides and phospholipids were all decreased [16]. Gene expression analysis generated 24 differentially expressed genes due to niacin treatment after multiple test correction (adjusted $p<0.05$, see Table 1). The global test was applied to identify KEGG pathways affected by niacin treatment. Table 2 depicts the top 5 pathways identified by global test, however only "biosynthesis of unsaturated fatty acids" remained significant after correction for false discovery rate ($q<0.05$). The differentially expressed genes from Table 1 were clustered and highlighted according to KEGG pathways. The top-hits from the "biosynthesis of unsaturated fatty acids" (*Elovl6*, *Tecr* and *Elovl5*) were all specifically involved in FA elongation, not FA desaturation, and were all up-regulated. Quantitative PCR measurements of *Elovl6* and *Elovl5* in gWAT confirmed up-regulation of mRNA levels of these enzymes after niacin treatment (Fig. 1). The rate-limiting desaturase enzyme of PUFA synthesis encoded by *Fads2* (Fatty acid desaturase 2) showed a trend towards increased expression after niacin.

Table 1: Differentially expressed gene hits from microarray analysis of gWAT after niacin treatment. P-value after multiple testing correction. The fold change was calculated as log_2((Niacin/Control). The gene symbols highlighted in black are part of the KEGG pathway "Biosynthesis of unsaturated fatty acids".

Gene symbol	Gene ID	Gene name	Adj. p-value	Log(fold change)
Pdzk1ip1	67182	PDZK1 interacting protein 1	0.002	1.190
Orm2	18406	Orosomucoid 2	0.002	0.857
Orm1	18405	Orosomucoid 1	0.003	0.550
Elovl6	170439	Elongation of long chain fatty acids 6	0.004	1.371
Lctl	235435	Lactase-like	0.004	1.107
Rdh11	17252	Retinol dehydrogenase 11	0.007	0.887
Nudt7	67528	Nudix (nucleoside diphosphate linked moiety X)-type motif 7	0.012	0.537
Acat2	110460	Acetyl-Coenzyme A acetyltransferase 2	0.013	0.695
Mup3	17842	Major urinary protein 3	0.013	1.047
1500017E21Rik	668215	RIKEN cDNA 1500017E21 gene	0.013	0.612
Clstn3	232370	Calsyntenin 3	0.013	0.607
Apoc1	11812	Apolipoprotein C-I	0.013	0.523
Comt	12846	Catechol-O-methyltransferase	0.014	0.536
Zfp385b	241494	Zinc finger protein 385B	0.014	-0.436
Tecr	106529	Trans-2,3-enoyl-CoA reductase	0.029	0.498
G6pdx	14381	Glucose-6-phosphate dehydrogenase X-linked	0.029	0.454
Elovl5	68801	Elongation of long chain fatty acids 5	0.033	0.405
Pkm2	18746	Pyruvate kinase, muscle	0.034	0.521
D430019H16Rik	268595	RIKEN cDNA D430019H16 gene	0.034	-0.505
Aacs	78894	Acetoacetyl-CoA synthetase	0.035	0.524
Lpcat3	14792	Lysophosphatidylcholine acyltransferase 3	0.035	0.504
Kcnj15	16516	Potassium inwardly-rectifying channel, subfamily J, member 15	0.035	0.450
Cyp51	13121	Cytochrome P450, family 51	0.039	0.747
Aard	239435	Alanine and arginine rich domain containing protein	0.039	-0.547
Fasn	14104	Fatty acid synthase	0.126	0.487
Acly	104112	ATP citrate lyase	0.139	0.691

Table 2: Pathways regulated on gene expression level by niacin in the gWAT according to global test. FDR: false discovery rate.

KEGG ID	KEGG pathway name	p-value	FDR q-value
map01040	Biosynthesis of unsaturated fatty acids	1.81E-05	0.00381
map00310	Lysine degradation	7.97E-04	0.16654
map00900	Terpenoid backbone biosynthesis	1.02E-03	0.21273
map00620	Pyruvate metabolism	1.09E-03	0.22603
map00100	Steroid biosynthesis	1.32E-03	0.27205

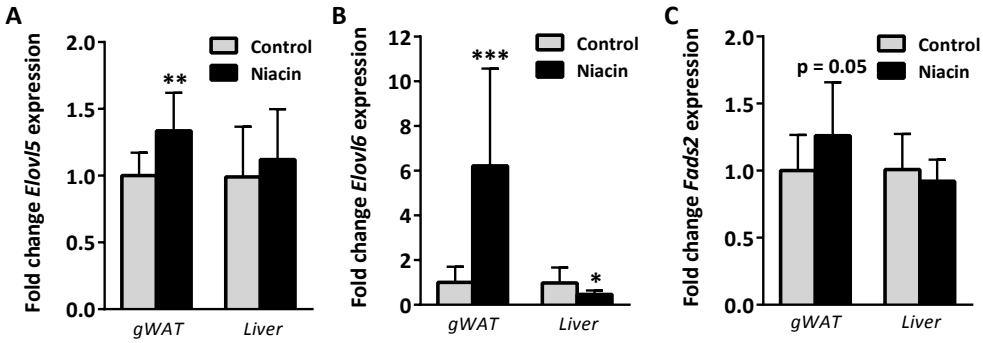

*Figure 1: Gene expression by qPCR of gWAT and liver tissue isolated from unfasted control and niacin treated mice. A) Elovl5, B) Elovl6 and C) Fads2 mRNA levels expressed as fold change from control. *p<0.05, **p<0.01, ***p<0.001 compared to control.*

gWAT fatty acid composition and adipocyte PUFA secretion

To investigate whether the increased mRNA levels of genes in the "biosynthesis of unsaturated fatty acids" translated to adipose tissue FA metabolism changes, we examined the FA composition of the gWAT by GC-MS. In the adipose tissue the fractions of the substrates for PUFA synthesis, the essential fatty acids α-linolenic acid (ALA, n-3) and linoleic acid (LA, n-6), were decreased after niacin treatment while their down-stream products were not fractionally different (Supplementary figure S1 and table S2). As the only source of essential FAs was the diet, of which the consumption was equal (data not shown), an increased enzymatic processing of essential FAs towards down-stream elongated and desaturated PUFAs would be plausible. To examine enzymatic processing, we investigated the substrate/product ratios for the enzymes in the PUFA synthesis pathway. We exclusively found differential elongase ratios and no desaturase ratios between control and niacin treatment (data not shown). Furthermore, the differential ratios that were decreased were the C18 to C20 elongation ratios, while the C20 to C22 ratios were increased indicating a possible increase in the metabolism and processing of essential FAs towards down-stream PUFAs in gWAT from niacin treated mice (Table 3). Given that niacin did no elevate the fractional content of the down-stream

PUFAs of the essential FAs, we studied whether niacin treatment increased PUFA secretion from freshly isolated adipocytes.

Although the fraction of medium chain fatty acids (MCFA, C10:0 / C12:0 / C14:0) was also increased in gWAT after niacin, adipocyte release of these MCFA was not different (Supplemental figure S 7). Of the PUFAs, both ALA and LA were secreted in equal amounts for control and niacin treated adipocytes (Figure 2A). Interestingly, down-stream metabolic products of the essential n-3 fatty acid ALA, namely EPA (non-significant after FRD correction) and DHA, were secreted to a greater extent after niacin treatment.

Table 3: Gene expression level of significant genes in the "Biosynthesis of unsaturated fatty acids" pathway and the associated enzymatic substrate/product ratio of FAs. The fold changes were calculated as log_2(niacin / control).

Gene name	Symbol	Adj. p-value	Fold change	Ratio	p-value	Fold change
Trans-2,3-enoyl-CoA reductase	*Tecr*	0.029	0.498(↑)	General fatty acid elongation		
Elongation of long chain fatty acids 6	*Elovl6*	0.004	1.371(↑)	C16:0 / C18:0	0.416	-0.152(↓)
				C16:1n-9 / C18:1n-9	0.019	-0.370(↓)
Elongation of long chain fatty acids 5	*Elovl5*	0.033	0.405(↑)	C18:3n-3 / C20:3n-3	0.007	-0.619(↓)
				C18:4n-3 / C20:4n-3	Sub & prod not measured	
				C18:2n-6 / C20:2n-6	0.028	-0.540(↓)
				C18:3n-6 / C20:3n-6	0.049	-0.390(↓)
Elongation of long chain fatty acids 5/2	*Elovl5/ Elovl2*			C20:5n-3 / C22:5n-3	0.155	0.529(↑)
				C20:4n-6 / C22:4n-6	0.032	0.387(↑)

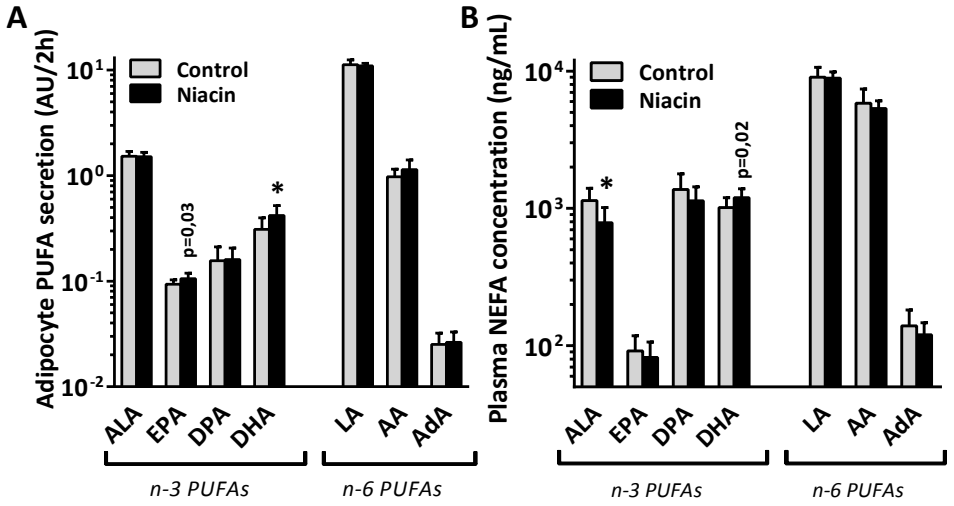

*Figure 2: A) PUFA release from ex vivo isolated adipocytes from control and niacin treated mice incubated for two hours in DMEM/F12 medium. B) PUFA concentration in unfasted plasma of control and niacin treated mice. Mean±SD, n=14 for Control/n=13 for Niacin. *p<0.05 compared to control gWAT after FDR correction. P-values listed were before FDR correction.*

Liver PUFA biosynthesis gene expression and fatty acid composition

As adipose tissue and the liver are the main sites of NEFA processing, we also examined the effects of prolonged niacin on the liver. We found by using qPCR that *Elovl5* and *Fads2* expression were unaffected by niacin treatment, while *Elovl6* expression was down-regulated (Figure 1). Liver fatty acid composition did not differ between control and niacin treated mice (supplementary figure S2 and table S3), neither did the substrate/product ratios relevant for PUFA biosynthesis (Data not shown). Although the PUFA fractions of the livers from niacin treated mice went in the inverse direction as seen in gWAT, this effect was non-significant.

Plasma PUFAs and oxylipins

In addition to measuring PUFA levels in adipocyte medium *ex vivo* we also examined PUFA levels in plasma by LC-MS/MS. Niacin reduced circulating levels of ALA and tended to increase the levels of its down-stream product DHA (Figure 2B and supplementary table S4, DHA was NS after FDR correction). EPA levels were not affected by niacin. We next examined the ratio of DHA over AA as a surrogate marker for PUFA associated cardiovascular risk [27–29] and found that the ratio was shifted towards DHA, both in adipocyte medium and in plasma (Figure 3A). PUFA derived oxylipin signaling molecules were also measured in the plasma (Figure 3B and supplementary table S4). Arachidonic acid metabolite prostaglandin

D_2 was not affected by niacin treatment, whereas thromboxane B_2 levels increased (NS after FDR correction). AA metabolite leukotriene E_4 decreased after niacin treatment (NS after FDR correction), whereas 12-hydroxy eicosatetraenoic acid (12-HETE) levels remained unchanged. The n-3 PUFA derived diol metabolite 19,20-dihydroxy docosapentaenoic acid (19,20-diHDPA) produced by cytochrome P450 was significantly increased. Due to the increase in DHA levels we investigated the presence of DHA derived resolvins [30], which could however not be detected by our approach.

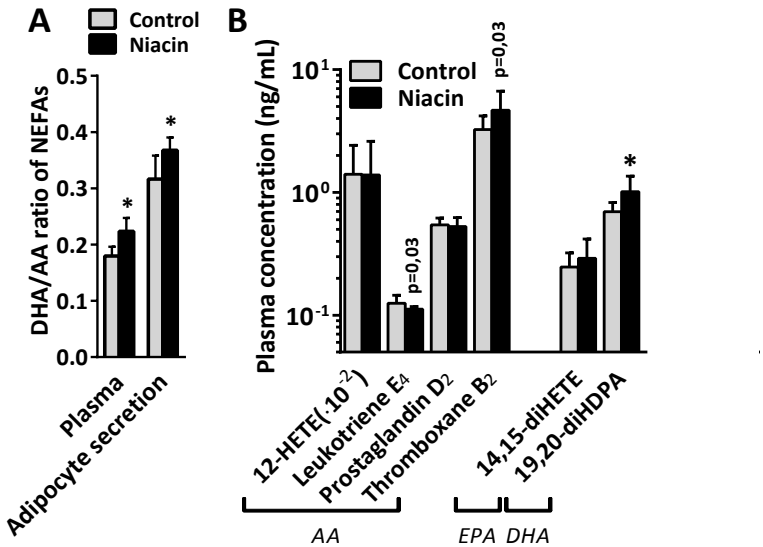

*Figure 3: A) Docosahexaenoic acid over arachidonic acid ratio in adipocyte secreted medium and in plasma. B) Oxylipin concentration in plasma of control and niacin treated mice. Mean±SD, n=14 per group. *p<0.05 compared to control gWAT after FDR correction. P-values listed were before FDR correction.*

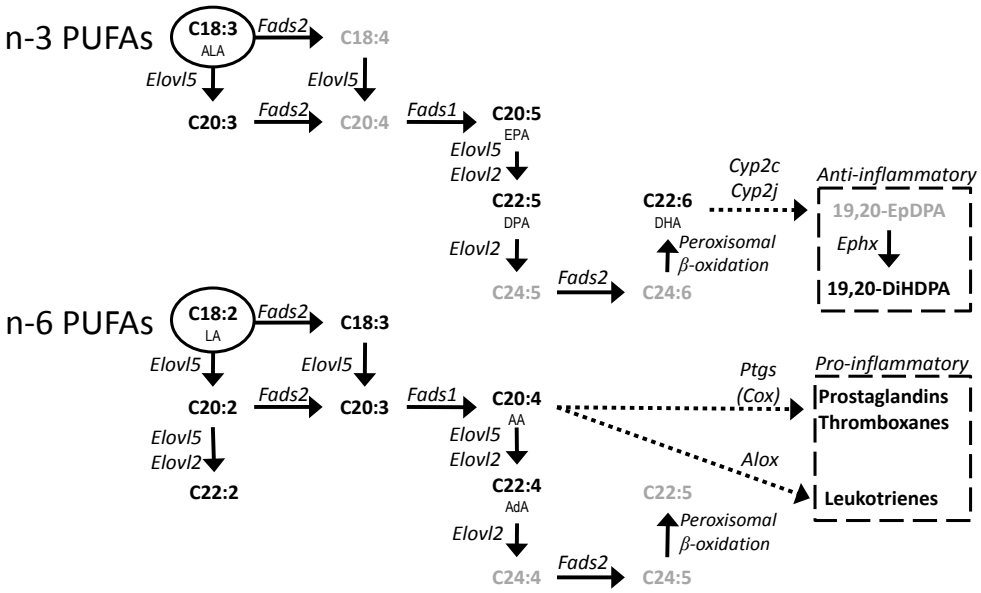

Figure 4: Schematic overview of the synthesis of poly unsaturated fatty acids and the subsequent conversion to a selection of oxylipins. Genes are in italic, metabolites in bold and essential FAs are encircled. Metabolites in grey were not measured. Based on the review by Guillou et al.[31]

Discussion

The current study demonstrates for the first time that prolonged niacin treatment results in an up-regulation of the n-3 PUFA synthesis pathway in adipose tissue. Gene expression analysis of gWAT showed that our hyperlipidemic mouse model responded to niacin by up-regulating genes involved in the unsaturated FA biosynthesis. Fatty acid composition analysis corroborated the increased PUFA synthesis. A higher degree of n-3 PUFA secretion from prolonged niacin treated adipocytes was seen, which was also reflected in increased n-3 PUFA plasma levels. Markedly, the plasma levels of n-3 PUFA derived oxylipins produced by cytochrome P450 and hydrolyzed by soluble epoxy hydrolases were increased. Oxylipins produced by cytochrome P450 from n-3 PUFAs and the n-3 PUFAs themselves suggest a beneficial vascular health profile, which might contribute to the prolonged niacin-induced atheroprotective effect.

Gene expression analysis of the gonadal white adipose tissue of hyperlipidemic mice treated with niacin for 15 weeks demonstrated an up-regulation of the "biosynthesis of unsaturated fatty acid" pathway, mostly by up-regulation of *Elovl6*, *Tecr* and *Elovl5*. All three genes are involved in FA elongation, not desaturation (as shown in figure 4 and table 3). This discovery was confirmed by qPCR, but also by gWAT FA composition and FA ratio analysis, which all pointed towards PUFA elongation. This increase in PUFA elongation was seen in adipose tissue, but not in liver tissue, where a more inverse trend towards PUFA accumulation could be seen in the fatty acid composition. When examining the PUFA secretion of adipocytes isolated from these mice, we found that specifically end-products of n-3 PUFA biosynthesis were secreted to a higher degree, as seen by DHA (C22:6) and also by EPA (C20:5) secretion. As the genes involved in PUFA biosynthesis are the same for n-3 PUFAs as for n-6 PUFAs, the specificity for increased n-3 PUFA secretion was puzzling. It is conceivable that the PUFA biosynthesis enzymes have a higher affinity for n-3 PUFAs, as was already shown for zebrafish desaturase enzymes [32]. The rat elongase 5 enzyme possesses a higher affinity for n-3 substrates than for n-6 substrates [33], and the mouse equivalent was found to be up-regulated in our study. Selective DHA biosynthesis, unlike AA or EPA, requires partial peroxisomal beta oxidation (Figure 4). Although the microarray did not point towards this pathway, increased peroxisomal beta oxidation after niacin could lead to preferential DHA synthesis. Asides from preferential n-3 PUFA biosynthesis, preferential mobilization from adipose tissue would also explain an increased n-3 PUFA release. A well-documented phenomenon is selective PUFA release from adipocytes [34], exemplified by fasting-induced preferential n-3 PUFA depletion of adipose tissue triglycerides [35]. Our preliminary results also indicate preferential n-3 PUFA release from adipocytes when (fasting-induced) lipolysis is stimulated by 8Br-cAMP (Supplemental figure S8c). Other potential mechanisms for preferential n-3 PUFA release might be phospholipid hydrolysis, as it has been previously shown that cytosolic PLA_2 releases AA and EPA from phospholipids whereas the release of DHA from phospholipids requires calcium-independent PLA_2 [36]. Although 99% of the

fatty acids are located in the triglyceride fraction, the contribution of the 1% fatty acids contained in the phospholipid fraction to n-3 PUFA release cannot be excluded. Additional research is required to investigate the underlying mechanisms for the preferential n-3 PUFA release after prolonged niacin treatment.

Adipocyte lipolysis contributes to the free fatty acid pool in the circulation. In the plasma of the niacin treated animals, we found a tendency for increased levels of the n-3 PUFA DHA in the NEFA pool. Although we do not have direct proof, our data suggest that DHA secretion by adipocytes is the main source of DHA in the plasma. Interestingly we did not find up-regulation of gene expression levels of *Elovl5*,*Elovl6* nor *Fads2*, or any change in fatty acid composition in the livers of the niacin treated mice, indicating that the niacin induced PUFA synthesis is selective for adipose tissue.

The n-3 PUFAs have been reported to confer CVD protective abilities via their conversion to anti-inflammatory oxylipins. For example, DHA can be converted to the oxylipin 19(20)-epoxy docosapentaenoic acid (19(20)-EpDPA) by cytochrome P450 (CYP) as can be seen in figure 4. Likewise, the n-3 PUFA EPA can be converted to 14(15)-epoxy eicosatetraenoic acid (14(15)-EpETE) by CYP. These epoxide metabolites have powerful biological effects on cardiovascular health. This was shown by previous studies where the epoxide metabolism pathway was genetically manipulated [37] or its compounds were pharmacologically elevated [38]. These studies showed the importance of epoxy metabolites in resolving inflammation, preserving vascular tone and general vascular homeostasis. The biologically active 19(20)-EpDPA and 14(15)-EpETE can be hydrolyzed by soluble epoxy hydrolases (encoded by the *Ephx2* gene in mice) to their respective diol metabolites 19,20-diHDPA and 14,15-dihydroxy eicosatetraenoic acid (14,15-diHETE). The levels of both these diol products were increased in plasma of niacin treated animals. The hydrolyzed diol metabolites have a far lower biological effect than their epoxide metabolites, but are more stable and can be detected in plasma by LC-MS/MS. Although we did not directly measure whether the levels of the bioactive epoxy metabolites 19(20)-EpDPA or 14(15)-EpETE were increased after niacin treatment, we found a positive correlation in plasma between the precursor and diol metabolite of 19(20)-EpDPA (DHA and 19,20-diHDPA) in niacin treated mice (Supplementary figure S3). This correlation suggests that the levels of 19(20)-EpDPA must also have increased after niacin treatment.

In general, the anti-inflammatory oxylipins such as epoxy metabolites produced by CYP (high affinity for n-3 PUFAs), are balanced by the pro-inflammatory oxylipins such as those produced by cyclooxygenases (COX) and arachidonate lipoxygenases (ALOX) (both with high affinity for n-6 PUFAs, such as AA) [39]. Prolonged niacin treatment did not dramatically affect AA derived oxylipin levels, although there was a tendency towards decreased levels of leukotriene E_4, a lipoxygenase pathway product stimulating inflammation, and towards increased levels of thromboxane B_2, a cyclooxygenase product stimulating coagulation.

Acute treatment of mouse adipocytes with niacin did not lead to an increased release of DHA or AA, nor a change in the ratio of DHA/AA in the adipocyte conditioned medium

(Supplemental figure S 9). Acute niacin treatment however, is a well-known trigger for AA-derived oxylipin synthesis in the skin. Irritative subcutaneous skin flushing is a common acute side-effect of niacin, induced by cyclooxygenase product prostaglandin D_2 [40] in Langerhans cells and keratinocytes. As mentioned above, we did not see an increase in pro-inflammatory prostaglandins after prolonged niacin treatment. These results are in line with results by Stern *et al.* [17] and suggest tolerance for flushing after prolonged niacin treatment. It is possible that the tolerance for flushing after prolonged niacin is mediated via n-3 PUFAs as suggested by vanHorn *et al.* [41]. Whether there is a role for anti-inflammatory n-3 PUFA derived oxylipins after acute niacin remains unclear. Inceoglu *et al.* [42] have acutely administered niacin to mice being treated with a soluble epoxide hydrolase inhibitor, which resulted in a blunted flushing response compared to wild type mice, while acute prostaglandin D_2 treatment did not blunt flushing. These results support a role for cytochrome P450 epoxide metabolites not only after prolonged niacin treatment, but also acutely in inhibiting the flushing response by niacin. Flushing severity also suggests an important balance between pro- and anti-inflammatory oxylipins, which can be modulated by niacin treatment. Most likely, the n-6 derived oxylipins prevail during acute niacin treatment, while after prolonged niacin treatment the n-3 derived oxylipins prevail.

Plasma DHA/AA ratio has been shown to be a diagnostic marker for PUFA associated cardiovascular health [27–29]. In addition to being metabolized to anti-inflammatory oxylipins, n-3 PUFA confer their CVD protective abilities by direct competition with n-6 PUFAs. Vanhorn *et al.* [41] have described that DHA supplementation increases the DHA/AA ratio in membrane phospholipids of Langerhans cells, thereby diminishing the relative availability of AA for pro-inflammatory prostaglandin synthesis. As a low n-3/n-6 ratio is associated with a risk for cardiovascular disease, increasing the ratio by supplementary n-3 PUFAs has been posed as a treatment target [43]. In our study, we see that the DHA/AA ratio has increased towards the anti-inflammatory DHA side without supplementary n-3 PUFAs. We have seen this increased DHA/AA ratio in both the *ex vivo* adipocyte PUFA secretion profile and in the *in vivo* plasma NEFA profile of niacin treated mice. These effects of niacin on adipose tissue and plasma PUFAs and oxylipins pose a potential contributing mechanism by which niacin treatment reduces cholesterol levels and CVD risk. Although we used mice in this study which are human like with respect to lipoprotein profile it remains to be investigated whether there are changes in the plasma DHA/AA ratio in humans treated with niacin.

In conclusion, prolonged niacin treatment of our hyperlipidemic mouse model with niacin resulted in up-regulation the entire pathway of PUFA biosynthesis in gWAT, increased n-3 PUFA secretion from the adipocytes and an increased plasma level of n-3 PUFAs and their anti-inflammatory oxylipins, which together point towards an atheroprotective plasma profile induced by prolonged niacin treatment.

Acknowledgements

This work was supported by grants from Center of Medical Systems Biology (CMSB), the Netherlands Consortium for Systems Biology (NCSB) established by The Netherlands Genomics Initiative/Netherlands Organization for Scientific Research (NGI/NWO), Leiden University Medical Center. Hulda Jónasdóttir is partially funded by the Stichting Prof. Jan Veltkamp Fonds (LUMC). This study was performed within the framework of the Center for Translational Molecular Medicine (http://www.ctmm.nl); project PREDICCt (grant 01C-104). We thank Dr. Makoto Arita from the department of Health Chemistry Graduate School of Pharmaceutical Sciences, University of Tokyo, Japan, for the kind gift of RvE1, RvE2, 18S-RvE3 and 18R-RvE3 used as standard material in the employed LC-MS/MS platform. The authors declare that there is no duality of interest associated with this manuscript.

References

1 Bruckert E, Labreuche J *et al.* **2010**; Meta-analysis of the effect of nicotinic acid alone or in combination on cardiovascular events and atherosclerosis. *Atherosclerosis* 210:353.

2 Morgan JM, Capuzzi DM *et al.* **2003**; Effects of extended-release niacin on lipoprotein subclass distribution. *American journal of cardiology* 91:1432.

3 Hernandez M, Wright SD *et al.* **2007**; Critical role of cholesterol ester transfer protein in nicotinic acid-mediated HDL elevation in mice. *Biochemical and biophysical research communications* 355:1075.

4 Wanders D, Graff EC *et al.* **2013**; Niacin Increases Adiponectin and Decreases Adipose Tissue Inflammation in High Fat Diet-Fed Mice. *PLoS ONE* 8:e71285.

5 Wu BJ, Chen K *et al.* **2012**; Niacin inhibits vascular inflammation via the induction of heme oxygenase-1. *Circulation* 125:150.

6 Chen X, Iqbal N *et al.* **1999**; The effects of free fatty acids on gluconeogenesis and glycogenolysis in normal subjects. *Journal of clinical investigation* 103:365.

7 Kasalicky J, Konopkova M *et al.* **2001**; 18F-fluorodeoxyglucose accumulation in the heart, brain and skeletal muscle of rats; the influence of time after injection, depressed lipid metabolism and glucose-insulin. *Nuclear medicine review. Central & Eastern Europe* 4:39.

8 Kaushik SV, Plaisance EP *et al.* **2009**; Extended-release niacin decreases serum fetuin-A concentrations in individuals with metabolic syndrome. *Diabetes/metabolism research and reviews* 25:427.

9 O'Neill M, Watt MJ *et al.* **2004**; Effects of reduced free fatty acid availability on hormone-sensitive lipase activity in human skeletal muscle during aerobic exercise. *Journal of applied physiology* 97:1938.

10 Oh YT, Oh K-S *et al.* **2011**; Continuous 24-h Nicotinic Acid Infusion in Rats Causes FFA Rebound and Insulin Resistance by Altering Gene Expression and Basal Lipolysis in Adipose Tissue. *American journal of physiology. Endocrinology and metabolism* 300:1012.

11 Quabbe H-J, Luyckx AS *et al.* **1983**; Growth Hormone, Cortisol, and Glucagon Concentrations during Plasma Free Fatty Acid Depression: Different Effects of Nicotinic Acid and an Adenosine Derivative (BM 11.189). *Journal of clinical endocrinology and metabolism* 57:410.

12 Watt MJ, Holmes AG *et al.* **2004**; Reduced plasma FFA availability increases net triacylglycerol degradation, but not GPAT or HSL activity, in human skeletal muscle. *American journal of physiology. Endocrinology and metabolism* 287:E120.

13 Hanson J, Gille A *et al.* **2010**; Nicotinic acid- and monomethyl fumarate-induced flushing involves GPR109A expressed by keratinocytes and COX-2-dependent prostanoid formation in mice. *Journal of clinical investigation* 120:2910.

14 Gadegbeku CA, Dhandayuthapani A *et al.* **2003**; Hemodynamic effects of nicotinic acid infusion in normotensive and hypertensive subjects. *American journal of hypertension* 16:67.

15 Wang W, Basinger A *et al.* **2000**; Effects of nicotinic acid on fatty acid kinetics, fuel selection, and pathways of glucose production in women. *American journal of physiology. Endocrinology and metabolism* 279:E50.

16 Heemskerk MM, van den Berg SA *et al.* **2014**; Long-term niacin treatment induces insulin resistance and adrenergic responsiveness in adipocytes by adaptive downregulation of phosphodiesterase 3B. *American journal of physiology. Endocrinology and metabolism* 306:E808.

17 Stern RH, Spence JD *et al.* **1991**; Tolerance to nicotinic acid flushing. *Clinical pharmacology and therapeutics* 50:66.

18 Choi S, Yoon H *et al.* **2011**; Widespread effects of nicotinic acid on gene expression in insulin-sensitive tissues: implications for unwanted effects of nicotinic acid treatment. *Metabolism* 60:134.

19 Westerterp M, van der Hoogt CC *et al.* **2006**; Cholesteryl ester transfer protein decreases high-density lipoprotein and severely aggravates atherosclerosis in APOE*3-Leiden mice. *Arteriosclerosis, Thrombosis, and Vascular Biology* 26:2552.

20 Kuhnast S, Louwe MC *et al.* **2013**; Niacin Reduces Atherosclerosis Development in APOE*3Leiden.CETP Mice Mainly by Reducing NonHDL-Cholesterol. *PLoS ONE* 8:e66467.

21 Du P, Kibbe WA *et al.* **2008**; lumi: a pipeline for processing Illumina microarray. *Bioinformatics* 24:1547.

22 Smyth GK. **2004**; Linear models and empirical bayes methods for assessing differential expression in microarray experiments. *Statistical applications in genetics and molecular biology* 3:3.

23 Goeman JJ, van de Geer SA *et al.* **2004**; A global test for groups of genes: testing association with a clinical outcome. *Bioinformatics* 20:93.

24 Kloos DP, Gay E *et al.* **2014**; Comprehensive GC–MS analysis of fatty acids and sterols using sequential one-pot silylation: quantification and isotopologue analysis. *Rapid communnications in mass spectrometry* 28:1507.

25 Giera M, Ioan-Facsinay A *et al.* **2012**; Lipid and lipid mediator profiling of human synovial fluid in rheumatoid arthritis patients by means of LC-MS/MS. *Biochimica et biophysica acta* 1821:1415.

26 Yang R, Chiang N *et al.* **2011**; Metabolomics-lipidomics of eicosanoids and docosanoids generated by phagocytes. *Current protocols in immunology* 14:26.

27 Nozue T, Yamamoto S *et al.* **2014**; Low serum docosahexaenoic acid is associated with progression of coronary atherosclerosis in statin-treated patients with diabetes mellitus: results of the treatment with statin on atheroma regression evaluated by intravascular ultrasound with virtual histology (TRUTH) study. *Cardiovascular diabetology* 13:13.

28 Nishizaki Y, Shimada K *et al.* **2014**; Significance of imbalance in the ratio of serum n-3 to n-6 polyunsaturated fatty acids in patients with acute coronary syndrome. *American journal of cardiology* 113:441.

29 Dohi T, Miyauchi K *et al.* **2011**; Long-term impact of mild chronic kidney disease in patients with acute coronary syndrome undergoing percutaneous coronary interventions. *Nephrology, dialysis, transplantation* 26:2906.

30 Serhan CN, Petasis NA. **2011**; Resolvins and protectins in inflammation resolution. *Chemical reviews* 111:5922.

31 Guillou H, Zadravec D *et al.* **2010**; The key roles of elongases and desaturases in mammalian fatty acid metabolism: Insights from transgenic mice. *Progress in lipid research* 49:186.

32 Hastings N, Agaba M *et al.* **2001**; A vertebrate fatty acid desaturase with Δ5 and Δ6 activities. *Proceedings of the National Academy of Sciences* 98:14304.

33 Gregory MK, Gibson RA *et al.* **2011**; Elongase Reactions as Control Points in Long-Chain Polyunsaturated Fatty Acid Synthesis. *PLoS ONE* 6:e29662.

34 Raclot T. **2003**; Selective mobilization of fatty acids from adipose tissue triacylglycerols. *Progress in lipid research* 42:257.

35 Nieminen P, Mustonen A-M *et al.* **2009**; Fatty Acid Composition and Development of Hepatic Lipidosis During Food Deprivation—Mustelids as a Potential Animal Model for Liver Steatosis. *Experimental biology and medicine* 234:278.

36 Strokin M, Sergeeva M *et al.* **2003**; Docosahexaenoic acid and arachidonic acid release in rat brain astrocytes is mediated by two separate isoforms of phospholipase A2 and is differently regulated by cyclic AMP and Ca2+. *British journal of pharmacology* 139:1014.

37 Imig JD. **2012**; Epoxides and Soluble Epoxide Hydrolase in Cardiovascular Physiology. *Physiological reviews* 92:101.

38 Askari AA, Thomson S *et al.* **2014**; Basal and inducible anti-inflammatory epoxygenase activity in endothelial cells. *Biochemical and biophysical research communications* 446:633.

39 Fischer R, Konkel A *et al.* **2014**; Dietary Omega-3 Fatty Acids Modulate the Eicosanoid Profile in Man Primarily via the CYP-epoxygenase Pathway. *Journal of Lipid Research* 55:1150.

40 Serebruany V, Malinin A *et al.* **2010**; The in vitro effects of niacin on platelet biomarkers in human volunteers. *Thrombosis and haemostasis* 104:311.

41 Vanhorn J, Altenburg JD *et al.* **2012**; Attenuation of niacin-induced prostaglandin D(2) generation by omega-3 fatty acids in THP-1 macrophages and Langerhans dendritic cells. *Journal of inflammation research* 5:37.

42 Inceoglu AB, Clifton HL *et al.* **2012**; Inhibition of soluble epoxide hydrolase limits niacin-induced vasodilation in mice. *Journal of cardiovascular pharmacology* 60:70.

43 Simopoulos AP. **2008**; The Importance of the Omega-6/Omega-3 Fatty Acid Ratio in Cardiovascular Disease and Other Chronic Diseases. *Experimental biology and medicine* 233:674.

Supplemental data

Table S1:

Gene	Forward primer	Reverse primer	Temperature
Rplp0	GGACCCGAGAAGACCTCCTT	GCACATCACTCAGAATTTCAATGG	60
Ppia	ACTGAATGGCTGGATGGCAA	TGTCCACAGTCGGAAATGGT	61
Elovl5	CAGCTTGCTTCTGTTCCCG	TCCATTTTAAAACCTCTCTGCCT	61
Elovl6	GCACTAAGACCGCAAGGCAT	CTACGTGTTCTCTGCGCCTC	61
Fads2	CTGGTGGAACCACCGACATT	TCTTGCCATACTCAAGGGGC	61

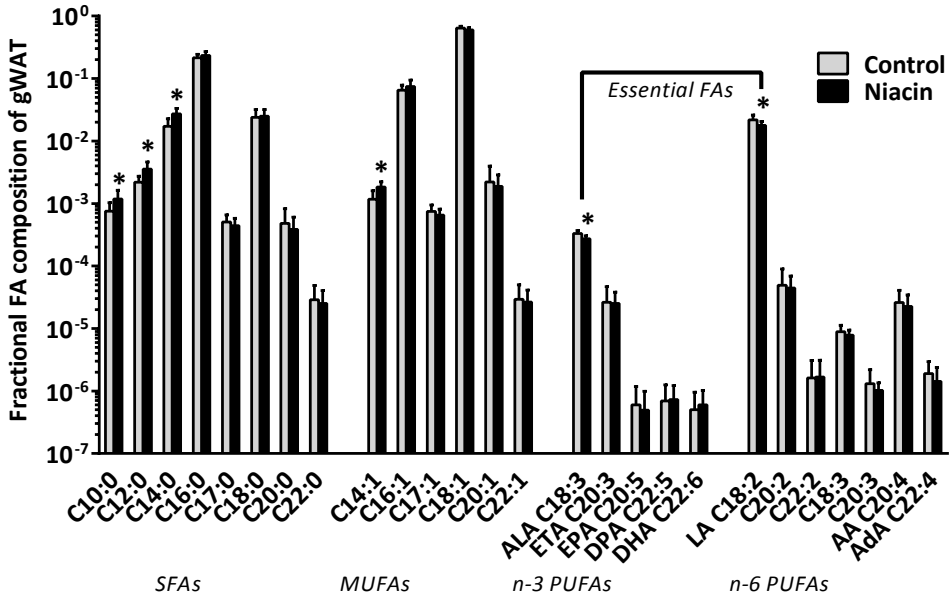

*Figure S1: Adipose tissue fatty acid composition of gWAT from APOE*3-Leiden.CETP mice fed a western type diet with 0.1% cholesterol with and without niacin. Mean±SD, N=14 for Control/N=13 for Niacin, *p<0.05 compared to control gWAT after false discovery rate correction.*

*Table S 2: Adipose tissue fatty acid composition of gWAT from APOE*3-Leiden.CETP mice fed a western type diet with 0.1% cholesterol with and without niacin and fatty acid composition of the western type diet. Fraction of total area corrected sum. Mean±SD, N=14 for Control/N=13 for Niacin/N=3 for diet. (*)Significant finding after false discovery rate correction.*

	Control gWAT		Niacin gWAT		Diet		Control vs Niacin
	Average	SD	Average	SD	Average	SD	P-value
SFA							
C10:0	0,0008	0,0003	0,0012	0,0004	0,0013	0,0009	(*)0,0078
C12:0	0,0022	0,0005	0,0036	0,0011	0,0019	0,0013	(*)0,0005
C14:0	0,0173	0,0054	0,0271	0,0061	0,0059	0,0038	(*)0,0003
C16:0	0,2153	0,0285	0,2339	0,0360	0,4351	0,0571	0,1679
C17:0	0,0005	0,0002	0,0004	0,0001	0,0014	0,0006	0,2804
C18:0	0,0239	0,0081	0,0250	0,0069	0,2162	0,0331	0,7049
C20:0	0,0005	0,0003	0,0004	0,0002	0,0030	0,0009	0,4066
C22:0	2,88E-05	1,99E-05	2,51E-05	1,55E-05	3,00E-04	7,01E-05	0,6070
MUFA							
C14:1	0,0012	0,0004	0,0018	0,0004	0,0003	0,0002	(*)0,0006
C16:1	0,0652	0,0131	0,0745	0,0202	0,0055	0,0035	0,1773
C17:1	0,0007	0,0002	0,0007	0,0002	0,0002	0,0001	0,1951
C18:1	0,6400	0,0459	0,6007	0,0532	0,3036	0,0445	0,0593
C20:1	0,0022	0,0018	0,0019	0,0010	0,0004	0,0002	0,5577
C22:1	2,94E-05	2,05E-05	2,65E-05	1,47E-05	1,62E-05	1,13E-05	0,6729
PUFA n-3							
ALA C18:3	3,32E-04	3,89E-05	2,72E-04	3,37E-05	4,58E-04	9,25E-05	(*)0,0003
ETA C20:3	2,63E-05	2,06E-05	2,51E-05	1,31E-05	2,82E-06	1,61E-06	0,8598
EPA C20:5	6,01E-07	5,83E-07	4,93E-07	4,93E-07	9,89E-07	9,91E-07	0,7985
DPA C22:5	6,95E-07	5,62E-07	7,28E-07	5,00E-07	4,11E-07	3,58E-07	0,8961
DHA C22:6	5,02E-07	4,58E-07	6,00E-07	4,28E-07	2,06E-06	4,75E-07	0,5940
PUFA n-6							
LA C18:2	2,19E-02	4,13E-03	1,78E-02	2,82E-03	2,32E-02	9,00E-03	(*)0,0080
C20:2	4,91E-05	4,09E-05	4,43E-05	2,49E-05	1,15E-05	4,28E-06	0,7206
C22:2	1,62E-06	1,47E-06	1,67E-06	1,45E-06	7,95E-06	1,70E-06	0,9370
C18:3	8,86E-06	2,45E-06	7,84E-06	1,59E-06	7,16E-07	4,56E-07	0,2231
C20:3	1,31E-06	8,78E-07	1,02E-06	3,31E-07	3,55E-07	1,66E-07	0,2789
AA C20:4	2,60E-05	1,47E-05	2,25E-05	1,18E-05	1,47E-06	9,51E-07	0,5065
AdA C22:4	1,90E-06	1,07E-06	1,42E-06	9,62E-07	2,86E-07	-	0,2540

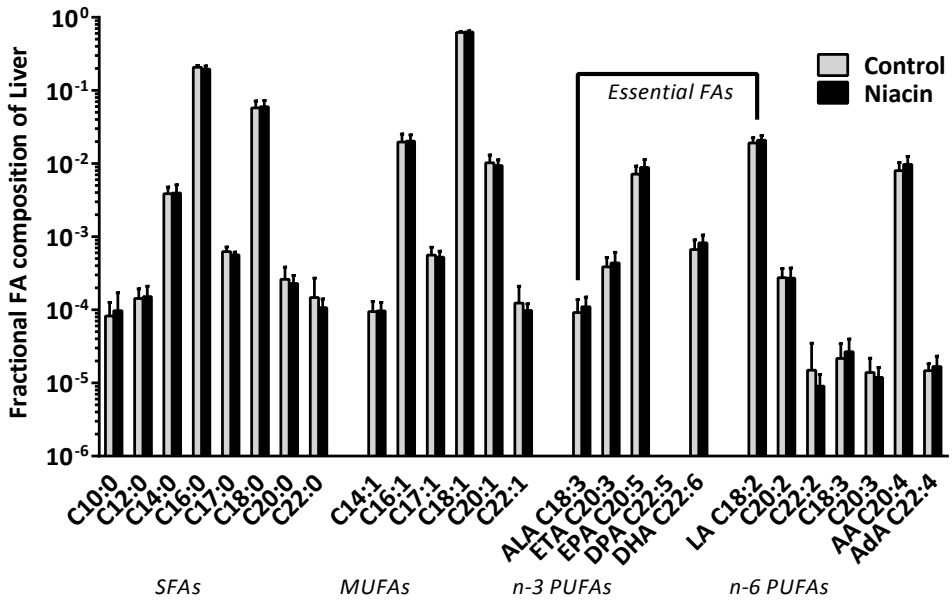

*Figure S2: Liver fatty acid composition from APOE*3-Leiden.CETP mice fed a western type diet with 0.1% cholesterol with and without niacin. Fraction of total area corrected sum. Mean±SD, N=14 for Control/N=13 for Niacin. *p<0.05 comparing control gWAT to niacin gWAT after false discovery rate correction.*

*Table S3: Liver fatty acid composition from APOE*3-Leiden.CETP mice fed a western type diet with 0.1% cholesterol with and without niacin. Fraction of total area corrected sum. Mean±SD, N=14 for Control/N=13 for Niacin. (*) Significant finding after false discovery rate correction.*

	Control Liver		Niacin Liver		Control vs Niacin
	Average	SD	Average	SD	P-value
SFA					
C10:0	8,23E-05	4,42E-05	9,74E-05	7,38E-05	0,5248
C12:0	0,000143	5,17E-05	0,000152	5,92E-05	0,6948
C14:0	0,003877	0,000907	0,003968	0,001167	0,8245
C16:0	0,20753	0,013181	0,196168	0,020302	0,0989
C17:0	0,000625	9,85E-05	0,000565	5,39E-05	0,0739
C18:0	0,057714	0,014338	0,059939	0,013182	0,6860
C20:0	0,000262	0,000122	0,000229	6,67E-05	0,4218
C22:0	0,000147	0,000125	0,000107	3,45E-05	0,2909
MUFA					
C14:1	9,46E-05	3,57E-05	9,7E-05	2,96E-05	0,8528
C16:1	0,019737	0,00563	0,020314	0,004366	0,7759
C17:1	0,00056	0,000161	0,000524	0,000112	0,5268
C18:1	0,621529	0,018559	0,628717	0,023243	0,3893
C20:1	0,010283	0,002869	0,009425	0,001852	0,3834
C22:1	0,000124	8,64E-05	9,79E-05	2,31E-05	0,3213
PUFA n-3					
ALA C18:3	9,17E-05	4,6E-05	0,00011	3,92E-05	0,2796
ETA C20:3	0,000388	0,000133	0,000438	0,000173	0,4111
EPA C20:5	0,00721	0,00204	0,00886	0,002503	0,0763
DPA C22:5	-	-	-	-	
DHA C22:6	0,000669	0,000237	0,000828	0,000228	0,0945
PUFA n-6					
LA C18:2	0,019119	0,003479	0,020887	0,003278	0,1973
C20:2	0,000276	9,29E-05	0,000271	0,000102	0,9115
C22:2	1,49E-05	2,02E-05	9,08E-06	4,02E-06	0,3334
C18:3	2,17E-05	1,29E-05	2,69E-05	1,31E-05	0,3204
C20:3	1,39E-05	7,87E-06	1,19E-05	4,41E-06	0,4437
AA C20:4	0,008023	0,002318	0,009784	0,002791	0,0916
AdA C22:4	1,47E-05	3,65E-06	1,69E-05	6,41E-06	0,3014

*Table S 4: Unfasted plasma PUFA and oxylipin concentrations of APOE*3-Leiden.CETP mice fed a western type diet with 0.1% cholesterol with and without niacin. Mean±SD, N=14 for Control/N=13 for Niacin. (*)Significant finding after false discovery rate correction.*

	Control		Niacin		Control vs Niacin
	Average (ng/mL)	**SD** (ng/mL)	**Average** (ng/mL)	**SD** (ng/mL)	**P-value**
PUFA					
ALA	1139,98	69,76	784,61	61,24	(*)0,0007
EPA	91,51	7,10	82,03	6,51	0,3342
DPA	1373,47	118,48	1133,20	81,11	0,0996
DHA	1012,96	52,65	1194,23	52,00	0,0226
LA	9033,60	427,04	8875,20	273,66	0,7614
AA	5833,59	417,18	5342,29	192,80	0,2949
AdA	139,25	11,33	119,86	7,21	0,1608
Oxylipins					
12-HETE	140,60	100,95	138,77	121,74	0,9666
Leukotriene E_4	0,125	0,020	0,112	0,005	0,0324
Prostaglandin D_2	0,545	0,073	0,528	0,097	0,6066
Thromboxane B_2	3,25	0,95	4,67	2,00	0,0252
14,15-diHETE	0,247	0,075	0,291	0,127	0,2891
19,20-diHDPA	0,696	0,131	1,011	0,345	(*)0,0065

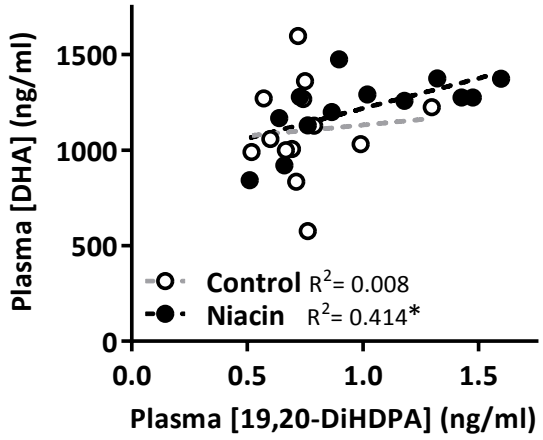

*Figure S3: Correlation between the plasma concentrations of 19,20-dihydroxydocosapentaenoic acid and docosahexaenoic acid. N=14 mice per group, *p<0.05 compared to a slope of zero.*

Table S5: Multiple Reaction Monitoring setup for ion transitions of the target compounds. Symbols in bold refer to internal standards. RT retention time, Q1 quadrupole 1 ion selection, Q3 quadrupole 3 ion selection, EP entrance potential, CE, collision energy, CCEP collision cell exit potential. HODEs, HOTrEs, HETEs, HEPEs, diHETEs and diHDPAs are given without chiral descriptors. Internal standards are indicated in grey.

Symbol	Lipid Maps ID	RT (min)	Q1 (m/z)	Q3 (m/z)	DP (Volts)	EP (Volts)	CE (Volts)	CCEP (Volts)
RvE1	LMFA03070019	4.0	349.1	195.0	-95	-10	-22	-13
20-hydroxy LTB_4	LMFA03020018	4.4	351.1	195.0	-60	-10	-24	-17
8-iso-$PGF_{2\alpha}$	LMFA03110001	5.1	353.1	193.0	-135	-10	-34	-11
15-keto-PGE_2	LMFA03010030	5.1	349.0	234.9	-65	-10	-20	-13
TxB_2	LMFA03030002	5.2	369.1	169.0	-55	-10	-24	-15
8-iso-PGE_2	LMFA03110003	5.3	351.1	271.0	-5	-10	-24	-19
13,14-dihydro-15-keto-PGE_2	LMFA03010031	5.6	351.1	235.0	-45	-10	-30	-13
PGE_2-d_4	LMFA03010008	5.6	355.1	193.0	-50	-10	-26	-17
PGE_2	LMFA03010003	5.7	351.2	271.1	-50	-10	-22	-21
PGD_2	LMFA03010004	5.8	351.1	233.0	-30	-10	-16	-13
LXB_4	LMFA03040002	6.0	351.1	220.9	-60	-10	-22	-13
$PGF_{2\alpha}$	LMFA03010002	6.1	353.1	193.0	-80	-10	-34	-11
RvD2	LMFA04000007	6.2	375.1	277.1	-60	-10	-18	-15
LXA_4	LMFA03040001	6.5	351.1	114.8	-40	-10	-20	-11
13,14-dihydro-15-keto-$PGF_{2\alpha}$	LMFA03010027	6.6	353.1	195.0	-110	-10	-32	-11
AT-RvD1	LMFA04000074	6.7	375.0	215.0	-50	-10	-26	-11
RvD1	LMFA04000006	6.7	375.1	215.0	-50	-10	-26	-11
epi-LXA_4	LMFA03040003	6.8	351.1	114.9	-20	-10	-22	-11
RvE2	LMFA03070036	7.8	333.1	114.9	-35	-10	-18	-15
18S-RvE3	LMFA03070048	8.8	333.1	245.2	-25	-10	-16	-17
6-trans-LTB_4	LMFA03020013	8.9	335.1	194.9	-105	-10	-22	-11
8S,15S-diHETE	LMFA03060050	8.9	335.1	207.9	-55	-10	-22	-17
LTD_4	LMFA03020006	9.0	495.1	177.0	-70	-10	-28	-19
6-trans-12-epi-LTB_4	LMFA03020014	9.1	335.1	194.9	-80	-10	-22	-25
10S,17S-diHDHA (PDX)	LMFA04000047	9.2	359.1	153.0	-70	-10	-22	-9
18R-RvE_3	LMFA03070049	9.2	333.1	245.0	-55	-10	-18	-23
7S-MaR1	n.a.	9.3	359.1	249.9	-20	-10	-20	-19
MaR1	LMFA04000048	9.4	359.2	250.2	-65	-10	-20	-13
LTB_4-d_4	LMFA03020030	9.4	339.1	196.9	-70	-10	-22	-19
LTB_4	LMFA03020001	9.4	335.1	195.0	-65	-10	-22	-21
14,15-diHETE	LMFA03060077	9.5	335.1	207.0	-65	-10	-24	-21
7,17-diHDPA	n.a.	9.5	361.1	198.9	-45	-10	-26	-23
LTE_4	LMFA03020002	9.6	438.1	333.1	-55	-10	-26	-15
19,20-diHDPA	LMFA04000043	10.2	361.1	273.0	-55	-10	-22	-15

Symbol	Lipid Maps ID	RT (min)	Q1 (m/z)	Q3 (m/z)	DP (Volts)	EP (Volts)	CE (Volts)	CCEP (Volts)
9-HOTrE	LMFA02000024	10.2	293.0	170.9	-75	-10	-20	-15
13-HOTrE	LMFA02000051	10.3	293.0	195.0	-45	-10	-24	-19
18-HEPE	LMFA03070038	10.4	317.1	259.0	-5	-10	-16	-7
15-HEPE	LMFA03070009	10.5	317.1	219.0	-65	-10	-18	-19
13-HODE	LMFA02000228	10.8	295.0	194.9	-110	-10	-24	-21
9-HODE	LMFA02000188	10.8	295.0	171.0	-130	-10	-22	-7
15-HETE-d_8	LMFA03060080	10.9	327.2	226.0	-85	-10	-18	-11
15-HETE	LMFA03060001	11.0	319.1	219.1	-55	-10	-18	-9
11-HETE	LMFA03060003	11.1	319.1	167.0	-70	-10	-22	-15
17-HDHA	LMFA04000072	11.1	343.1	245.0	-65	-10	-16	-15
12-HETE	LMFA03060007	11.2	319.1	179.0	-65	-10	-20	-23
8-HETE	LMFA03060006	11.2	319.1	154.9	-70	-10	-20	-19
5-HETE	LMFA03060002	11.3	319.1	115.0	-65	-10	-18	-11
ALA	LMFA01030152	12.4	277.0	233.0	-90	-10	-22	-29
EPA	LMFA01030759	12.4	301.0	202.9	-125	-10	-18	-21
DHA-d_5	LMFA01030762	12.4	332.0	288.1	-75	-10	-16	-13
DHA	LMFA01030185	12.7	327.1	229.2	-115	-10	-18	-11
AA	LMFA01030001	12.7	303.0	205.1	-155	-10	-20	-11
LA	LMFA01030120	12.8	279.0	261.0	-115	-10	-28	-13
DPA n-3	LMFA04000044	13.0	329.1	231.1	-50	-10	-20	-17
AdA	LMFA01030178	13.1	331.1	233.0	-130	-10	-22	-11

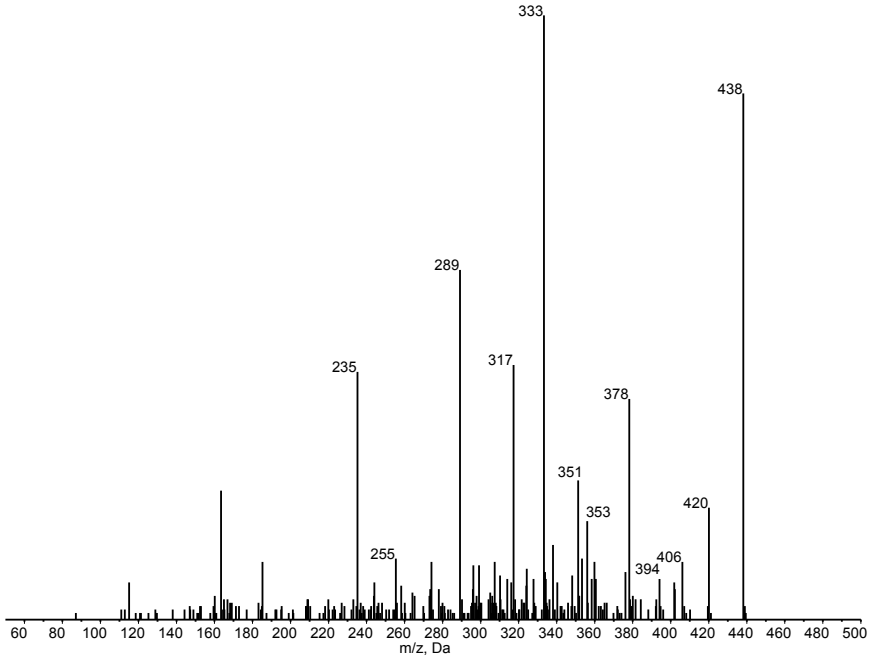

Figure S4a: MS/MS of 0.1 ng/mL standard sample at Relative RT 1.016 (Leukotriene E_4).

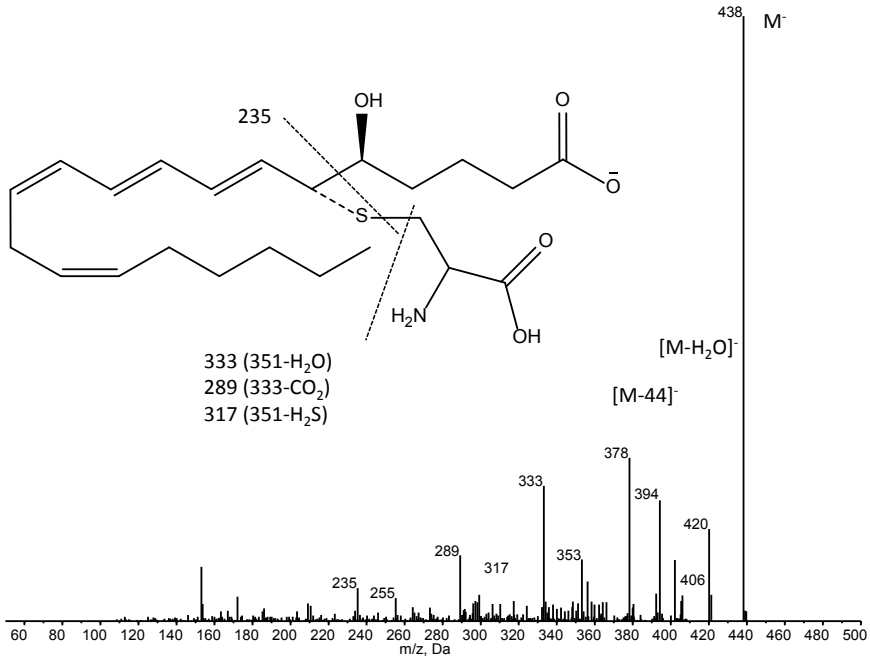

Figure S4b: MS/MS spectra of representative sample at Relative RT 1.015 (Leukotriene E_4).

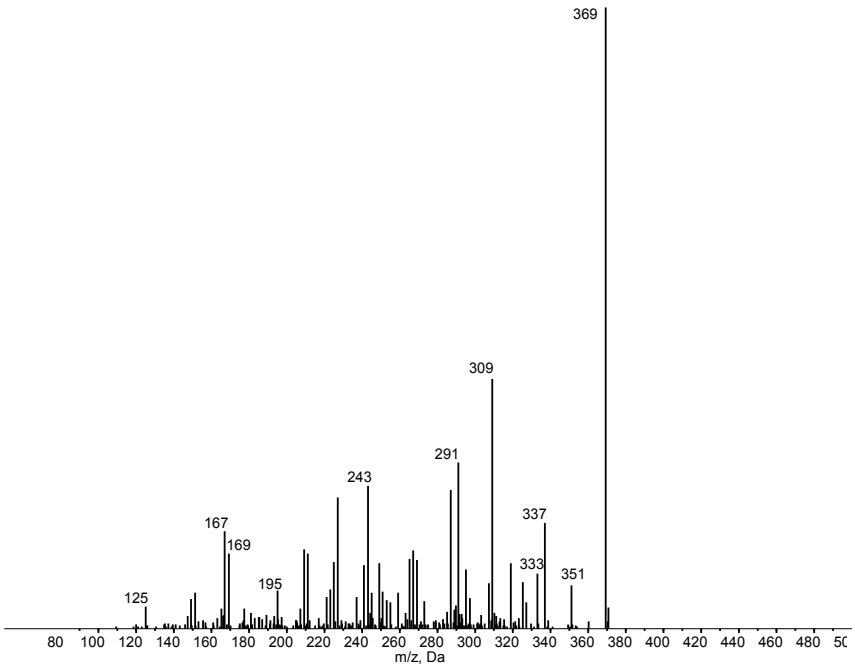

Figure S5a: MS/MS spectra of 0.1 ng/mL standard sample at Relative RT 0.925 (Thromboxane B_2).

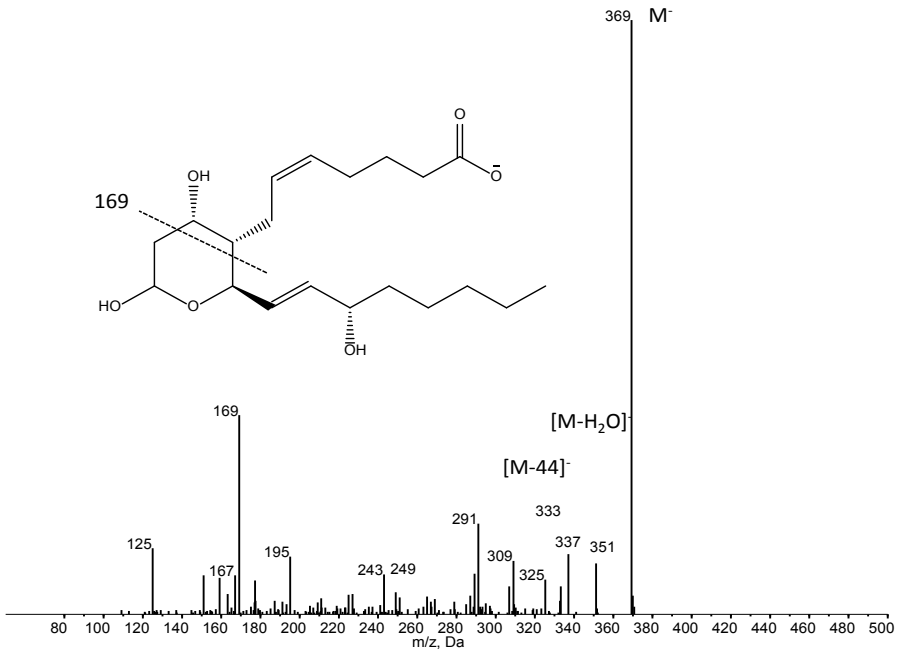

Figure S5b: MS/MS spectra of representative sample at Relative RT 0.927 (Thromboxane B_2).

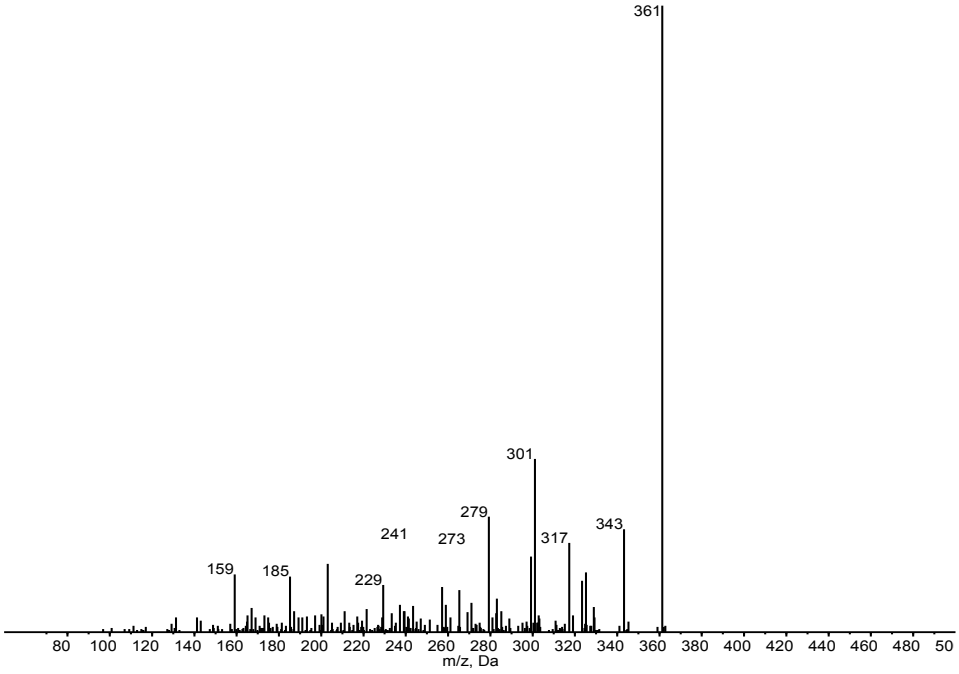

Figure S6a: MS/MS spectra of 0.1 ng/mL standard sample at Relative RT 1.087 (19,20-diHDPA).

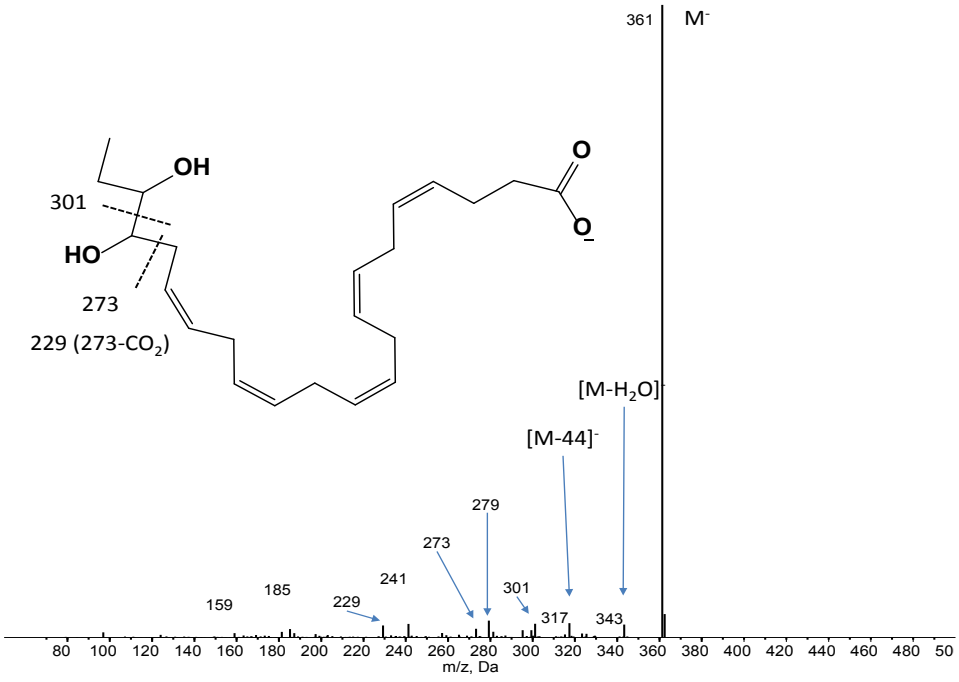

Figure S6b: MS/MS spectra of representative sample at Relative RT 1.087 (19,20-diHDPA).

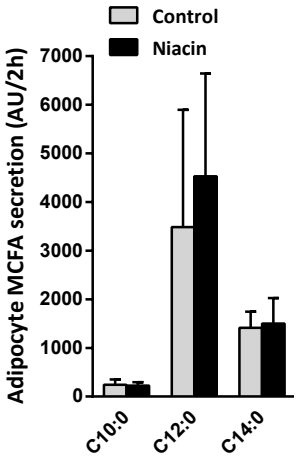

*Figure S7: Release of medium chain saturated fatty acids from adipocytes isolated from APOE*3-Leiden.CETP mice fed a western type diet with 0.1% cholesterol with and without niacin. Fatty acid release in arbitrary units during a 2 hour ex vivo basal incubation. Mean±SD, N=14 for Control/N=13 for Niacin.*

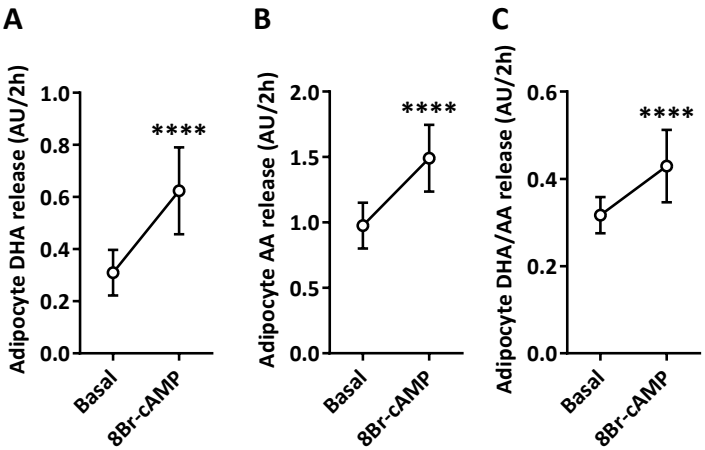

*Figure S8: Release of DHA and AA from adipocytes isolated from APOE*3-Leiden.CETP mice fed a western type diet with 0.1% cholesterol without niacin. Fatty acid release in arbitrary units during a 2 hour ex vivo incubation in basal and 8Bromo-cAMP stimulated conditions. Mean±SD, N=14 for Control/N=13 for Niacin. **** p<0,0001 for Basal vs 8Br-cAMP.*

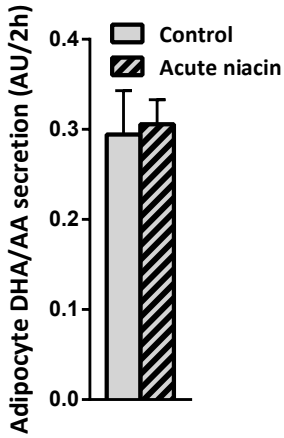

*Figure S9: Ratio of DHA/AA released fatty acids from adipocytes isolated from APOE*3-Leiden.CETP mice fed a western type diet with 0.1% cholesterol without niacin. Fatty acid release in arbitrary units during a 2 hour ex vivo incubation under basal and acute niacin conditions. Mean±SD, N=14 for Control/N=10 for Acute niacin.*

6

Increased PUFA content and 5-lipoxygenase pathway activity are associated with subcutaneous adipose tissue inflammation in obese women

Mattijs M. Heemskerk, Martin A. Giera, Fatiha el Bouazzaoui, Mirjam A. Lips, Hanno Pijl, Ko Willems van Dijk, Vanessa van Harmelen

Submitted to Nutrients **2015**

Abstract

Background/Objectives: White adipose tissue inflammation plays an important role in the development of insulin resistance and type 2 diabetes mellitus (T2DM). We have previously shown that obese women with T2DM have more inflammation in their subcutaneous adipose tissue than age and BMI similar obese women with normal glucose tolerance (NGT). The aim of the current study was to investigate whether adipose tissue fatty acids and/or oxylipins are associated with the enhanced inflammatory state in adipose tissue of the T2DM women.

Subjects/Methods: Fatty acid profiles were measured by GC-MS in both subcutaneous (sWAT) and visceral adipose tissue (vWAT) of 19 obese (BMI>40kg/m^2) women with NGT and 16 BMI-and age-comparable women with T2DM. Oxylipin levels (in total 49 lipid mediators) were measured in sWAT of all women.

Results: Arachidonic acid (AA) and docosahexaenoic acid (DHA) percentages were higher in sWAT but not vWAT of the T2DM women and correlated positively (trend for DHA) to *CD68* gene expression levels. For the oxylipins there were tendencies for higher concentrations of the leukotrienes, LTD_4, 6-*trans* LTB_4 and 6-*trans*-12-*epi* LTB_4, in sWAT of T2DM women. Gene expression of *ALOX5, ALOX5AP* and *DPEP2* (involved in the 5-LOX leukotriene biosynthesis pathway) was significantly higher in sWAT of T2DM women.

Conclusions: In conclusion, AA and DHA content were higher in sWAT of T2DM women and correlated to the inflammatory state in the tissue. The increased AA content was accompanied by an up-regulation of the 5-LOX pathway and this seems to have led to a modest increase in the conversion of AA into pro-inflammatory leukotrienes in the subcutaneous adipose tissue.

Introduction

Obesity is closely associated with insulin resistance, type-2 diabetes mellitus (T2DM), dyslipidemia, hypertension and cardiovascular disease. Expanding adipose tissue plays an important role in the patho-physiology of obesity-associated disorders as it responds to the energy overload with stress signals which in turn can elicit local immune responses and inflammation [1]. Although the majority of obese individuals (~80%) will eventually develop metabolic disorders associated with a reduced life expectancy, there seems to be a subset of obese individuals that remains relatively insulin sensitive and metabolically healthy throughout life [2, 3]. The reason why these individuals are unaffected is still not completely understood**.** We have previously shown that subcutaneous white adipose tissue (sWAT) from obese women with T2DM contained a larger number of crown-like-structures (CLS) than sWAT of similarly obese women with normal glucose tolerance (NGT) [4]. In a parallel study, we analyzed the transcriptome in adipose tissue samples by RNA deep sequencing in the same cohort of women and observed an up-regulation of genes in inflammatory pathways and a down-regulation of genes in metabolic pathways in WAT of the women with T2DM [5]. Our data thus indicate that metabolically healthy and unhealthy obese women can be differentiated by the inflammatory status of their adipose tissue.

Adipose tissue inflammation involves the accumulation of macrophages in CLS around adipocytes that are stressed or dying due to cellular lipid overload [6]. The enlarged stressed adipocytes exhibit an increased release of pro-inflammatory adipocytokines and chemokines which attract immune cells into the adipose tissue [7]. Hypertrophic adipocytes also store and release increased levels of fatty acids which are known to mediate inflammatory processes as well [8]. Not only the amount of fatty acids released, but also the type of fatty acid stored in adipose tissue has been associated to systemic inflammation [9] and T2DM [10, 11]. For example, an increased percentage of saturated fatty acids or their metabolites has been suggested to induce inflammation by activating Toll-like receptor 4, which in turn leads to an up-regulation of the ceramide biosynthesis pathway [12]. Ceramides activate the NLPR3 inflammasome which is an important contributor to obesity induced inflammation and insulin resistance [13]. Other fatty acids that are involved in inflammation are the polyunsaturated fatty acids (PUFAs). n-3 and n-6 PUFAs can induce pro- and anti-inflammatory pathways respectively [14] via a variety of different mechanisms including signaling via GPR120. PUFAs can be converted to inflammatory lipid mediators called oxylipins. Oxylipin synthesis usually occurs via the cyclooxygenase (COX), lipoxygenase (LOX) or cytochrome P450 (CYP) pathways [15]. All three pathways can metabolize both n-3 and n-6 PUFAs, but the affinity for these substrates differs as does the pro- or anti-inflammatory potency of the different resulting products. For example the 2-series prostaglandins, synthesized from arachidonic acid (AA; C20:4n-6) via the COX pathway, induce mainly pro-inflammatory effects; while the 3-series prostaglandins, synthesized from eisosapentaenoic acid (EPA; 20:5n-3) via COX, induces less potent inflammatory effects [16] and the epoxy metabolites derived from n-3 PUFAs via the

CYP pathway induce anti-inflammatory effects [17]. PUFA-derived oxylipin synthesis can be rapidly induced when triggered by inflammasome signaling [18]. A wide range of oxylipins has been identified in both human [19] and mouse WAT [20]. Oxylipins have been shown to play a role in WAT inflammation, mostly in rodent studies [8]. In the current study we hypothesized that the adipose fatty acid composition is linked to the enhanced inflammatory state in adipose tissue of obese women with T2DM. To test this hypothesis, we determined fatty acid profiles by GC-MS and oxylipin profiles by LC-MS/MS in white adipose tissue of both obese women with T2DM and obese women with NGT.

Subjects and methods

Subjects

The study group consisted of 19 obese women with normal fasting glucose (i.e. normal glucose tolerant (NGT)) and 16 women with T2DM. The women were part of a clinical trial of which the research methods and design have been described elsewhere [21]. The groups were comparable for age and BMI (see Table 1). All women had been morbidly obese (mean BMI=43.4 ± 3.8 kg/m^2) for at least five years. Women who reported the use of weight loss medications within 90 days prior to enrolment in the study were excluded. Body weight of all women had been stable for at least 3 months prior to inclusion. All women were non-smokers, had no signs of any infections nor had any history of auto-immune diseases. The women underwent bariatric surgery (gastric bypass or banding). Within 1h after opening the abdominal wall adipose tissue specimens were taken from the epigastric region of the abdominal wall (subcutaneous sWAT) and from the major omentum (visceral vWAT). These samples were used for determination of fatty acid composition and oxylipin profiles. The study (ClinicalTrials.gov: NTC01167959) was approved by the p5. All subjects gave informed consent to participate in the study.

Medication

For obvious reasons we could not restrict obese individuals to not using any type of medication. All T2DM women were treated with oral medication only (metformin or sulfonylurea derivatives). Participants were allowed to use cholesterol lowering statins and antihypertensive medication. The use of drugs such as statins and antihypertensive drugs was slightly higher in the T2DM women. The patients were not using any anti-inflammatory agents (i.e. NSAIDS, thiazolidinediones or steroids (prednisone)).

Analysis of number of crown like structures and adipocyte size

In a previous study the number of crown like structures in the adipose tissue of our participants was determined by immunohistochemistry and the adipocyte size by direct microscopy [4].

Fatty acid composition of WAT by GC-MS

FA composition analysis of sWAT and vWAT was carried out as described recently by Kloos *et al.* [22]. Briefly: approximately 10 mg WAT was weighed from the obese women. 1 ml of water, 3 ml of methanol and 1 ml of 10M NaOH were added, the samples flushed with argon and hydrolyzed for 1 h at 90 °C. After acidification with 2 ml of 6M HCl, 10 µl of an internal standard solution ([$^2H_{31}$]palmitic acid and ergosterol 10 µg/ml each) was added. The

samples were extracted twice with 3 ml *n*-hexane and the combined organic extracts were dried under a gentle stream of nitrogen. Dried samples were derivatized using 25 µl of *N*-tert.-butyldimethylsilyl-*N*-methyltrifluoroacetamide (Sigma Aldrich, Schnelldorf, Germany) for 10 min at 21 °C, subsequently 25 µl of *N*,*O*-bis(trimethylsilyl)trifluoroacetamide containing 1% trimethylchlorosilane (Thermo Scientific, Waltham, MA, USA) and 2.5 µl of pyridine were added and the sample was heated for 15 min to 50 °C. Next, 947.5 µl of *n*-hexane, containing 10 µg/ml octadecane (C18) as system monitoring component, was added.

Samples were analyzed in SIM mode on a Scion TQ GC-MS (Bruker, Bremen, Germany) equipped with a 15 m × 0.25 mm × 0.25 mm BR5MS column (Bruker). The injection volume was 1 µl, the injector was operated in splitless mode at 280 °C and the oven program was as follows: 90 °C kept constant for 0.5 min, then ramped to 180 °C with 30 °C/min then to 250 °C with 10 °C/min then to 266 °C with 2 °C/min and finally to 300 °C with 120 °C/min, kept constant for 2 min. Helium (99.9990%, Air Products, The Netherlands) was used as carrier gas. For data analysis a total area correction was applied.

Oxylipin measurements in WAT by LC-MS/MS

Oxylipin analysis was carried out as described elsewhere ([23],[24]) with some modifications. Approximately 100 mg of tissue were cut using a razor blade on a glass plate, transferred into a 2 ml Eppendorf tube and accurately weighed. Three µl of an internal standard solution containing 50 ng/ml each of PGE_2-d4, LTB_4-d4, 15-HETE-d8 and DHA-d5 was added. Subsequently 3-5 stainless steel beads, 500 µl of methanol and 2 µl of a 20 mg/ml butylated hydroxyl toluene solution were added. Next, the samples were homogenized in a bead beater for 4 min centrifuged at 16100 g for 3 min. 400 µl of the supernatant were transferred into a 12 ml glass tube. The samples were re-extracted using 500 µl of methanol by shaking for 5 min. The combined organic extracts were diluted with approximately 9 ml of water, acidified with 6M HCl and further cleaned up using solid phase extraction (employing 100 mg SPE columns) as described elsewhere [25] and finally reconstituted in 150 µl 40% methanol before LC-MS/MS analysis.

Statistics

Data are expressed as mean ± SD or as median and range of the values. Differences between NGT and T2DM were analyzed using unpaired non-parametric t-test's. Linear regression was used to analyze correlations using the F-test in Graphpad Prism 6 (GraphPad Software, CA, USA).

Results

Characteristics of participants

Characteristics of the participants are shown in Table 1. Fasting plasma glucose and LDL-cholesterol levels were significantly higher in T2DM than in NGT women. HOMA-IR index and triglyceride levels tended to be higher in the T2DM women. The gene expression of *CD68* (a macrophage marker) and the number of CLS per area adipose tissue on immunohistochemistry slides was used as an index for the extent of adipose tissue inflammation. The sWAT but not the vWAT of the T2DM women had a significantly higher gene expression of *CD68* and contained more CLS. Adipocyte sizes did not differ between NGT and T2DM women both for sWAT and vWAT.

Table 1: Characteristics of the NGT and T2DM women. Crown like structures (CLS) were determined by immunohistochemistry of CD68 and expressed as number (#) of CLS per area of adipose tissue (AT) section on the slide. Adipocyte size was expressed as mean adipocyte diameter in µm. CLS counts and adipocyte sizes have been published previously [4]. Gene expression was determined by RNA deep sequencing in a previous study [5] and expressed as log transformed normalized gene expression levels (relative units [RU]: log2-scale). Data are expressed as mean ± SD.

	NGT	T2DM	P-value t-test
N	19	16	
BMI (kg/m^2)	43.4 ±3.3	43.4±4.5	NS
Age (y)	47±7	52±6	NS
Weight (kg)	121±8	127±12	NS
HOMA-IR	2.7±2.2	4.0±3.0	0.08
Fasting glucose (mmol/l)	5.0±0.6	9.0±2.6	<0.01
Fasting insulin (mU/l)	10.9±7.7	13.3±7.3	NS
Total cholesterol (mmol/l)	4.7±1.1	4.2±0.8	NS
HDL cholesterol (mmol/l)	1.1±0.3	1.1±0.3	NS
LDL cholesterol (mmol/l)	3.0±1.0	2.2±0.6	0.03
Triglycerides (mmol/l)	1.5±0.7	2.0±0.7	0.08
CRP (mg/l)	7.8±7.5	8.2±6.3	NS
CD68 gene expression in sWAT	8.2±0.4	8.9±0.7	0.003
CD68 gene expression in vWAT	8.2±0.4	8.4±0.5	NS
# of CLS in sWAT (no/AT section)	2.3±1.4	12.3±7.1	0.05
# of CLS in vWAT (no/AT section)	1.9±1.2	2.7±1.0	NS
Adipocyte size in sWAT (µm)	122±16	126±15	NS
Adipocyte size in vWAT (µm)	112±16	118±8	NS

Differences in adipose tissue content of saturated fatty acids and PUFAs between NGT and T2DM obese women

The fatty acid composition of sWAT and vWAT samples from the NGT and T2DM obese women was determined by GC-MS. For both sWAT and vWAT for the T2DM women, we found lower percentages of C10:0 (Decanoic acid) and C12:0 (Lauric acid) (Fig. 1A). The MUFAs did not show large differences between the NGT and T2DM women (Fig. 1B). For the PUFAs in vWAT of the T2DM women, a lower percentage of C18:3n-6 (gamma-linolenic acid) was seen. In the sWAT of the T2DM women, differences in both n-6 and n-3 PUFAs were found. For the n-6 PUFAs higher percentages of C20:4n-6 (Arachidonic acid (AA)) and C22:4n-6 (Adrenic acid (AdA)) were found (Fig. 1C), whereas for the n-3 PUFAs higher percentages of C20:3n-3 (Eicosatetraenoic acid (ETA)), C20:5n-3 (Eicosapentaenoic acid (EPA)), C22:5n-3 (Docosapentaenoic acid (DPA)) and C22:6n-3 (Docosahexaenoic acid (DHA)) were found (Fig. 1D).

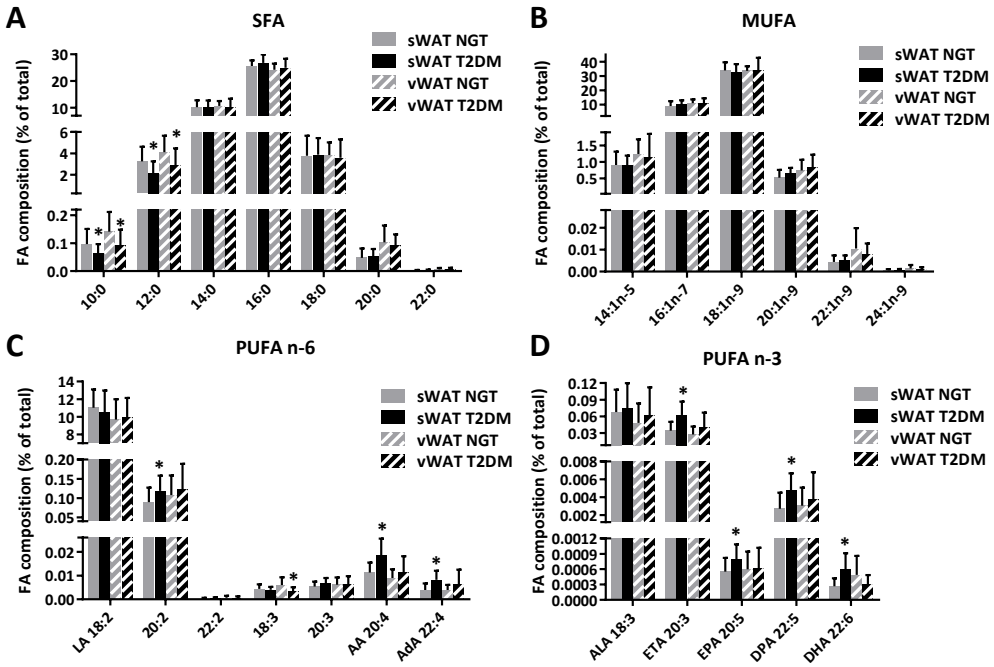

*Figure 1: Fatty acid composition of sWAT and vWAT for NGT versus T2DM individuals. A) Saturated fatty acids. B) Mono-unsaturated fatty acids. C) n-6 and D) n-3 poly-unsaturated fatty acids. Data are expressed as mean ± SD. *p<0.05 for NGT vs T2DM.*

Arachidonic acid and docosahexaenoic acid correlated to CD68 expression in sWAT

The percentage AA of the total fatty acid pool correlated to the gene expression level of *CD68* in sWAT and a trend was visible for DHA. For the correlation of AA with *CD68* expression the goodness-of-fit was r=0.42, p=0.029 (Fig. 2A). For the correlation of DHA with *CD68* expression the goodness-of-fit was r=0.34, p=0.087 (Fig. 2B). There were no significant correlations between any other fatty acid percentage and *CD68* expression in sWAT.

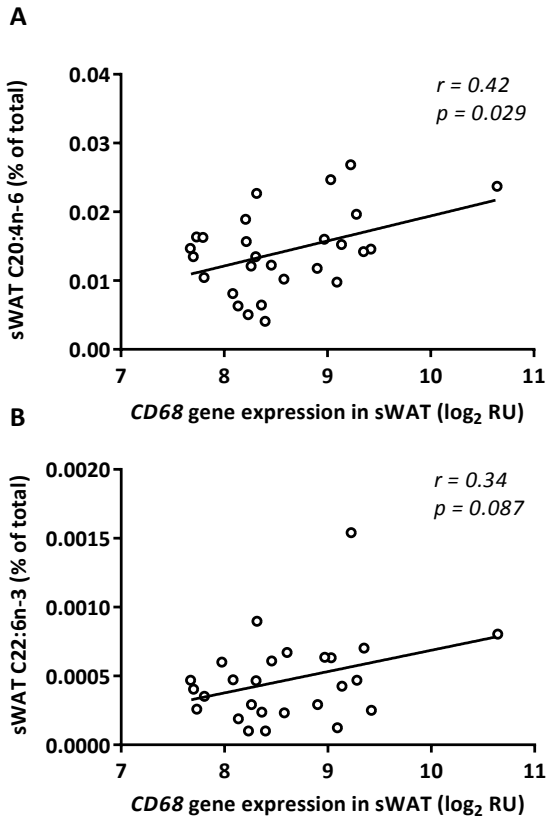

Figure 2: CD68 expression versus PUFA percentage in sWAT. Linear regression of sWAT gene expression of the macrophage marker CD68 with the sWAT percentage of C20:4n-6 (AA) and C22:6n-3 (DHA). Data are log transformed normalized gene expression levels (relative units [RU]: log2-scale). Data are expressed as mean ± SD.

Oxylipin levels in sWAT of women with NGT and T2DM

Table 2 shows the list of the oxylipins that were measured and the levels that were detected per mg of sWAT of the women with NGT and with T2DM. Many of the oxylipins measured, in particular the resolvins, were below the detection limit (see Table 2). There was a large variation in oxylipin concentrations between the women. Of the detectable oxylipins there was a tendency for higher content of some leukotrienes; i.e. LTD_4, 6-*trans* LTB_4 and 6-*trans*-12-*epi* LTB_4 in sWAT of women with T2DM (See Fig. 3A).

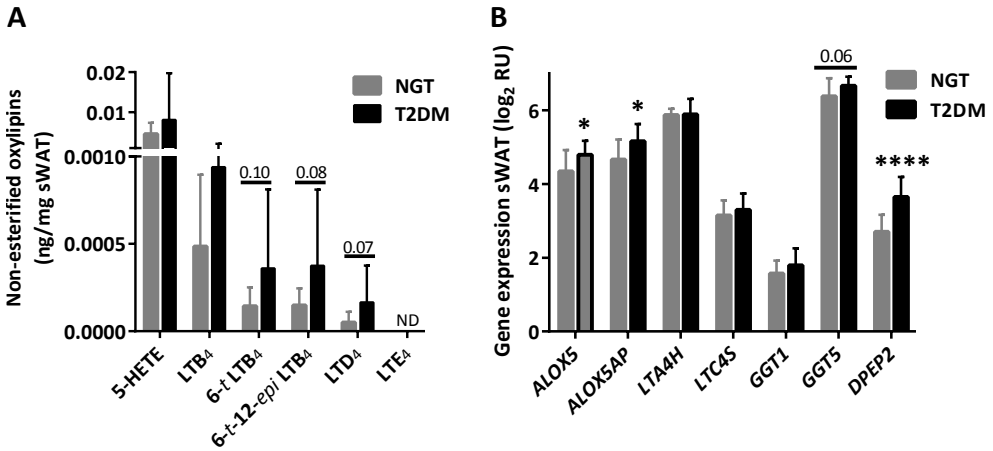

*Figure 3: 5-LOX oxylipins in sWAT. A) Non-esterified oxylipins derived from arachidonic acid via the 5-LOX pathway in sWAT of NGT vs T2DM obese individuals. LTE_4 was below the detection limit (ND=not detectable). LTA_4, LTC_4 and LTF_4 were not included in the LC-MS/MS method. B) Gene expression of genes involved in the leukotriene biosynthesis pathway in sWAT of NGT versus T2DM individuals (ALOX5, ALOX5AP, LTA4H, LTC4S, GGT1, GGT5 and DPEP2). Data are log transformed normalized gene expression levels (relative units [RU]: log2-scale). Data are expressed as mean ± SD. *p<0.05 and ****p<0.0001 for NGT vs T2DM.*

*Table 2: Oxylipins in sWAT of NGT versus T2DM obese women. NGT vs T2DM values were compared using non-parametric t-test. ND= non-detectable. NS= non-significant. *= Compound not in calibration line. P-value calculated from area ratios compared to internal standard. #= Detected, but only in fewer than five individuals in total. Data are expressed as median and range of the concentrations.*

	NGT		T2DM		NGT vs T2DM
Oxylipin (ng/mg sWAT)	**Range**	**Median**	**Range**	**Median**	**P-value**
5-HETE	7.91E-04 - 3.19E-02	3.70E-03	1.47E-03 - 5.07E-02	5.01E-03	NS
8-HETE	4.53E-04 - 1.83E-02	2.28E-03	5.56E-04 - 2.24E-02	2.86E-03	NS
11-HETE	3.58E-04 - 1.46E-02	1.55E-03	3.90E-04 - 1.84E-02	1.89E-03	NS
12-HETE	1.63E-03 - 8.36E-02	1.06E-02	2.77E-03 - 7.90E-02	1.17E-02	NS
15-HETE	7.36E-04 - 3.20E-02	3.49E-03	8.13E-04 - 4.62E-02	4.04E-03	NS
15-HEPE	9.23E-05 - 3.13E-03	4.36E-04	1.54E-04 - 2.62E-03	5.72E-04	NS
18-HEPE	1.25E-04 - 4.94E-03	5.55E-04	2.40E-04 - 3.91E-03	5.04E-04	NS
7-HDHA	*		*		NS
10-HDHA	*		*		NS
17-HDHA	0 - 3.17E-03	5.34E-04	0 - 3.23E-03	1.14E-03	NS
LTB_4	6.42E-05 - 2.69E-03	4.10E-04	4.66E-05 - 4.17E-03	4.24E-04	NS
6-*trans*-12-*epi* LTB_4	2.97E-05 - 3.22E-04	1.29E-04	5.98E-05 - 1.71E-03	1.90E-04	0.08
6-*trans* LTB_4	3.91E-05 - 4.36E-04	1.14E-04	6.39E-05 - 1.86E-03	1.57E-04	0.10
20-OH LTB_4	ND		ND		
LTD_4	0 - 2.08E-04	3.80E-05	0 - 7.75E-04	7.74E-05	0.06
LTE_4	ND		ND		
PGD_2	5.79E-05 - 1.14E-03	2.26E-04	3.93E-05 - 2.65E-03	2.68E-04	NS
PGE_2	7.06E-05 - 2.12E-03	5.95E-04	7.68E-05 - 3.58E-03	4.76E-04	NS
$PG_{F2}\alpha$	0 - 2.12E-03	6.94E-04	1.02E-04 - 2.53E-03	5.11E-04	NS
TxB_2	0 - 1.24E-02	1.54E-03	4.49E-05 - 2.05E-02	1.59E-03	NS
LXA_4	0 - 2.49E-04	0	0 - 1.53E-03	1.52E-05	NS
LXB_4	ND		ND		
AT LXA_4	ND		ND		
8-*iso* PGE_2	ND		ND		
8-*iso* $PGF_{2\alpha}$	0 - 1.83E-04	4.50E-05	0 - 7.64E-04	4.39E-05	NS
15-*keto* PGE_2	1.69E-05 - 3.62E-04	8.60E-05	6.63E-06 - 1.21E-03	6.35E-05	NS
13,14-dihydro-15-*keto* $PGF_{2\alpha}$	0 - 5.05E-03	0	0 - 4.60E-03	0	NS
RvD1	ND		ND		
RvD2	ND		ND		
AT RvD1	ND		ND		
RvE1	ND		ND		
RvE2	#		#		
18S-RvE3	ND		ND		
18R-RvE3	ND		ND		

	NGT		T2DM		NGT vs T2DM
Oxylipin (ng/mg sWAT)	**Range**	**Median**	**Range**	**Median**	**P-value**
7,17-DiHDPA	0 - 1.68E-03	7.39E-05	0 - 8.76E-04	0.00E+00	NS
19,20-DiHDPA	0 - 3.53E-04	9.56E-05	5.99E-05 - 4.30E-04	1.11E-04	NS
10S,17S-diHDHA (PDX)	0 - 1.97E-04	4.00E-05	0 - 2.44E-04	3.93E-05	NS
MaR1	#		#		
7S-MaR1	ND		ND		
5,15-diHETE	0 - 2.08E-02	2.20E-03	0 - 8.71E-02	3.43E-03	NS
14,15-diHETE	0 - 6.32E-04	2.21E-04	0 - 2.15E-03	1.85E-04	NS
8S,15S-diHETE	4.00E-05 - 1.32E-03	1.47E-04	0 - 1.63E-03	1.85E-04	NS
9-HoDE	7.46E-02 - 9.24E-01	3.17E-01	1.27E-01 - 8.32E-01	2.59E-01	NS
13-HoDE	4.74E-02 - 5.27E-01	1.61E-01	6.52E-02 - 4.71E-01	1.42E-01	NS
9-HoTrE	3.41E-03 - 4.90E-02	2.08E-02	3.89E-03 - 3.74E-02	1.49E-02	NS
13-HoTrE	4.45E-02 - 5.02E-01	2.85E-01	5.68E-02 - 3.96E-01	1.95E-01	NS
8(9)EET	*		*		NS
11(12)EET	*		*		NS
14(15)EET	*		*		NS

Differential expression of ALOX5, ALOX5AP and DPEP2 in sWAT between NGT and T2DM women

In a previous study, the adipose tissues of 15 of the NGT and 15 of the T2DM women included in the current study were used for transcriptome analysis by RNA deep sequencing [5]. From the gene expression profiles obtained in that study we could extract gene expression levels of the genes involved in the leukotriene biosynthesis pathway (i.e. *ALOX5*, *ALOX5AP*, *LTA4H*, *LTC4S*, *GGT1*, *GGT5* and *DPEP2*). See Fig. 4 for a scheme of the leukotriene biosynthesis pathway and the genes involved therein. Of these genes *ALOX5*, *ALOX5AP* and *DPEP2* were significantly higher expressed and *GGT5* tended (p=0.06) to be higher expressed in sWAT of T2DM women (see Fig. 3B).

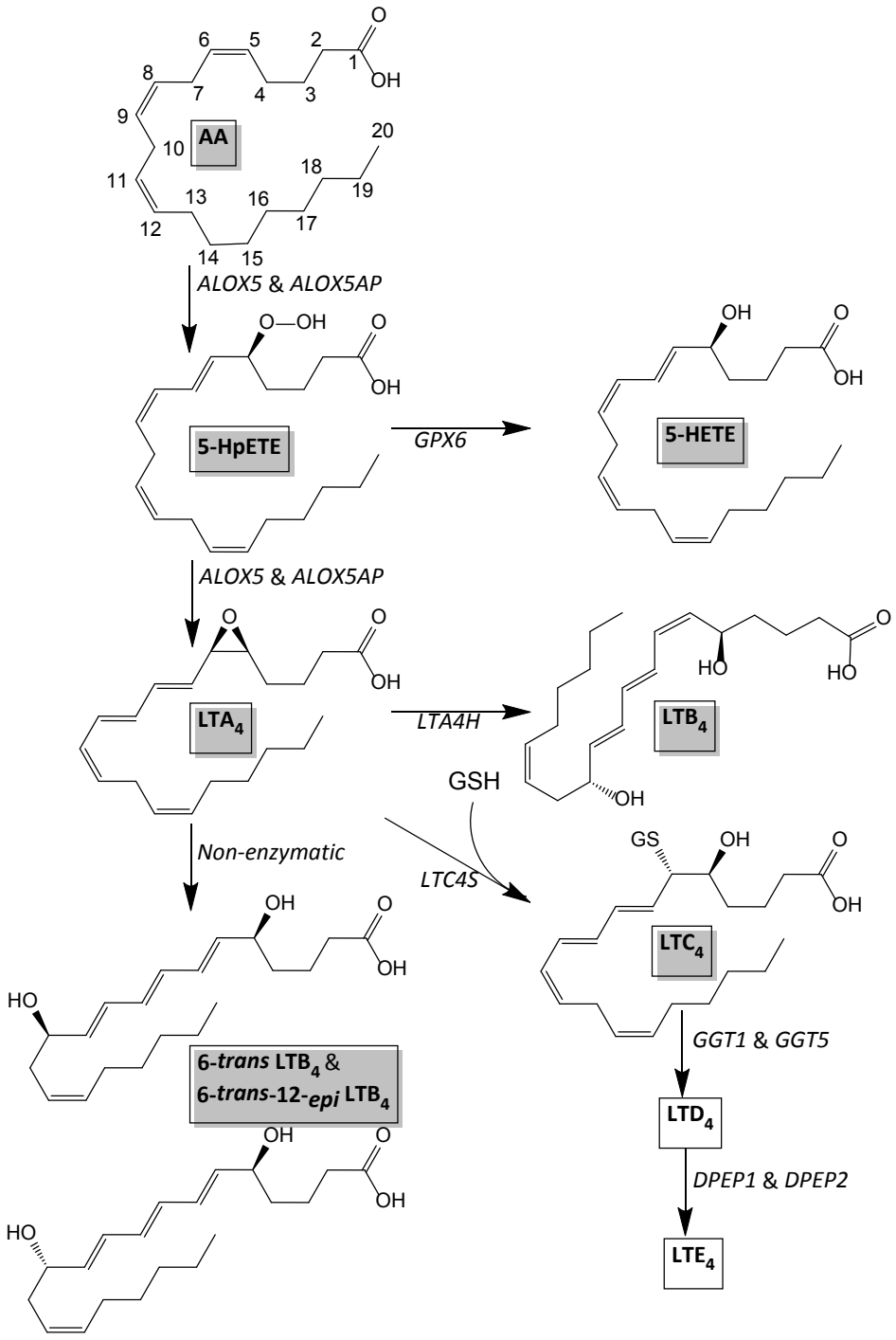

Figure 4: Leukotriene biosynthesis pathway based on Murphy et al. [26]

Discussion

We have previously shown that the macrophage content in the sWAT but not the vWAT of obese women with T2DM was higher. In the current study we investigated whether this increased inflammatory state was linked to a higher percentage of fatty acids that mediate inflammatory processes such as the saturated fatty acids or the PUFAs. We found that the higher inflammatory state in the sWAT of T2DM women was not associated with a higher percentage of saturated fatty acids. The saturated fatty acid percentages of C10:0 and C12:0 were even lower in T2DM women, both in sWAT and vWAT. Interestingly, the sWAT of T2DM women showed increased percentages of both n-3 and n-6 long-chain PUFAs (including AA and DHA) which was not seen in vWAT. AA percentage in sWAT correlated positively with gene expression of the macrophage marker *CD68* (trend for DHA) indicating that PUFAs were associated with the macrophage infiltration in the adipose tissue.

The content of PUFAs in adipose tissue is dependent on several processes including uptake of PUFAs into the cell via fatty acid transporters or passive transport, the biosynthesis of PUFAs within a cell, the degradation of PUFAs and the release of PUFAs from a cell. Previously, we analyzed the transcriptome of adipose tissue by RNA sequencing in the same individuals as included in this study [5]. By using a network-based approach to analyze gene expression in NGT versus T2DM women, we identified the down-regulation of the complete acetyl-CoA metabolic network in the adipose tissue of the T2DM women. This network included a down-regulation of fatty acid biosynthesis, fatty acid degradation as well as fatty acid release. Thus, although there seem to be clear differences in gene expression of PUFA metabolism, we cannot determine the net flux of PUFAs in the adipose tissue based on this gene expression analysis. Further research is required to determine the PUFA mass balance *in vivo* in the adipose tissue to be able to explain the increased PUFA content in the T2DM individuals.

Although most of the fatty acids in adipose tissue are stored in triglycerides within the adipocytes (99%) there is a small fraction of the fatty acids present in phospholipids. We could not determine which of the fatty acid based lipid species in the adipose tissue contributed to the difference in PUFAs in T2DM women. In addition, the (immune) cells of the stromal vascular fraction in adipose tissue contribute to the fatty acid pool and can produce fatty acid-derived mediators. Immune cells are the main producers of oxylipins [27]. It is possible that the observed difference in FA and oxylipin content are due to differences in the cellular composition of the adipose tissues. Additional research is necessary to determine whether the cellular composition of adipose tissue contributed to the observed differences in FA and oxylipin content.

Both AA and DHA can be metabolized into oxylipins with pro or anti-inflammatory properties. We detected several oxylipins in human sWAT, derived either from AA, DHA or EPA. The levels of most of these oxylipins did not differ between NGT and T2DM women, but there were tendencies for higher concentrations of some of the AA derived leukotrienes (LTD_4, 6-*trans* LTB_4 and 6-*trans*-12-*epi* LTB_4). For the leukotriene biosynthesis pathway (see Fig. 4),

AA is metabolized by 5-lipoxygenase (5-LOX) in the presence of an integral nuclear membrane protein, 5-LOX activating protein (also called FLAP). In this reaction, AA is metabolized into the sequential intermediates 5-hydroperoxyeicosatetraenoic acid (5-HpETE) and LTA_4. LTA_4 is conjugated with reduced glutathione by LTC_4 synthase (LTC4S) and released from the cell for extracellular conversion to LTD_4 and LTE_4. Alternatively, cytosolic LTA_4 hydrolase (LTA4H) converts LTA_4 to LTB_4. LTA_4 is also hydrolyzed non-enzymatically into 6-*trans* LTB_4 and 6-*trans*-12-*epi* LTB_4. To further study the leukotriene biosynthesis pathway we analyzed gene expression of genes involved in this pathway. We found a significant higher expression of *ALOX5* (5-LOX), *ALOX5AP* (FLAP) and *DPEP2* (Dipeptidase 2), indicating an overall up-regulation of the 5-LOX pathway in sWAT of T2DM women. The fact that both LTD_4 and the non-enzymatically hydrolyzed LTB_4's tended to be higher (and not only one particular leukotriene) is in line with this notion. Subcutaneous adipose tissue expression of *ALOX5AP* has previously been shown to be positively associated to body weight and insulin resistance as determined by HOMA-IR index [28]. The 5-LOX pathway has also been shown to be increased in obese adipose tissue [29]. Mouse and human adipocytes produce leukotrienes *in vitro* and this production is increased in hypertrophic adipocytes in obesity in mice [30]. Taken together, previous studies and our study suggest that the 5-LOX pathway may provide a link between adipose tissue, inflammation and insulin resistance.

The results obtained in this study differ from those of a previous study by Lieb *et al.* [31] who measured fatty acids and some downstream oxylipins in obese non-diabetic and T2DM individuals. They did not observe any differences in AA or DHA content between the subjects groups neither in sWAT nor vWAT. Instead, they observed an up-regulation of *ALOX12* expression and its metabolite 12(S)-hydroxyeicosatetraenoic acid in vWAT but not sWAT of the T2DM individuals and suggested that the ALOX12 pathway may have a critical role in adipose tissue inflammation. Differences in the subject groups (their study also included males) may explain the discrepancies between their and our study.

Most of the studies on lipid signaling and oxylipins in adipose tissue have been performed in rats or mice. We have performed a study in humans and have made a thorough analysis of several types of oxylipins and concentrations thereof in adipose tissue. We did not detect resolvins in adipose tissue apart from 10S,17S-diHDHA (PDX) and in fewer than five women we could detect some Resolvin E2 and Maresin 1. This is in contrast with several mouse studies that detected more resolvins in adipose tissue and suggested a role for these mediators in counteracting adipose tissue inflammation [32],[33],[34]. Apart from the fact that there may be species specific differences between the studies it is also possible that discrepancies can be explained by the stage of adipose tissue inflammation studied. Most of the mouse studies examine adipose tissue inflammation during a high fat diet feeding, thus during progressive adipose tissue expansion and inflammation. Our obese women had been obese for a relatively long period of time and their adipose tissue inflammation was likely fairly established. Further research is required to determine whether species-specificity or the stage and duration of obesity is responsible for the observed differences. Additionally,

the analysis of oxylipins in adipose tissue is a challenging task due to the large amounts of triglycerides and other hydrophobic matrix constituents. In the presented study we adapted a published protocol for the analysis of adipose tissue, however it has to be mentioned that the recoveries particularly for the internal standards 15-HETE-d8 and DHA-d5 were rather low (< 40%), suggesting that an improvement of the described method for further studies might be of importance. In conclusion, AA and DHA content were higher in sWAT of T2DM women and associated with the inflammatory state in the tissue. The increased AA content was accompanied by an up-regulation of the genes in the leukotriene pathway and this seems to have led to a modest increase in the conversion of AA into pro-inflammatory leukotrienes in the subcutaneous adipose tissue of individuals with T2DM.

Acknowledgements

This work was supported by grants from the Leiden University Medical Center, the Dutch Obesity Clinic, the Center of Medical Systems Biology (CMSB) and the Netherlands Consortium for Systems Biology (NCSB) established by The Netherlands Genomics Initiative/ Netherlands Organization for Scientific Research (NGI/NWO). This study was performed within the framework of the Center for Translational Molecular Medicine (http://www.ctmm.nl); project PREDICCt (grant 01C-104).

References

1 Hotamisligil GS. **2010**; Endoplasmic Reticulum Stress and the Inflammatory Basis of Metabolic Disease. *Cell* 140:900.

2 Bluher M. **2010**; The distinction of metabolically 'healthy' from 'unhealthy' obese individuals. *Current opinion in lipidology* 21:38.

3 Rey-López JP, de Rezende LF *et al.* **2014**; The prevalence of metabolically healthy obesity: a systematic review and critical evaluation of the definitions used. *Obesity reviews* 15:781.

4 van Beek L, Lips MA *et al.* **2013**; Increased systemic and adipose tissue inflammation differentiates obese women with T2DM from obese women with normal glucose tolerance. *Metabolism* 63:492.

5 Dharuri H, t Hoen PA *et al.* **2014**; Downregulation of the acetyl-CoA metabolic network in adipose tissue of obese diabetic individuals and recovery after weight loss. *Diabetologia*.

6 Cinti S, Mitchell G *et al.* **2005**; Adipocyte death defines macrophage localization and function in adipose tissue of obese mice and humans. *Journal of Lipid Research* 46:2347.

7 Vachharajani V, Granger DN. **2009**; Adipose tissue: A motor for the inflammation associated with obesity. *IUBMB Life* 61:424.

8 Masoodi M, Kuda O *et al.* **2014**; Lipid signaling in adipose tissue: Connecting inflammation & metabolism. *Biochimica et biophysica acta*.

9 Jacobsson L, Lindgarde F *et al.* **1990**; Correlation of fatty acid composition of adipose tissue lipids and serum phosphatidylcholine and serum concentrations of micronutrients with disease duration in rheumatoid arthritis. *Annals of the rheumatic diseases* 49:901.

10 Korani M, Firoozrai M *et al.* **2012**; Distribution of fatty acids in adipose tissue of patients with type 2 diabetes. *Clinical laboratory* 58:457.

11 Pezeshkian M, Mahtabipour MR. **2013**; Epicardial and subcutaneous adipose tissue Fatty acids profiles in diabetic and non-diabetic patients candidate for coronary artery bypass graft. *Bioimpacts* 3:83.

12 Masi LN, Rodrigues AC *et al.* **2013**; Fatty acids regulation of inflammatory and metabolic genes. *Current opinion in clinical nutrition and metabolic care* 16:418.

13 Vandanmagsar B, Youm Y-H *et al.* **2011**; The NLRP3 inflammasome instigates obesity-induced inflammation and insulin resistance. *Nature medicine* 17:179.

14 Simopoulos AP. **2008**; The Importance of the Omega-6/Omega-3 Fatty Acid Ratio in Cardiovascular Disease and Other Chronic Diseases. *Experimental biology and medicine* 233:674.

15 Tourdot BE, Ahmed I *et al.* **2014**; The emerging role of oxylipins in thrombosis and diabetes. *Frontiers in pharmacology* 4.

16 Ricciotti E, FitzGerald GA. **2011**;

17 Fischer R, Konkel A *et al.* **2014**; Dietary Omega-3 Fatty Acids Modulate the Eicosanoid Profile in Man Primarily via the CYP-epoxygenase Pathway. *Journal of Lipid Research* 55:1150.

18 von Moltke J, Trinidad NJ *et al.* **2012**; Rapid induction of inflammatory lipid mediators by the inflammasome in vivo. *Nature* 490:107.

19 Claria J, Nguyen BT *et al.* **2013**; Diversity of lipid mediators in human adipose tissue depots. *American journal of physiology. Cell physiology* 304:C1141.

20 Balvers MG, Verhoeckx KC *et al.* **2012**; Fish oil and inflammatory status alter the n-3 to n-6 balance of the endocannabinoid and oxylipin metabolomes in mouse plasma and tissues. *Metabolomics* 8:1130.

21 Lips MA, de Groot GH *et al.* **2014**; Calorie Restriction is a Major Determinant of the Short-Term Metabolic Effects of Gastric Bypass Surgery in Obese Type 2 Diabetic Patients. *Clinical endocrinology* 80:834.

22 Kloos DP, Gay E *et al.* **2014**; Comprehensive gas chromatography-electron ionisation mass spectrometric analysis of fatty acids and sterols using sequential one-pot silylation: quantification and isotopologue analysis. *Rapid communnications in mass spectrometry* 28:1507.

23 Heemskerk MM, Dharuri HK *et al.* **2014**; Prolonged niacin treatment leads to increased adipose tissue poly-unsaturated fatty acid synthesis and an anti-inflammatory lipid and oxylipin plasma profile. *Journal of Lipid Research* 55.

24 Jónasdóttir H, Ioan-Facsinay A *et al.* **2014**; An Advanced LC–MS/MS Platform for the Analysis of Specialized Pro-Resolving Lipid Mediators. *Chromatographia*:1.

25 Giera M, Ioan-Facsinay A *et al.* **2012**; Lipid and lipid mediator profiling of human synovial fluid in rheumatoid arthritis patients by means of LC-MS/MS. *Biochim Biophys Acta* 1821:1415.

26 Murphy RC, Gijon MA. **2007**; Biosynthesis and metabolism of leukotrienes. *Biochemical journal* 405:379.

27 Gonzalez-Periz A, Claria J. **2010**; Resolution of adipose tissue inflammation. *Scientific world journal* 10:832.

28 Kaaman M, Ryden M *et al.* **2006**; ALOX5AP expression, but not gene haplotypes, is associated with obesity and insulin resistance. *International journal of obesity* 30:447.

29 Martinez-Clemente M, Claria J *et al.* **2011**; The 5-lipoxygenase/leukotriene pathway in obesity, insulin resistance, and fatty liver disease. *Current opinion in clinical nutrition and metabolic care* 14:347.

30 Mothe-Satney I, Filloux C *et al.* **2012**; Adipocytes secrete leukotrienes: contribution to obesity-associated inflammation and insulin resistance in mice. *Diabetes* 61:2311.

31 Lieb DC, Brotman JJ *et al.* **2014**; Adipose tissue 12/15 lipoxygenase pathway in human obesity and diabetes. *Journal of clinical endocrinology and metabolism* 99:E1713.

32 Claria J, Dalli J *et al.* **2012**; Resolvin D1 and resolvin D2 govern local inflammatory tone in obese fat. *Journal of immunology* 189:2597.

33 Hellmann J, Tang Y *et al.* **2011**; Resolvin D1 decreases adipose tissue macrophage accumulation and improves insulin sensitivity in obese-diabetic mice. *FASEB journal* 25:2399.

34 Neuhofer A, Zeyda M *et al.* **2013**; Impaired local production of proresolving lipid mediators in obesity and 17-HDHA as a potential treatment for obesity-associated inflammation. *Diabetes* 62:1945.

Supplemental data

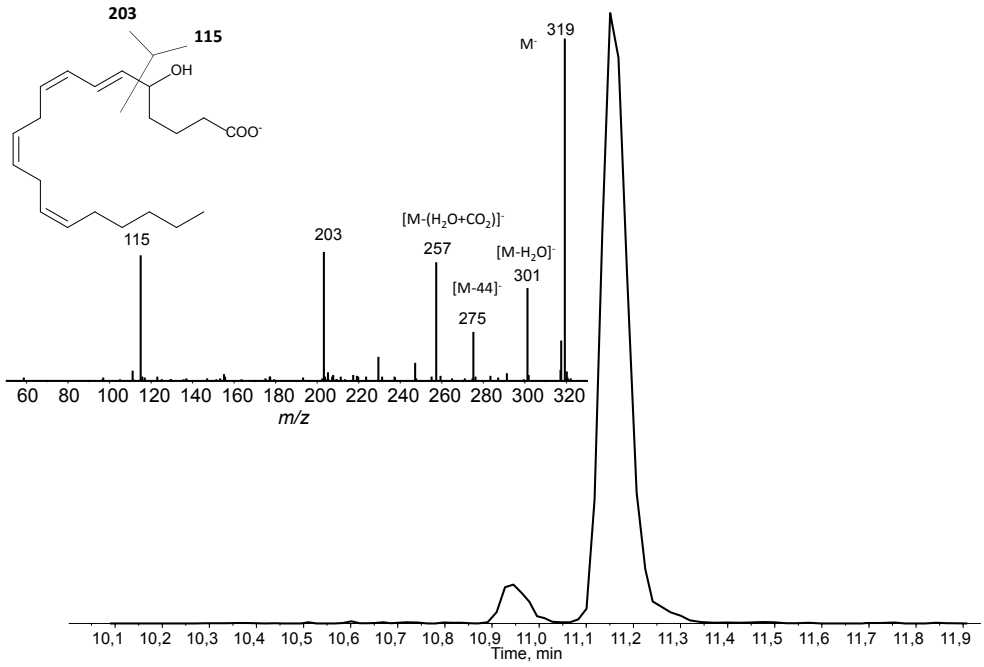

Figure S1: SRM transition m/z 319 -> 115 showing 5-HETE at RT=11.2 min and its two isomers. Upper left corner characteristic MS/MS spectrum and fragmentation of 5-HETE.

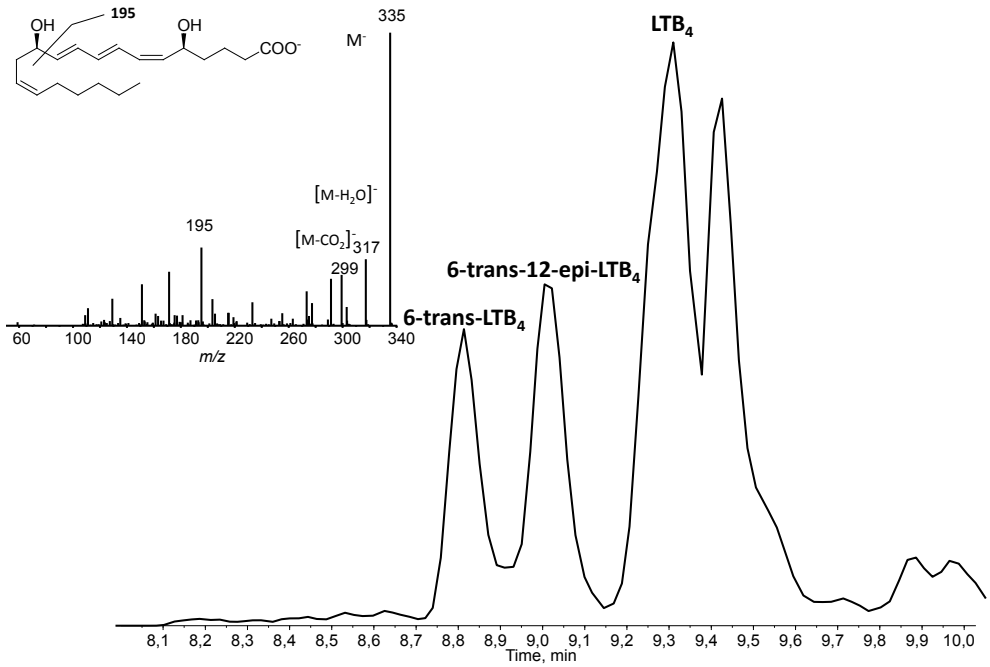

Figure S2: SRM transition m/z 335 -> 195 showing LTB_4 at RT=9.3 min and its two isomers. Upper left corner characteristic MS/MS spectrum and fragmentation of LTB_4.

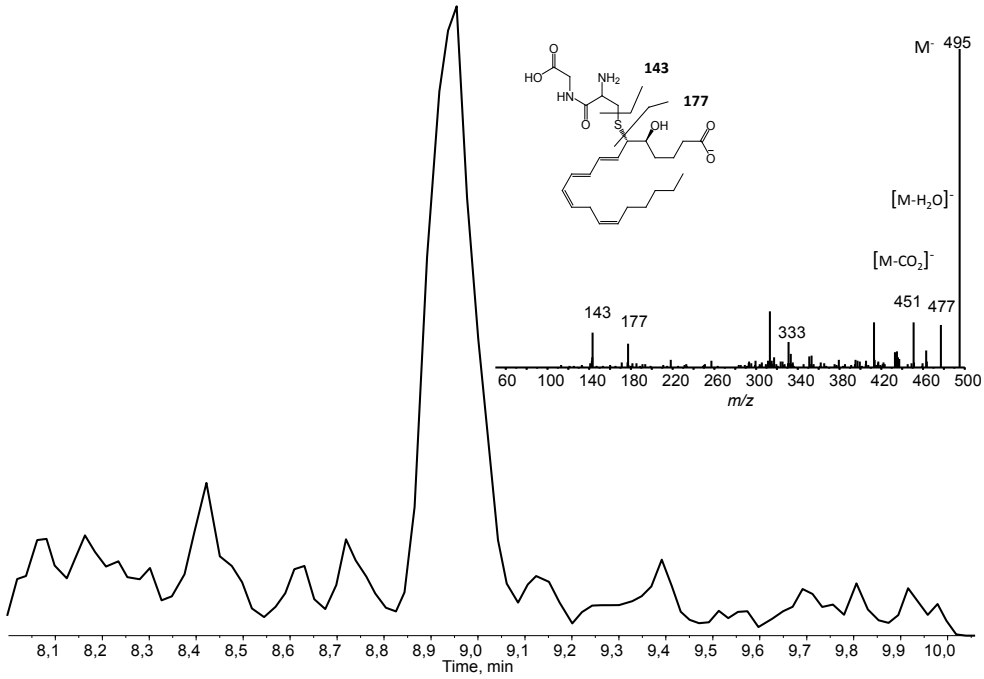

Figure S3: SRM transition m/z 495 -> 177 showing LTD_4 at RT=8.9 min. Upper right corner characteristic MS/MS spectrum and fragmentation of LTD_4.

Table S1: Multiple Reaction Monitoring setup for ion transitions of the target compounds. Symbols in bold refer to internal standards. RT=retention time, Q1=quadrupole 1 ion selection, Q3=quadrupole 3 ion selection, EP=entrance potential, CE=collision energy, CCEP=collision cell exit potential. HODEs, HOTrEs, HETEs, HEPEs, diHETEs and diHDPAs are given without chiral descriptors. Internal standards are indicated in grey.

Symbol	Lipid Maps ID	RT (min)	Q1 (m/z)	Q3 (m/z)	DP (Volts)	EP (Volts)	CE (Volts)	CCEP (Volts)
RvE1	LMFA03070019	4.0	349.1	195.0	-95	-10	-22	-13
20-hydroxy LTB_4	LMFA03020018	4.4	351.1	195.0	-60	-10	-24	-17
8-*iso*-$PGF_{2\alpha}$	LMFA03110001	5.1	353.1	193.0	-135	-10	-34	-11
15-*keto*-PGE_2	LMFA03010030	5.1	349.0	234.9	-65	-10	-20	-13
TxB_2	LMFA03030002	5.2	369.1	169.0	-55	-10	-24	-15
8-*iso*-PGE_2	LMFA03110003	5.3	351.1	271.0	-5	-10	-24	-19
PGE_2-d_4	LMFA03010008	5.6	355.1	193.0	-50	-10	-26	-17
PGE_2	LMFA03010003	5.7	351.2	271.1	-50	-10	-22	-21
PGD_2	LMFA03010004	5.8	351.1	233.0	-30	-10	-16	-13
LXB_4	LMFA03040002	6.0	351.1	220.9	-60	-10	-22	-13
$PGF_{2\alpha}$	LMFA03010002	6.1	353.1	193.0	-80	-10	-34	-11
RvD2	LMFA04000007	6.2	375.1	277.1	-60	-10	-18	-15
LXA_4	LMFA03040001	6.5	351.1	114.8	-40	-10	-20	-11
13,14-dihydro-15-*keto*-$PGF_{2\alpha}$	LMFA03010027	6.6	353.1	195.0	-110	-10	-32	-11
AT-RvD1	LMFA04000074	6.7	375.0	215.0	-50	-10	-26	-11
RvD1	LMFA04000006	6.7	375.1	215.0	-50	-10	-26	-11
AT-LXA_4	LMFA03040003	6.8	351.1	114.9	-20	-10	-22	-11
RvE2	LMFA03070036	7.8	333.1	114.9	-35	-10	-18	-15
18S-RvE3	LMFA03070048	8.8	333.1	245.2	-25	-10	-16	-17
6-*trans*-LTB_4	LMFA03020013	8.9	335.1	194.9	-105	-10	-22	-11
8S,15S-diHETE	LMFA03060050	8.9	335.1	207.9	-55	-10	-22	-17
5,15-diHETE	LMFA03060010	9.2	`335.0	173.1	-55	-10	-20	-11
8(9)-EET	LMFA03080003	11.4	319.0	155.0	-60	-10	-10	-13
11(12)-EET	LMFA03080004	11.4	319.0	167.0	-90	-10	-18	-19
14(15)-EET	LMFA03080005	11.2	319.0	219	-5	-10	-16	-55
LTD_4	LMFA03020006	9.0	495.1	177.0	-70	-10	-28	-19
6-*trans*-12-*epi*-LTB_4	LMFA03020014	9.1	335.1	194.9	-80	-10	-22	-25
10S,17S-diHDHA (PDX)	LMFA04000047	9.2	359.1	153.0	-70	-10	-22	-9
18R-RvE_3	LMFA03070049	9.2	333.1	245.0	-55	-10	-18	-23
7S-MaR1	n.a.	9.3	359.1	249.9	-20	-10	-20	-19
MaR1	LMFA04000048	9.4	359.2	250.2	-65	-10	-20	-13
LTB_4-d_4	LMFA03020030	9.4	339.1	196.9	-70	-10	-22	-19
LTB_4	LMFA03020001	9.4	335.1	195.0	-65	-10	-22	-21
14,15-diHETE	LMFA03060077	9.5	335.1	207.0	-65	-10	-24	-21
7,17-diHDPA	n.a.	9.5	361.1	198.9	-45	-10	-26	-23

Symbol	Lipid Maps ID	RT (min)	Q1 (m/z)	Q3 (m/z)	DP (Volts)	EP (Volts)	CE (Volts)	CCEP (Volts)
LTE_4	LMFA03020002	9.6	438.1	333.1	-55	-10	-26	-15
19,20-diHDPA	LMFA04000043	10.2	361.1	273.0	-55	-10	-22	-15
9-HOTrE	LMFA02000024	10.2	293.0	170.9	-75	-10	-20	-15
13-HOTrE	LMFA02000051	10.3	293.0	195.0	-45	-10	-24	-19
18-HEPE	LMFA03070038	10.4	317.1	259.0	-5	-10	-16	-7
15-HEPE	LMFA03070009	10.5	317.1	219.0	-65	-10	-18	-19
13-HODE	LMFA02000228	10.8	295.0	194.9	-110	-10	-24	-21
9-HODE	LMFA02000188	10.8	295.0	171.0	-130	-10	-22	-7
15-HETE-d_8	LMFA03060080	10.9	327.2	226.0	-85	-10	-18	-11
15-HETE	LMFA03060001	11.0	319.1	219.1	-55	-10	-18	-9
11-HETE	LMFA03060003	11.1	319.1	167.0	-70	-10	-22	-15
7-HDHA	n.a.	11.3	343.1	141.1	-85	-10	-18	-23
10-HDHA	n.a.	11.2	343.1	153.0	-25	-10	-20	-15
17-HDHA	LMFA04000072	11.1	343.1	245.0	-65	-10	-16	-15
12-HETE	LMFA03060007	11.2	319.1	179.0	-65	-10	-20	-23
8-HETE	LMFA03060006	11.2	319.1	154.9	-70	-10	-20	-19
5-HETE	LMFA03060002	11.3	319.1	115.0	-65	-10	-18	-11
ALA	LMFA01030152	12.4	277.0	233.0	-90	-10	-22	-29
EPA	LMFA01030759	12.4	301.0	202.9	-125	-10	-18	-21
DHA-d_5	LMFA01030762	12.4	332.0	288.1	-75	-10	-16	-13
DHA	LMFA01030185	12.7	327.1	229.2	-115	-10	-18	-11
AA	LMFA01030001	12.7	303.0	205.1	-155	-10	-20	-11
LA	LMFA01030120	12.8	279.0	261.0	-115	-10	-28	-13
DPA n-3	LMFA04000044	13.0	329.1	231.1	-50	-10	-20	-17
AdA	LMFA01030178	13.1	331.1	233.0	-130	-10	-22	-11

7

Discussion

New functional roles of genes in disturbed energy metabolism

Some 10-50% of the variation in blood (energy) metabolites can be explained by hereditary factors, the remaining variation most likely by environmental factors or by a combination of genetic and environmental factors. The technology for measuring genetic and epigenetic parameters is one of the fastest growing fields at the moment. Linking these parameters to diseases, disease markers and biological variation in general has resulted in the association of many new genes with metabolic diseases. This thesis has investigated the association of certain genes with metabolites to gain more mechanistic insight into the gene-disease relationship. Here, I will discuss some of the questions which followed from the research into the functional roles of the genes in general and in particular the genes involved in BCAA metabolism (Chapter 2), the *APOA5* gene (Chapter 3) and genes showing an interaction with PUFAs (Chapter 5 & 6).

How to improve research towards the functional effects of SNPs?

Currently, 150 genetic loci have been associated with obesity or T2DM [1]. Unfortunately the translation of these genotype-disease associations into a molecular disease mechanism is lagging. The technology for measuring DNA variation has advanced rapidly. On the other hand, the effects of changes to DNA sequence on DNA functionality can be very diverse, require many different measurement technologies and are less compatible for computer analysis. Therefore an increased effort in discovering the functional roles of genes involved in disturbed energy metabolism is required to gain mechanistic insight.

In Chapter 2, we have designed and utilized a new bioinformatics tool to assist researchers in discovering functional associations between SNPs, genes and metabolites. Typically, a SNP is assumed to affect the nearest gene, and knowledge of this gene is used to explain the associated disease(marker). Our tool accumulates information from various databases in order to assist the user in rationally exploring more distal genes as possible candidates. Using this tool, we provided evidence in Chapter 2 for an alternative SNP-to-gene mapping with a more distal gene, which was functionally more plausible.

Smemo *et al.* recently also showed that the nearest gene to the SNP is not always the gene being affected [2]. SNPs in introns of the *FTO* gene have consistently and repeatedly been associated to obesity and SNPs in this region are able to explain several kilograms of variation in body weight between individuals. For years, genetic studies have explained the body weight consequences of the SNPs by their influence on the *FTO* gene itself. But Smemo *et al.* argue that the SNPs in fact do not influence the *FTO* gene, but the *IRX3* gene further away. They functionally pursued the *IRX3* gene, to discover its role in hypothalamic energy metabolism control. Research by Smemo and by our group shows that high-throughput genetic screening techniques need to be combined with bio-informatic data analyses, knowledge-based inferences and a subsequent functional validation by physiological and biochemical

laboratory work. Cooperation between bioinformatics and biological disciplines is needed to unravel the story from genetic architecture up to the cellular functions triggered by the relevant circumstances.

How is branched-chain amino acid metabolism functionally involved in T2D?

As an example of new functional roles for genes, Chapter 2 of this thesis describes the functional association of branched-chain keto and hydroxy acids to a SNP that most likely affects the gene expression of Lactate dehydrogenase A (*LDHA*). The functional association of the SNP with *LDHA* was more rational than with the nearest gene, *HPS5*. This was based on the theoretical capability of lactate dehydrogenase to convert branched-chain α keto acids into branched-chain α hydroxy acids and this was confirmed experimentally. This association is interesting from an energy metabolism standpoint, as we and others have previously found that increased levels of branched-chain amino acids (BCAA) and branched-chain α keto acids (BCKA) are associated with obesity and T2DM, but functionally little is known about this association [3].

There is discussion on whether increased BCAAs are a cause or a consequence of obesity and T2DM. If BCAAs are causally involved in developing obesity and T2DM, then DNA variants that influence BCAAs must also be associated to the diseases. Indeed, several SNPs affecting genes involved in BCKA degradation have been shown to increase the risk of obesity and T2DM (*BCKDHA, IVD, PPM1K* and *KLF15*) [4]. In contrast, subjects with SNPs affecting *BCAT1* or mice deficient for *Bcat2* have a reduced risk of obesity and T2DM [4, 5]. As these genes are involved in BCKA formation, these results would point towards a pathogenic role of BCKA and its down-stream metabolites, but not of the upstream BCAAs. The SNP affecting *LDHA* described in this thesis is involved in BCKA degradation; therefore it seems likely that the SNP would increase the risk of obesity and T2DM.

A variety of possible mechanisms by which increased BCAA degradation metabolites increase the risk of obesity and T2DM have been proposed, summarized by Lynch *et al.* [4]. One mechanism involves the persistent activation of the indirect amino acid sensor mTORC1. The intracellular signaling of activated mTORC1 can interfere with intracellular insulin signaling, thereby inducing insulin resistance. On the other hand, other observations do not support a role of mTORC1. For instance, BCAA supplementation leads to persistent mTORC1 activation and would therefore be expected to induce insulin resistance. However, BCAA supplementation leads to metabolic improvements [4].

Another mechanism involves defective metabolism of BCAA. Valine, leucine and isoleucine are transaminated to BCKAs by BCAT enzymes, which are then further reduced to branched-chain α hydroxy acids by the BCKDC enzymes. A toxic accumulation of BCKA metabolic products has been shown to result in lipid peroxidation and oxidative stress [4], leading to mitochondrial bioenergetic dysfunction and the activation of stress kinases. All

these effects are associated with the development of insulin resistance.

We and others have shown that genetic defects in the BCKA degradation pathway lead to defective BCKA metabolism and therefore accumulation of BCKA metabolites [3-6]. High levels of these metabolites can induce insulin resistance via several mechanisms. Whether mutations affecting *LDHA* expression could also induce these effects will require further research.

How is APOA5 functionally capable of inducing neuronal satiety signaling?

A second gene of which SNPs have been shown to be associated with energy metabolism disorders and for which the functional mechanism is currently incomplete, is *APOA5*. In Chapter 3 we describe a newly discovered role for APOA5 in inducing neuronal satiety signaling. However the exact mechanism of inducing this neuronal signaling remains unclear. First, the source and trigger for *APOA5* expression is unknown. An appealing mechanism was introduced by Guardiola *et al.* who proposed that the intestinal expression of *APOA5* is triggered by PPARα, a (dietary) fatty acid sensor [7]. Our data confirm that a high fat dietary trigger is necessary to induce food intake differences between WT and *Apoa5*$^{-/-}$ mice. Unpublished follow-up experiments corroborate the fact that small intestinal *Apoa5* expression is detectable at low levels and that intestinal expression is up-regulated on a high fat diet. However, the expression levels were very low. It seems more likely that the majority of APOA5 originates from the liver, where different nuclear receptors, PPARα, FXR, ROR, HNF4, Nur77 and CREBPH could trigger *APOA5* expression [8, 9].

After induction of *APOA5* gene expression in either the intestine or the liver, most of the APOA5 is secreted into the bloodstream [10, 11]. Due to its hydrophobic nature most APOA5 is bound to the lipoprotein particles chylomicrons, VLDL and HDL. In order to induce satiety signaling, APOA5 must bind to a neuronal receptor. Several potential binding partners of APOA5 have been suggested, including members of the LDL receptor family and VPS10P domain containing receptors (such as Sortilin-1 and Sortilin-related receptor [12]), but also heparin and glycosylphosphatidylinositol HDL-binding protein 1 (GPIHBP1) [9]. SNPs in the VPS10P domain containing receptors themselves were found to associate with plasma TG, LDL-cholesterol and CVD in a GWAS [13] and potentially play important roles in neuronal signaling [14]. A role for GPIHBP1 in binding APOA5 was suggested when an *iv* injection of APOA5 bound to recombinant HDL lowered plasma TG in *Apoa5*$^{-/-}$ mice, while *Gpihbp1*$^{-/-}$ mice did not show TG lowering after APOA5-rHDL injection [15].

In order for APOA5 to bind to neuronal receptors in the brain, it must first cross the blood brain barrier (BBB). Certain apolipoproteins, namely APOA1, APOE and APOB100 are capable of crossing the BBB by endocytosis [16]. Whether APOA5 is capable of crossing the BBB is unknown, although proteomics studies have identified APOA4 in cerebrospinal fluid [17, 18]. As was pointed out in the discussion of Chapter 3, APOA4 is also capable of

inducing satiety, but at a 500 fold higher dose than is required for APOA5 to induce satiety. APOA4, the closest protein homologue of APOA5, was shown to interact with the satiety inducting melanocortin system in the paraventricular nucleus of the hypothalamus, but did not activate proopiomelanocortin positive neurons in the arcuate nucleus [19]. Therefore it is possible that APOA5 also passes the BBB and binds to certain neurons of the melanocortin system to induce satiety signaling.

For future research, it is necessary to verify the role of the intestinal *APOA5* expression in response to dietary fat and to investigate whether APOA5 crosses over the BBB and binds to a receptor in certain brain cells of the melanocortin system in order to induce neuronal satiety signaling.

Is APOA5 a target to reduce CVD risk?

With the newly discovered satiety-inducing properties of APOA5 described in Chapter 3, it is tempting to speculate about any therapeutic possibilities. If hyperphagia could be prevented, obesity and its co-morbidities might also be reduced. Obesity has been widely associated to hyperphagia-inducing SNPs in several GWA studies [20, 21]. Therapy aimed at reducing food intake has been attempted using several strategies before. One of the first drugs that have proven very effective as appetite suppressants were amphetamine-like drugs. However these drugs can only be used short-time due to side effects and become less effective over time [22]. Therapy with endogenous hormones, such as leptin, has gained attention, as leptin-deficiency resulted in constant hunger and overeating [23]. Unfortunately, it quickly became clear that the intended obese target individuals demonstrated hyperleptinemia as a result of leptin resistance [24]. Therefore therapies aimed at reducing food intake using leptin in the obese (leptin-resistant) individuals have proven challenging [24]. Currently glucagon-like peptide 1 (GLP-1) analogues and inhibitors of GLP-1 degradation are being tested for their anti-hyperphagia properties [25, 26]. Unfortunately, desensitization to GLP-1 analogue-induced satiety signaling has been shown upon long-term treatment in hyperphagic rodent models [27, 28].

An important question that needs to be addressed is therefore whether APOA5 resistance also occurs in obese individuals. Similar to leptin resistant obese subjects with hyperleptinemia, obese subjects might also be APOA5 resistant indicated by increased APOA5 concentrations. Interestingly, there is controversy about the direction of the association of obesity and plasma APOA5. Unpublished data from our group indicates that a higher BMI is associated with higher plasma APOA5 levels, while Hahne *et al.* has found equal APOA5 levels in a large BMI range [29] and Huang *et al.* have even found lower plasma APOA5 levels in individuals with a high BMI [30]. Overexpression of *Apoa5* as a prolonged appetite suppressant therapy was tested in mice fed a high fat diet for 18 weeks, but did not result in reduced body weight or reduced plasma cholesterol levels [31].

Modulating appetite control has proven to be resilient to pharmacological interventions

due to neuronal adaptations that appear to defend a certain body weight and fat mass set point [32]. On the other hand, bariatric surgery, such as implemented in the individuals of Chapter 6, has proven very effective not only against obesity, but also against hyperphagia. Intestinal hormone secretion (e.g. GLP-1) as a consequence of bariatric surgery was increased, perhaps partly explaining its appetite-reducing effect [33]. Interestingly, unpublished work from our group indicated a consistent increase in the APOA5 plasma levels after bariatric surgery, possibly indicating an appetite-reducing effect via APOA5. Further research into resistance to satiety hormones such as APOA5 and the effect of bariatric surgery on intestinal satiety hormones, will be required before APOA5 could be pursued as a treatment to reduce overeating.

How do interactions between genes and PUFAs modulate CVD risk?

The new roles of recently discovered genes in disturbed energy metabolism have also implicated the importance of triggers to which these genes respond. For example, a high fat trigger is required to bring about the satiety signaling function of APOA5. Recently PUFAs have gained attention both as triggers and as markers in relation to a disturbed energy metabolism. Multiple GWA studies have detected significant interactions between the risk-markers for CVD or CVD itself and the amount of dietary PUFAs consumed or the amount of endogenous PUFAs in the blood [34, 35].

Intriguingly, SNP rs662799 affecting *APOA5* interacts with the amount of n-6 PUFAs in the diet, modulating the risk of developing hypertriglyceridemia [36, 37]. If more than 6 energy-percent of the diet is derived from n-6 PUFAs, subjects with SNP rs662799 are more prone to develop hypertriglyceridemia. The interaction between *APOA5* and n-6 PUFAs could involve the intestinal *APOA5* expression, triggered by consumption of dietary fat (more specifically n-6 PUFAs). If this feedback signal is compromised by a SNP in *APOA5*, it would result in less satiety signaling and therefore more fat consumption and possibly higher plasma TG levels. This hypothetical mechanism would require further experimentation.

In Chapters 5 & 6 we found associations between PUFAs in adipose tissue and adipose tissue inflammation. Recently, nutrigenomic interactions between PUFA content in the diet and the genes involved in the production of PUFA-derived inflammatory mediators have been found, which modulate risk-markers of CVD [34, 35]. The SNPs interacting with PUFAs on risk markers for CVD showed only a small overlap with the SNPs found to associate directly with risk markers of CVD, indicating the complementary importance of gene-environment interactions in explaining the variation in CVD risk markers [34]. The interaction between genes and PUFAs on CVD indicate sensor proteins triggered by PUFAs, which can directly or indirectly affect gene expression of genes involved in CVD. These interactions point towards metabolic regulatory mechanisms that can be influenced by the environment. Whether or not these regulatory mechanisms can be influences by adjusting PUFA metabolism or the dietary intake of the PUFA triggers will be discussed in more detail below.

Adipose tissue characteristics during a disturbed energy metabolism

Dysfunctional adipose tissue is an important feature associated with metabolic diseases. Therefore, in the second part of this thesis, we performed studies investigating the characteristics of dysfunctional adipose tissue. In Chapters 4 & 5, we pharmacologically influenced adipose tissue function using niacin to learn more about the adipose tissue changes that could occur during disease development. We found that niacin critically modifies cAMP signaling in the adipocyte, while also increasing long-chain n-3 PUFA biosynthesis, secretion and conversion. Changes in PUFA metabolism of adipose tissue were also detected in obese women that developed T2DM compared to obese women resistant to T2DM development (Chapter 6).

What is the impact of niacin treatment on cAMP metabolism in adipocytes?

Niacin, nicotinic acid or vitamin B3 (Chapter 4 & 5) has been known for almost 60 years to be an effective treatment of dyslipidemia when given in gram-dosages daily. However the mechanism by which it conveys these beneficial properties has not been completely unraveled. For example, niacin displays effects that are initiated acutely, but most of the beneficial effects leading to CVD risk reduction only occur after days of continuous niacin treatment. Niacin acutely binds to the HCA2 receptor expressed by certain immune cells and adipocytes. Binding this G-protein coupled receptor in skin Langerhans cells and keratinocytes leads to the activation of phospholipase A2, releasing arachidonic acid, which is converted to prostaglandins. These prostaglandins acutely induce vasodilation and thereby skin flushing. Also, binding of HCA2 acutely inhibits cAMP formation in adipocytes, leading to reduced lipolysis and fatty acid release from adipose tissue.

These acute effects are followed by later-stage effects of prolonged niacin administration. These effects bring about marked improvements of dyslipidemia, inflammation and free-radical formation, which help reduce CVD-risk. Although these prolonged effects are preceded by the acute effects induced by HCA2 receptor signaling, the necessity of the HCA2 receptor in inducing the beneficial prolonged effect is questioned. Prolonged niacin treatment of *Hcar2*-deficient mice still resulted in improvements to dyslipidemia, mostly by cholesterol lowering [38]. Therefore, cholesterol-lowering by niacin is likely not dependent on the HCA2 receptor and independent of lipolysis inhibition or skin prostaglandin release.

The adipocyte signaling effects after prolonged niacin treatment described in Chapter 4 on the other hand are most likely dependent on the HCA2 receptor. As niacin binding inhibits the production of an important signaling metabolite, cAMP, signaling events are distorted. In order to restore signaling functionality, adaptions are made in the adipocyte. First, on the protein phosphorylation level [39] and later on gene expression level as described in Chapter

4. Most importantly, the expression of the cAMP degrading enzyme phosphodiesterase 3B was diminished. The adaptation made to the cAMP signaling, likely induced to counteract the effect of niacin binding to the HCA2 receptor, also modified cAMP-dependent insulin and adrenergic signaling. A side effect of prolonged niacin treatment is therefore decreased insulin sensitivity and increased adrenergic sensitivity of adipocytes. Despite niacin's beneficial anti-dyslipidemic properties combined with its disadvantageous insulin resistant and adrenergic hypersensitivity properties, it is a potent treatment for dyslipidemia to reduce atherosclerosis [40]. The fact that niacin treatment is equally effective as statin treatment in mice, despite these side-effects suggests that improvements could be possible [41]. However further research would be required to dissociate the HCA2 receptor-mediated disadvantageous effects from the beneficial non-HCA2 receptor mediated effects on dyslipidemia. Whether the effects on PUFA metabolism after prolonged niacin described in Chapter 5 are dependent on the HCA2 receptor is unknown.

What are the consequences of modulating adipose PUFA metabolism on CVD?

The therapeutic role of PUFAs in CVD prevention is disputed. There are several PUFA-based therapeutic strategies currently being investigated. The first is dietary supplementation of additional n-3 PUFAs. The second is induction of endogenous n-3 PUFA biosynthesis. The third is modulation of the PUFA-derived oxylipin profile. Combination approaches are also being investigated. The effect of dietary n-3 PUFA supplementation showed significant improvements of risk factors of CVD, such as reduced hypertriglyceridemia and hypertension [42] and hepatosteatosis [43]. However in a systematic review of the randomized clinical trials of n-3 PUFA supplementation in a primary and/or secondary CVD prevention setting [44], a meta-analysis showed no effect of supplementing the diet with n-3 PUFAs on CVD outcomes itself. Therefore, PUFA supplementation might not have the desired effects on CVD endpoints.

Another therapeutic strategy is the endogenous induction of PUFA biosynthesis. Increasing n-3 PUFA and decreasing n-6 PUFA synthesis in transgenic mouse models led to resistance to obesity, dyslipidemia and diabetes [45]. In Chapter 5 we have detected an endogenous increase in PUFA biosynthesis after niacin treatment, which was associated with an anti-inflammatory PUFA metabolite plasma profile. The niacin treated mice with increased PUFA biosynthesis also showed improvements of dyslipidemia. Reversely, in Chapter 6 we detected a decreased PUFA biosynthesis in adipose tissue from obese women with T2DM compared to obese without T2DM. This result is in concordance with a beneficial effect of increased PUFA biosynthesis on metabolic diseases. Outside the context of metabolic disease, increased PUFA biosynthesis might be harmful due to their potential oxidation to lipoperoxide inflammatory triggers. Reducing PUFA biosynthesis by knockdown of PUFA elongation genes in non-diseased *C. elegans* increased their lifespan [46]. Therefore pursuing increased (n-3) PUFA

biosynthesis as a therapeutic strategy must have a proper disease indication.

Therapies aimed at modulating PUFA conversion to specific (sets of) oxylipins is an active research field for possible vascular disease therapies. For example inhibition of soluble epoxide hydrolase, which increases the levels of cytochrome P450 metabolites, may assist in maintaining vascular homeostasis in patients at risk of CVD [47, 48]. On the other hand, modulating the inflammatory pathway by this way could be a double-edged sword, as these metabolites also play an important role in cancer progression [49].

The PUFA dependent therapeutic strategies described above have shown clear improvements on metabolic disease-markers, such as improved plasma triglycerides, inflammation and vascular homeostasis. Whether these advantages will propagate to reduced CVD risk is less clear. PUFA consumption seems to be ineffective. Although PUFA biosynthesis and PUFA conversion modulation both seem promising, using these treatments might harm the patient when they are prescribed without a proper indication of dysfunctional PUFA metabolism.

Conclusions and outlook

In a world where the genetic basis for the risk of developing diseases is gaining more and more attention, it is important to pursue the functional mechanism behind the genetic associations as well. In this thesis we have looked further into the mechanisms of some of the risk alleles for cardiovascular diseases. In doing so, we have found new roles for two genes. We show that if the regulation of these genes is altered by a genetic mutation, the role of these genes provide a mechanism by which they could be involved in the development of metabolic disease. APOA5 can suppress appetite, while mutations affecting APOA5 induce overeating leading to obesity. LDHA can metabolize branched chain amino acid metabolites, while mutations affecting LDHA induce BCAA dysmetabolism and accumulation of toxic BCAA metabolites which is associated with insulin resistance. These studies provide scientific insight into the pathology of metabolic disease, which could point to possible new therapeutic targets to prevent and treat cardiovascular disease and T2DM.

Aside from possible genetic contributors to metabolic diseases, this thesis has also investigated some of the consequences of metabolic diseases, especially on adipose tissue. As energy continues to accumulate in the body due to a positive energy balance, the stressful consequences on adipose tissue become visible. Adipose tissue is also an important location where the accumulated lipids and fatty acids can modify inflammatory processes. In our studies we have seen important modifications to PUFA metabolism, both in human and mice. As PUFA metabolism is closely linked to the production of inflammatory mediators, PUFAs can connect the accumulating lipids to the development of inflammation during obesity. Endogenous up-regulation of PUFA synthesis could modify the inflammatory processes involved in obesity related diseases. The studies from this thesis have proven once again that PUFA metabolism is a powerful marker of CVD health and it provides new insights in the dysregulation that occurs during metabolic diseases.

References

1 OMIM. **2014**; Online Mendelian Inheritance in Man, http://omim.org/, McKusick-Nathans Institute of Genetic Medicine, Johns Hopkins University (Baltimore, MD) ("125853 OR 601665": accessed 15-12-2014).

2 Smemo S, Tena JJ *et al.* **2014**; Obesity-associated variants within FTO form long-range functional connections with IRX3. *Nature* 507:371.

3 Lips MA, Van Klinken JB *et al.* **2014**; Roux-en-Y Gastric Bypass Surgery, but Not Calorie Restriction, Reduces Plasma Branched-Chain Amino Acids in Obese Women Independent of Weight Loss or the Presence of Type 2 Diabetes Mellitus. *Diabetes care* 37:3150.

4 Lynch CJ, Adams SH. **2014**; Branched-chain amino acids in metabolic signalling and insulin resistance. *Nat Rev Endocrinol* 10:723.

5 Rampersaud E, Damcott CM *et al.* **2007**; Identification of Novel Candidate Genes for Type 2 Diabetes From a Genome-Wide Association Scan in the Old Order Amish: Evidence for Replication From Diabetes-Related Quantitative Traits and From Independent Populations. *Diabetes* 56:3053.

6 Dharuri H, t Hoen PA *et al.* **2014**; Downregulation of the acetyl-CoA metabolic network in adipose tissue of obese diabetic individuals and recovery after weight loss. *Diabetologia.* 57:2384.

7 Guardiola M, Alvaro A *et al.* **2012**; APOA5 gene expression in the human intestinal tissue and its response to in vitro exposure to fatty acid and fibrate. *Nutrition, metabolism, and cardiovascular diseases* 22:756.

8 Song KH, Park AY *et al.* **2013**; Identification and Characterization of Cyclic AMP Response Element-Binding Protein H Response Element in the Human Apolipoprotein A5 Gene Promoter. *BioMed research international* 2013:892491.

9 Zheng XY, Zhao SP *et al.* **2013**; The role of apolipoprotein A5 in obesity and the metabolic syndrome. *Biological reviews* 88:490.

10 Landau BR, Wahren J *et al.* **1996**; Glycerol production and utilization in humans: sites and quantitation. *American journal of physiology. Endocrinology and metabolism* 271:E1110.

11 Shu X, Ryan RO *et al.* **2008**; Intracellular lipid droplet targeting by apolipoprotein A-V requires the carboxyl-terminal segment. *Journal of Lipid Research* 49:1670.

12 Nilsson SK, Christensen S *et al.* **2008**; Endocytosis of apolipoprotein A-V by members of the low density lipoprotein receptor and the VPS10p domain receptor families. *J Biol Chem* 283:25920.

13 Kleber ME, Renner W *et al.* **2010**; Association of the single nucleotide polymorphism rs599839 in the vicinity of the sortilin 1 gene with LDL and triglyceride metabolism, coronary heart disease and myocardial infarction: The Ludwigshafen Risk and Cardiovascular Health Study. *Atherosclerosis* 209:492.

14 Dekker E, Hellerstein MK *et al.* **1997**; Glucose homeostasis in children with falciparum malaria: precursor supply limits gluconeogenesis and glucose production. *Journal of clinical endocrinology and metabolism* 82:2514.

15 Shu X, Nelbach L *et al.* **2010**; Intravenous Injection of Apolipoprotein A-V Reconstituted High-Density Lipoprotein Decreases Hypertriglyceridemia in apoav−/− Mice and Requires Glycosylphosphatidylinositol-Anchored High-Density Lipoprotein–Binding Protein 1. *Arteriosclerosis, Thrombosis, and Vascular Biology* 30:2504.

16 Kreuter J. **2013**; Mechanism of polymeric nanoparticle-based drug transport across the blood-brain barrier (BBB). *Journal of microencapsulation* 30:49.

17 Chiasserini D, van Weering JRT *et al.* **2014**; Proteomic analysis of cerebrospinal fluid extracellular vesicles: A comprehensive dataset. *Journal of proteomics* 106:191.

18 Guldbrandsen A, Vethe H *et al.* **2014**; In-depth Characterization of the Cerebrospinal Fluid (CSF) Proteome Displayed Through the CSF Proteome Resource (CSF-PR). *Molecular & cellular proteomics* 13:3152.

19 Gotoh K, Liu M *et al.* **2006**; Apolipoprotein A-IV interacts synergistically with melanocortins to reduce food intake. *Am.J.Physiol Regul.Integr. Comp Physiol* 290:R202.

20 Yang W, Kelly T *et al.* **2007**; Genetic Epidemiology of Obesity. *Epidemiologic reviews* 29:49.

21 Schneeberger M, Gomis R *et al.* **2014**; Hypothalamic and brainstem neuronal circuits controlling homeostatic energy balance. *Journal of endocrinology* 220:T25.

22 Bray GA. **1993**; Use and Abuse of Appetite-Suppressant Drugs in the Treatment of Obesity. *Annals of internal medicine* 119:707.

23 Frederich RC, Hamann A *et al.* **1995**; Leptin levels reflect body lipid content in mice: evidence for diet-induced resistance to leptin action. *Nature medicine* 1:1311.

24 Myers Martin G, Jr., Heymsfield Steven B *et al.* **2012**; Challenges and Opportunities of Defining Clinical Leptin Resistance. *Cell metabolism* 15:150.

25 Schlögl H, Kabisch S *et al.* **2013**; Exenatide-Induced Reduction in Energy Intake Is Associated With Increase in Hypothalamic Connectivity. *Diabetes care* 36:1933.

26 Ando T, Haraguchi A *et al.* **2014**; Liraglutide as a potentially useful agent for regulating appetite in diabetic patients with hypothalamic hyperphagia and obesity. *Internal medicine* 53:1791.

27 Duca FA, Sakar Y *et al.* **2013**; Combination of obesity and high-fat feeding diminishes sensitivity to GLP-1R agonist exendin-4. *Diabetes* 62:2410.

28 Lin D, Wang Q *et al.* **2014**; Abnormal response to the anorexic effect of GHS-R inhibitors and exenatide in male Snord116 deletion mouse model for Prader-Willi syndrome. *Endocrinology* 155:2355.

29 Hahne P, Krempler F *et al.* **2008**; Determinants of plasma apolipoprotein A-V and APOA5 gene transcripts in humans. *Journal of internal medicine* 264:452.

30 Huang XS, Zhao SP *et al.* **2010**; Decreased apolipoprotein A5 is implicated in insulin resistance-related hypertriglyceridemia in obesity. *Atherosclerosis* 210:563.

31 Pamir N, McMillen TS *et al.* **2009**; Overexpression of apolipoprotein A5 in mice is not protective against body weight gain and aberrant glucose homeostasis. *Metabolism* 58:560.

32 Farias MM, Cuevas AM *et al.* **2011**; Set-point theory and obesity. *Metabolic syndrome and related disorders* 9:85.

33 Thomas S, Schauer P. **2010**; Bariatric surgery and the gut hormone response. *Nutrition in clinical practice* 25:175.

34 Parnell LD, Blokker BA *et al.* **2014**; CardioGxE, a catalog of gene-environment interactions for cardiometabolic traits. *BioData mining* 7:21.

35 Chilton FH, Murphy RC *et al.* **2014**; Diet-gene interactions and PUFA metabolism: a potential contributor to health disparities and human diseases. *Nutrients* 6:1993.

36 Corella D. **2009**; Diet-gene interactions between dietary fat intake and common polymorphisms in determining lipid metabolism. *Grasas y aceites* 60:22.

37 Park JY, Paik JK *et al.* **2010**; Interactions between the APOA5 -1131T>C and the FEN1 10154G>T polymorphisms on ω6 polyunsaturated fatty acids in serum phospholipids and coronary artery disease. *Journal of Lipid Research* 51:3281.

38 Lauring B, Taggart AKP *et al.* **2012**; Niacin Lipid Efficacy Is Independent of Both the Niacin Receptor GPR109A and Free Fatty Acid Suppression. *Science translational medicine* 4:148ra115.

39 Oh YT, Oh K-S *et al.* **2011**; Continuous 24-h Nicotinic Acid Infusion in Rats Causes FFA Rebound and Insulin Resistance by Altering Gene Expression and Basal Lipolysis in Adipose Tissue. *American journal of physiology. Endocrinology and metabolism* 300:1012.

40 Lee JM, Robson MD *et al.* **2009**; Effects of high-dose modified-release nicotinic acid on atherosclerosis and vascular function: a randomized, placebo-controlled, magnetic resonance imaging study. *Journal of the American College of Cardiology* 54:1787.

41 Kuhnast S, Louwe MC *et al.* **2013**; Niacin Reduces Atherosclerosis Development in APOE*3Leiden.CETP Mice Mainly by Reducing NonHDL-Cholesterol. *PLoS ONE* 8:e66467.

42 Lorente-Cebrian S, Costa AG *et al.* **2013**; Role of omega-3 fatty acids in obesity, metabolic syndrome, and cardiovascular diseases: a review of the evidence. *Journal of physiology and biochemistry* 69:633.

43 Parker HM, Johnson NA *et al.* **2012**; Omega-3 supplementation and non-alcoholic fatty liver disease: A systematic review and meta-analysis. *Journal of hepatology* 56:944.

44 Rizos EC, Ntzani EE *et al.* **2012**; Association between omega-3 fatty acid supplementation and risk of major cardiovascular disease events: A systematic review and meta-analysis. *JAMA* 308:1024.

45 Li J, Li FR *et al.* **2014**; Endogenous omega-3 Polyunsaturated Fatty Acid Production Confers Resistance to Obesity, Dyslipidemia, and Diabetes in Mice. *Molecular endocrinology* 28:1316.

46 Shmookler Reis RJ, Xu L *et al.* **2011**; Modulation of lipid biosynthesis contributes to stress resistance and longevity of C. elegans mutants. *Aging (Albany NY)* 3:125.

47 Imig JD. **2012**; Epoxides and Soluble Epoxide Hydrolase in Cardiovascular Physiology. *Physiological reviews* 92:101.

48 Deng Y, Theken KN *et al.* **2010**; Cytochrome P450 epoxygenases, soluble epoxide hydrolase, and the regulation of cardiovascular inflammation. *Journal of molecular and cellular cardiology* 48:331.

49 Wang D, DuBois RN. **2012**; Epoxyeicosatrienoic acids: a double-edged sword in cardiovascular diseases and cancer. *Journal of clinical investigation* 122:19.

&

Addendum

Abbreviations

Chapter 3:

[^{3}H]-TO	Glycerol tri(9,10(n)[^{3}H]oleate
[^{14}C]-CO	[1α,2α(n)-^{14}C]cholesteryl oleate
aCSF	Artificial cerebrospinal fluid
APOA5	Apolipoprotein A5
CHox	Carbohydrate oxidation
EE	Energy expenditure
FAox	Fat oxidation
FI	Food intake
GIR	Glucose infusion rate
HFD	High fat diet
HSL	Hormone sensitive lipase
MCR	Metabolic clearance rate
NPY	Neuropeptide Y
PLIN1	Perilipin-1
RER	Respiratory exchange ratio
VCO_2	Carbon dioxide production
VO_2	Oxygen consumption
WT	Wild type

Chapter 4:

AC	Adenyl cyclase,
ADRB1,2,3	β-Adrenoceptor 1,2,3,
ARRB1	β-Arrestin 1,
CETP	Cholesteryl ester transfer protein,
HSL	Hormone sensitive lipase,
ip	Intraperitoneal,
INSR	Insulin receptor,
IRS1	Insulin receptor substrate 1,
PDE3B	Phosphodiesterase 3B,
PKA/B	Protein kinase A/B,
TG	Triglyceride.

Chapter 5:

12-HETE	12-hydroxy eicosatetraenoic acid
14(15)-EpETE	14(15)-epoxy eicosatetraenoic acid
14,15-diHETE	14,15-dihydroxy eicosatetraenoic acid
19(20)-EpDPA	19(20)-epoxy docosapentaenoic acid
19,20-diHDPA	19,20-dihydroxy docosapentaenoic acid
AA	Arachidonic acid
AdA	Adrenic acid
ALA	α-Linolenic acid
ALOX	Arachidonate lipoxygenases
APOE*3-Leiden	Apolipoprotein E3 Leiden
CETP	Cholesteryl ester transfer protein
COX	Cyclooxygenase
CVD	Cardiovascular disease
CYP	Cytochrome P450
DHA	Docosahexaenoic acid
DPA	Docosapentaenoic acid
EPA	Eicosapentaenoic acid
FDR	False discovery rate
GC-MS	Gas chromatography mass spectrometry
gWAT	Gonadal white adipose tissue
LA	Linoleic acid
LC-MS/MS	Liquid chromatography tandem mass spectrometry
NEFA	Non-esterified fatty acid
PUFA	Poly-unsaturated fatty acid

Summary

Overweight and obesity have been on the rise since the late 1970's. With it, the risks of developing metabolic disorders such as the metabolic syndrome, type 2 diabetes and cardiovascular disease have also risen. This sudden increase in the prevalence of obesity and related metabolic disorders is most likely due to a sudden change in our environment. Most of us are ill-adapted to deal with the recent 'obesogenic environment'. In Chapter 1, an overview of our energy metabolism and regulation of the energy balance is introduced, showing that animals and humans are well-adapted for energy conservation and storage, but ill-adapted for energy overload. The subsequent work presented in this thesis focused on the development of obesity and insulin resistance by investigating the underlying energy,- and fatty acid metabolism.

Differences in our energy metabolism can have a genetic origin. Genome Wide Association Studies (GWAS) have revealed numerous single nucleotide polymorphisms (SNPs) associated with differences in energy metabolism. However, translating this genetic information to a mechanism by which the disease could arise has proven difficult. In order to assist scientists in reviewing possible mechanisms by which a SNP could be associated with a disease or disease-marker, we describe the application of a newly developed knowledge-based workflow in Chapter 2. This workflow assists users in mapping SNPs to genes. Suhre *et al.* have described metabolic variation in plasma metabolite levels and their association to SNPs in the general population. By applying our workflow to the 37 quantitative trait loci associated with metabolite levels described by Suhre *et al.* we generated metabolite-gene-SNP reports for these associations. We found that the report generated for SNP rs2403254 indicated that an alternative candidate gene (*LDHA*) might be affected by this SNP, which could account for the observed association with branched chain amino acid (BCAA) degradation products. To further strengthen the new-found association, we demonstrated using chromatin interaction databases that the SNP rs2403254 could indeed interact with *LDHA* and using *in vitro* experiments we demonstrated that the enzyme transcribed from the *LDHA* gene could indeed generate the BCAA degradation products that it associates with. Therefore it is plausible that SNP rs2403254 affects the transcription of *LDHA*, which could lead to changes in the levels of BCAA degradation products.

Other GWAS have shown that the *APOA5* gene is associated with triglyceride metabolism and obesity. In Chapter 3 we investigated the mechanism underlying this association by using a mouse model deficient for *Apoa5*. We observed that *Apoa5*$^{-/-}$ mice consume more food and gain more body weight, but only on a high fat diet. As APOA5 plasma levels are very low and increase after consumption, we hypothesized that APOA5 might be involved in satiety signaling after fat consumption. We tested this hypothesis by injecting APOA5 into the blood and by injecting APOA5 into the brain of fasted *Apoa5*$^{-/-}$ mice. In both cases APOA5 injection resulted in decreased high fat diet consumption. Also, hepatic overexpression of *APOA5* prevented the increased high fat diet consumption observed in *Apoa5*$^{-/-}$ mice. Together, these

experiments demonstrate a role for APOA5 as a fat-inducible satiety hormone.

Aside from genetic influences, the development of metabolic diseases can also be affected by drugs. For example, the drug niacin inhibits atherosclerosis, but as a side-effect niacin treatment induces the development of insulin resistance. Niacin is known to influence energy metabolism by acutely inhibiting fatty acid release from adipocytes. However, the mechanisms by which niacin induces its long-term effects are not entirely understood. In Chapter 4 we further investigated the niacin-induced insulin resistance of adipocytes. After prolonged niacin treatment we confirmed that mice developed whole-body insulin resistance and that their isolated adipocytes were less sensitive to lipolysis-inhibition by insulin. We also showed that the adipocytes from niacin-treated mice were more sensitive to lipolysis-stimulation by cAMP (via both 8Br-cAMP and adrenergic stimulation). Subsequently, we examined gene expression of the proteins in the insulin signaling pathway and the adrenergic signaling pathway controlling lipolysis and found that both pathways were down-regulated. This included the gene *Pde3b* encoding for a cAMP degradation protein, which is involved in both pathways. Using a PDE3B inhibitor on isolated adipocytes, we showed that decreasing PDE3B activity can stimulate lipolysis. Therefore, the niacin-induced decreased PDE3B activity could lead to both the observed insulin resistance and the increased sensitivity towards cAMP stimulation.

In Chapter 5, we further investigated the effect of niacin on adipose tissue gene expression and composition. Microarray analysis demonstrated up-regulation of gene expression of the pathway of biosynthesis of (poly) unsaturated fatty acid. By examining the fatty acid composition of the adipose tissue, we found that increased substrate-product ratios in the PUFA biosynthesis pathway matched the increased gene expression for the catalyzing enzyme. By measuring the adipocyte secreted fatty acid levels and the plasma NEFA levels, which are mostly determined by adipose lipolysis, an increased level of the end-products of the PUFA biosynthesis pathway was found. Specifically, increased levels of n-3 PUFAs were found, which can be converted to anti-inflammatory oxylipins. Indeed, increased plasma levels of the hydrolysis products of these n-3 PUFA derived oxylipins were found, which suggests an anti-inflammatory plasma profile that could contribute to the anti-inflammatory vascular effects of niacin.

In Chapter 6, the role of fatty acids in the development of obesity and diabetes was examined in an obese human population. We previously found that adipose tissue of obese women with type 2 diabetes mellitus (T2DM) was more inflamed than adipose tissue from obese women without T2DM (NGT). As this inflammatory difference might be partially mirrored by differences in adipose PUFA composition and PUFA-derived oxylipin formation, the fatty acid composition was determined. Long chain PUFAs of both n-3 and n-6 were more abundant in the adipose tissue of T2DM women compared to NGT women. Measuring the oxylipin concentrations in the adipose tissue suggested an increased conversion of the n-6 PUFA arachidonic acid towards leukotrienes. Moreover, as gene expression of the leukotriene biosynthesis pathway was up-regulated and leukotriene metabolites tended to be increased

in the subcutaneous adipose tissue of the T2DM women. The increased arachidonic acid conversion to chemo-attractant leukotrienes might explain the positive correlation between the adipose arachidonic acid content and the gene expression of the macrophage marker *CD68*, suggesting a role for PUFAs and leukotrienes in the development of adipose tissue inflammation.

Taken together, these studies provide novel insight into the role of dysfunctional energy and fatty acid metabolism in the development of obesity and insulin resistance. As discussed in Chapter 7, our results illustrate the importance of functional research into the discovered genetic associations to gain more mechanistic insight. A better insight may lead to new therapeutic strategies to combat metabolic diseases. We have also seen the extensive changes in adipose tissue in obesity and insulin resistance, especially with regard to PUFA metabolism. Adipose tissue PUFA storage and PUFA conversion to inflammatory mediators provide a clear link between obesity and inflammation, which can be targeted to improve inflammation and metabolic disease.

Samenvatting

Overgewicht is een groeiend probleem wereldwijd. Meer mensen sterven aan de gevolgen van overgewicht dan aan de gevolgen van ondergewicht. Overgewicht op zichzelf is schadelijk voor bijvoorbeeld knie- en heupgewrichten, maar is vooral een risico door de nadelige gevolgen van de verstoorde energiestofwisseling. Deze stofwisseling veranderingen kunnen leiden tot ziektes, zoals het metabool syndroom, diabetes mellitus type 2 (DM2) en aderverkalking. Al deze ziektes dragen bij aan een vergrote kans op hart en vaatziekten (HVZ). Overgewicht en obesitas worden veroorzaakt door een hogere energie inname dan een energie verbruik, ofwel door meer te eten dan te verbranden. Er zijn sterke aanwijzingen dat de huidige obesitas epidemie vooral veroorzaakt wordt door een hogere energie inname, met name van koolhydraten, ook al is men zeker ook minder gaan bewegen. Het onderzoek wat hier beschreven is gaat niet zozeer over de vraag waarom de bevolking als geheel dikker wordt, maar waarom sommige mensen wèl en sommige mensen géén nadelige gevolgen van de energiestofwisseling ontwikkelen. De aandacht gaat in het bijzonder uit naar welke onderlinge verschillen in bijvoorbeeld het DNA en het dieet een rol spelen. Daarnaast onderzoeken we het mechanisme van een ooit veelbelovend geneesmiddel.

In Hoofdstuk 1 wordt beschreven hoe de energiestofwisseling van voornamelijk vet en suiker in elkaar zit. De stofwisseling is zorgvuldig afgestemd op het conserveren van energie voor tijden van schaarste. Echter, in onze overvloedige maatschappij waar schaarste zeldzaam is raakt de regulatie uit balans. De gevolgen van een toenemende energieopslag in de vorm van vet, in de levercellen (hepatocyten) en de vetcellen (adipocyten), kunnen stress veroorzaken in deze cellen wat kan leiden tot een verminderde gevoeligheid voor bijvoorbeeld het voedselhormoon insuline. Insuline wordt vrijgegeven aan het bloed wanneer voedingsstoffen van een maaltijd het bloed bereiken. Vervolgens geeft insuline het signaal aan voorraadcellen om hun voorraad op te bouwen en te stoppen met de afgifte van hun voorraad aan het bloed. Tevens geeft insuline het signaal aan niet-voorraad cellen zoals spiercellen en zenuwcellen om de voedingsstoffen op te nemen en te gebruiken. Bij een verminderde gevoeligheid (resistentie) voor insuline worden voedingsstoffen niet efficiënt opgenomen uit het bloed en blijft de concentratie voedingsstoffen in het bloed hoog. Dit heet insuline resistentie en kan uiteindelijk leiden tot DM2. Dit proefschrift is gewijd aan de rol die de energiestofwisseling en vetzuurstofwisseling spelen bij de ontwikkeling van obesitas en insuline resistentie, met name in het vetweefsel.

In het eerste deel van mijn proefschrift hebben we geprobeerd om genetische aanwijzingen die in verband staan met een verstoorde stofwisseling, te vertalen naar een verfijnder werkingsmechanisme voor die aanwijzing. Obesitas is gedeeltelijk genetisch bepaald. Vele studies hebben variatie in DNA-volgorde (bijvoorbeeld een SNP) in verband gebracht met variatie in lichaamsgewicht, metabole ziektes en energie metabolisme. Maar ondanks alle kennis over DNA is nog steeds grotendeels onbekend wat voor uitwerking een SNP kan hebben op eiwitproductie. Vandaar dat genetische studies die een verband laten zien tussen

SNPs en metabolisme soms niet verder komen dan precies dat: een (indirect) verband waarbij mechanistisch inzicht in het metabolisme ontbreekt. Door gebruik te maken van een door ons ontwikkelde koppeling van computerprogramma's (workflow) kunnen de verschillende mechanismen waarop een SNP in verband staat met een ziekte of een ziekte-marker worden vergeleken. In Hoofdstuk 2 laten we zien dat onze workflow helpt om te beredeneren of een verschil in de productie van een bepaald eiwit, veroorzaakt door een SNP, logischerwijze zou kunnen passen bij de verschillen in het gemeten metabolisme. Een eerder onderzoek in de algemene populatie heeft 37 nieuwe verbanden gevonden, namelijk dat bepaalde SNPs in verband staan met hogere of lagere concentraties van metabolieten in het bloed. Door onze workflow toe te passen op de 37 verbanden uit dat onderzoek hebben we resultaten gegenereerd voor ieder van deze 37 verbanden van een SNP via een eiwit naar een metaboliet. Zo vonden we in ons onderzoek dat SNP *rs2403254* mogelijk de eiwitproductie van een ander eiwit kan beïnvloeden dan de eiwitproductie gesuggereerd door eerdere onderzoekers. De productie van dit andere eiwit, Lactaat dehydrogenase A (LDHA), zou een directe invloed hebben op de bloed metaboliet concentraties van de afbraak producten van de vertakte-keten aminozuren, waar de SNP *rs2403254* mee in verband staat. Om onze hypothese ten aanzien van dit kandidaat-eiwit verder te onderbouwen hebben wij in databases gevonden dat de DNA positie van SNP *rs2403254* en van het *LDHA* gen een interactie hebben. Ook hebben we met onze experimenten aangetoond dat Lactaat dehydrogenase A de afbraak producten van de vertakte-keten aminozuren waar de SNP mee geassocieerd is direct kan omzetten. Het is daarom waarschijnlijk dat SNP *rs2403254* de eiwitproductie van LDHA verlaagd waardoor minder afbraak producten van de vertakte-keten aminozuren omgezet kunnen worden. Via dit mechanisme zou de SNP *rs2403254* veranderingen in de concentratie van deze metabolieten in het bloed kunnen bewerkstelligen.

Andere genetische studies hebben aangetoond dat SNPs die de eiwitproductie voor Apolipoproteïne A5 (APOA5) beïnvloeden ook in verband staan met obesitas en nadelige veranderingen in het vet metabolisme. In Hoofdstuk 3 onderzoeken we het onderliggende mechanisme voor dit verband in een muismodel wat het *Apoa5* eiwit niet aanmaakt. Deze *Apoa5*$^{-/-}$ muizen worden sneller zwaarlijvig en eten ook meer dan muizen die het *Apoa5* gen wèl hebben, echter deze bevindingen werden alleen geobserveerd bij een vetrijk dieet. Normaliter is de concentratie van het APOA5 eiwit in het bloed zeer laag, maar deze stijgt na inname van (vetrijk)voedsel. Hieruit vormden wij de hypothese dat het APOA5 eiwit wellicht betrokken is bij het doorgeven van het verzadigingsgevoel na het eten van een vetrijke maaltijd. Deze hypothese hebben we getoetst door het APOA5 eiwit niet alleen in het bloed, maar ook direct in de hersenen van gevaste *Apoa5*$^{-/-}$ muizen te injecteren. In beide gevallen resulteerde APOA5 eiwit injectie in een verlaagde inname van vetrijk voedsel. Daarnaast hebben wij ook gevonden dat als het *APOA5* gen weer terug geïntroduceerd werd in *Apoa5*$^{-/-}$ muizen, dan voorkomt dat het overeten aan vetrijke voedsel wat de *Apoa5*$^{-/-}$ muis kenmerkt. Deze experimenten laten samen zien dat APOA5 een rol speelt als verzadigingshormoon wat vrijkomt bij het eten van vetrijk voedsel.

Het tweede deel van mijn proefschrift gaat vooral over de rol van het vetzuurmetabolisme in vetweefsel van obese mensen en muizen. Niacine is een voorbeeld van een medicijn wat hart- en vaatziekte voorkomt door in te grijpen op onder andere de vetafbraak in vetweefsel. Niacine werkt door een centrale regelaar van allerlei cel processen (zo ook vetafbraak), cAMP, te beïnvloeden. Als bijwerking veroorzaakt niacine insuline resistentie. Het mechanisme waarmee niacine behandeling pas na dagen leidt tot insuline resistentie niet volledig bekend. In Hoofdstuk 4 wordt dit verder onderzocht. Na langdurige niacine behandeling van muizen laten we inderdaad zien dat insuline resistentie is opgetreden op lichaamsniveau, maar ook geïsoleerde vetcellen waren resistent voor insuline-gemedieerde remming van de vetafbraak. Daarnaast werd duidelijk dat vetcellen geïsoleerd uit niacine behandelde muizen gevoeliger waren voor vetafbraak-stimulatie door cAMP, zowel via het synthetische 8Bromo-cAMP als via adrenerge (stress) stimulatie. Vervolgens hebben we naar de genexpressie gekeken van de insuline signaal transductie eiwitten en de adrenerge signaal transductie eiwitten die vetafbraak reguleren, maar de genen in beide signaal transductieketens kwamen verminderd tot expressie. Eén van deze genen, *Pde3b*, codeert voor een cAMP afbrekend eiwit, wat betrokken is in beide transductieketens via cAMP. Met behulp van een PDE3B-remmer lieten we in geïsoleerde vetcellen zien dat een verminderde PDE3B activiteit de vetafbraak kan stimuleren. We concluderen uit deze resultaten dat de verlaging van PDE3B activiteit veroorzaakt door niacine kan leiden tot zowel de geobserveerde insuline resistentie als de verhoogde gevoeligheid voor cAMP stimulatie.

In Hoofdstuk 5 vervolgen we ons onderzoek van de effecten van niacine op vetweefsel. Een genexpressie microarray liet zien dat vetweefsels van niacine behandelde muizen een verhoogde genexpressie hadden van de eiwitten betrokken bij de(poly) onverzadigde vetzuur (PUFA) productie. Het vetweefsel van langdurig met niacine behandelde muizen bleek na analyse van de vetzuursamenstelling verhoogde substraat-product ratio's in de PUFA biosyntheseketen te hebben. Deze verhoogde ratio's overlapten met de verhoogde genexpressie van het corresponderende eiwitten die het substraat tot product omzetten. Door te meten welke vetzuren worden uitgescheiden vanuit de vetcellen en welke vetzuren in het bloed zitten werd een verhoging van de eindproducten van de PUFA biosyntheseketen gevonden. Specifiek werden er verhoogde concentraties van n-3 PUFAs gevonden, welke omgezet kunnen worden naar ontstekingsremmende oxylipines. Daarnaast werden ook verhoogde concentraties van het hydrolyse product van een oxylipine gevonden wat geproduceerd word van deze n-3 PUFAs. Dit wijst op een ontstekingsremmend bloedplasma profiel wat zou kunnen bijdragen aan de verminderde ontsteking van bloedvaten die typisch zijn bij niacine behandeling van hart- en vaatziekte patiënten.

De rol van vetzuren in de ontwikkeling van overgewicht en suikerziekte wordt verder onderzocht in Hoofdstuk 6 bij een populatie van vrouwen met obesitas. Vetweefsel van obese vrouwen met DM2 was meer ontstoken dat vetweefsel van obese vrouwen zonder DM2 (NGT). Dit verschil in vetweefsel ontsteking zou gedeeltelijk verklaard kunnen worden door verschillen in de PUFA vetzuursamenstelling van het vetweefsel en de oxylipines die

geproduceerd worden van PUFAs. Er waren meer langketenige PUFAs van zowel n-3 als n-6 in het vetweefsel van vrouwen met DM2 vergeleken met NGT vrouwen. Metingen aan het oxylipine metabolisme in het vetweefsel leken te wijzen op een verhoogde omzetting van de n-6 PUFA arachidonzuur naar leukotriënen, omdat de genexpressie van de leukotrieen biosyntheseketen hoger was en er een trend was tot verhoogde leukotrieen metabolieten in het onderhuidse vetweefsel van vrouwen met DM2. De mogelijk verhoogde leukotrieen metaboliet concentraties zouden kunnen verklaren waarom de arachidonzuur hoeveelheid in onderhuids vetweefsel gecorreleerd is aan de vetweefsel genexpressie van de macrofaag marker *CD68*. Dit zou kunnen wijzen op een rol voor PUFAs en leukotriënen in de ontwikkeling van vetweefsel inflammatie.

Samengenomen laten deze studies zien dat een slechtwerkende energie en vetzuur stofwisseling sterke voorbodes zijn voor de ontwikkeling van obesitas en diabetes. Zoals beschreven in Hoofdstuk 7, benadrukken deze studies het belang van functioneel laboratoriumonderzoek naar de ontdekte genetische verbanden tussen SNPs en ziektemarkers om meer inzicht te krijgen in het werkingsmechanisme. Een beter inzicht kan leiden tot nieuwe behandelstrategieën in de strijd tegen metabole ziektes. We hebben ook de grote veranderingen van vetweefsel tijdens de ontwikkeling van obesitas en insuline resistentie beter in kaart gebracht, specifiek van het PUFA metabolisme. Vetweefsel PUFA opslag en PUFA omzetting naar ontstekingsmediatoren zijn een duidelijke verbinding tussen obesitas en ontsteking, wat het mogelijk maakt om gerichtere behandelingen te kunnen ontwikkelen die ontsteking en metabole ziektes tegengaan.

List of publications

1 M.M. Heemskerk, S.A.A. van den Berg, A.M.C. Pronk, K. Willems van Dijk, A. Aartsma, M. van Putten. **2015**. Metabolic effects of high fat diet in dystrophine deficient mice. *In preparation*.

2 S. Janssens, M.M. Heemskerk, S. van den berg, N. van Riel, K. Nicolay, K. Willems van Dijk, and J. J. Prompers. **2015**. Effects of low-stearate and high-stearate high-fat diets on liver lipid metabolism and glucose tolerance. *Submitted to J Lipid Res*.

3 L. van Beek, I.O.C.M. Vroegrijk, S. Katiraei, M.M. Heemskerk, A.D. van Dam, S. Kooijman, P.C.N. Rensen, F. Koning, J.S. Verbeek, K. Willems van Dijk, and V. van Harmelen. **2015**. Fcγ-chain deficiency restricts the development of diet-induced obesity. *Accepted in Obesity.*

4 M.M. Heemskerk, M. Giera, F. el Bouazzaoui, K. Willems van Dijk, and V. van Harmelen. **2015.** Increased PUFA content and 5-lipoxygenase pathway activity are associated with subcutaneous adipose tissue inflammation in obese women. *Submitted to Nutrients*.

5 M.M. Heemskerk, V.J.A. van Harmelen, K. Willems van Dijk, and J.B. van Klinken. **2014.** Reanalysis of mGWAS results and in vitro validation show that lactate dehydrogenase interacts with branched-chain amino acid metabolism. *Accepted in Eur J Hum Gen*.

6 L. Hussaarts, N. García-Tardón, L. van Beek, M.M. Heemskerk, S. Haeberlein, G.C. van der Zon, A. Ozir-Fazalalikhan, J.F.P. Berbée, K. Willems van Dijk, V. van Harmelen, M. Yazdanbakhsh, and B. Guigas. **2015** Chronic helminth infection and helminth-derived egg antigens promote adipose tissue M2 macrophages and improve insulin sensitivity in obese mice. *Accepted in FASEB journal*.

7 M.M. Heemskerk *, H.K. Dharuri*, S.A. van den Berg, H.S. Jónasdóttir, D.P. Kloos, M. Giera, K.Willems van Dijk, and V. van Harmelen. **2014**. Prolonged niacin treatment leads to increased adipose tissue PUFA synthesis and anti-inflammatory lipid and oxylipin plasma profile. *J Lipid Res* 55: 2532-2540.

8 M.M. Heemskerk *, S.A. van den Berg*, A.C. Pronk, J.B. van Klinken, M.R. Boon, L.M. Havekes, P.C. Rensen, K. Willems van Dijk, and V. van Harmelen. **2014**. Long-term niacin treatment induces insulin resistance and adrenergic responsiveness in adipocytes by adaptive downregulation of phosphodiesterase 3B. *AJP Endo Met* 306: E808-813.

9 R. Stienstra, W. Dijk, L. van Beek, H. Jansen, M.M. Heemskerk, R.H. Houtkooper, S. Denis, V. van Harmelen, K. Willems van Dijk, C.J. Tack, and S. Kersten. **2014**. Mannose-binding lectin is required for the effective clearance of apoptotic cells by adipose tissue macrophages during obesity. *Diabetes* 63: 4143-4153.

10 A.D. van Dam, K.J. Nahon, S. Kooijman, S.M. van den Berg, A.A. Kanhai, T. Kikuchi, M.M. Heemskerk, V. van Harmelen, M. Lombes, A.M. van den Hoek, M.P. de Winther, E. Lutgens, B. Guigas, P.C. Rensen, and M.R. Boon. **2015**. Salsalate activates brown adipose tissue in mice. *Diabetes* 64: 1544-1554.

11 S.A. van den Berg*, M.M. Heemskerk*, J.J. Geerling, J.B. van Klinken, F.G. Schaap, S. Bijland, J.F. Berbee, V.J. van Harmelen, A.C. Pronk, M. Schreurs, L.M. Havekes, P.C. Rensen, and K. Willems van Dijk. **2013**. Apolipoprotein A5 deficiency aggravates high-fat diet-induced obesity due to impaired central regulation of food intake. *FASEB journal* : 27: 3354-3362.

12 S. Kuhnast, M.C. Louwe, M.M. Heemskerk, E.J. Pieterman, J.B. van Klinken, S.A. van den Berg, J.W. Smit, L.M. Havekes, P.C. Rensen, J.W. van der Hoorn, H.M. Princen, and J.W. Jukema. **2013**. Niacin Reduces Atherosclerosis Development in APOE*3Leiden. CETP Mice Mainly by Reducing NonHDL-Cholesterol. *PLoS One* 8: e66467.

13 P.K. Wawrzyniak, A. Alia, R.G. Schaap, M.M. Heemskerk, H.J. de Groot, and F. Buda. **2008**. Protein-induced geometric constraints and charge transfer in bacteriochlorophyll-histidine complexes in LH2. *Phys chem chem phys* 10: 6971-6978.

*Authors contributed equally.

Curriculum Vitae

Mattijs Maria Heemskerk werd geboren op 23 mei 1985 te Rijpwetering. In 2003 behaalde hij zijn atheneum diploma aan het Visser 't Hooft Lyceum te Leiden. In september van dat jaar begon hij aan de studie Life Science & Technology aan zowel de Universiteit Leiden als aan de Technische Universiteit Delft. Na het *cum laude* afronden van de Bachelor in 2007, volgde hij de Master Life Science & Technology met de specialisatie "modelleren van levende materie". Tijdens een studiereis naar Barcelona, raakte Mattijs gefascineerd door regulatie van de stofwisseling. Zo heeft hij een half jaar lang onderzoek gedaan bij de groep van prof. Marta Cascante aan de Universitat de Barcelona. Bij dit onderzoek werden systeembiologie-databases gebruikt om longziektes op metabool- eiwit- en genetisch niveau te bekijken. Mattijs heeft zijn afstudeeronderzoek uitgevoerd bij prof. Sef Heijnen aan de TU Delft, waar hij computer modellen ontwierp van de schimmel *Penicillium chrysogenum*. Hij onderzocht welke combinatie van stabiele isotoop gelabelde voedingsstoffen het beste inzicht zouden geven in de energie- en penicillinestofwisseling van deze schimmel.

Na het behalen van zijn ingenieurstitel in 2009 heeft hij zijn interesse voor stofwisselingsregulatie voortgezet bij het LUMC. Onder begeleiding van prof. Ko Willems van Dijk is hij in 2010 met zijn promotie onderzoek begonnen aan de afdeling Humane Genetica, waarvan de resultaten zijn beschreven in dit proefschrift getiteld "The role of energy & fatty acid metabolism in obesity and insulin resistance". Voor de Medical Genetics Center PhD workshop won hij de beste presentatieprijs. Mattijs werkt momenteel als docent Scheikunde bij het Scala College in Alphen aan de Rijn en behaalt via het Rijksoverheid Onderwijstrainee programma zijn eerstegraads lesbevoegdheid.

&

Dankwoord

Een onderzoeker zit allang niet meer alleen in het laboratorium experimenten uit te voeren, maar het is juist een inspanning van velen die geholpen hebben, dan wel bewust of onbewust.

Eerst mijn promotor en co-promotor. Ko, je gaf mij de vrijheid om te leren, maar hield vanaf jouw vogel-perspectief het proces in de gaten, wat soms pijnlijke maar altijd verhelderende 'kill-your-darlings' momenten opleverde. Daarnaast heb je een gezonde balans gevonden tussen het noodzakelijke en het prettige, waar ik mij altijd heel prettig bij heb gevoeld. Vanessa, jouw manier van steeds fris naar resultaten kunnen kijken en dan toch nieuwe verbanden zien stelt mij iedere keer weer verbaasd. Jouw optimisme en enthousiasme sleepten mij door de mindere momenten van onderzoek doen en maakten werken met jou tot een groot plezier. Dan ook Sjoerd in den beginne, jij hebt mij aan de hand genomen bij mijn eerste stapjes in het metabool onderzoek en we hebben samen veel bereikt! Ook Jan verdient nog een vette pluim voor de begeleiding bij data analyse en bij nee-zeggen.

Ik ben zeer verdienstelijk voor de hulp van mijn paranimfen. Amanda, jij bent de spin in het web voor je gezin, je werk en zeker ook voor mij, waarbij je humor, positiviteit en verantwoordelijkheidsgevoel van jou een topvrouw maken! Sietske, jouw Randstedelijke/ Friese/ Barcelonese kijk op de wereld is heerlijk verfrissend. Ik heb geluk dat ik een inkijkje heb in jouw fantastische wereld.

De Lipido's over de tijd: Emma, wat fijn om jou een vriendin te mogen noemen. Sam & Lianne, zo leuk om samen met jullie hard te werken en ook hard te genieten. Fatiha, ik heb bewondering voor je. Saeed & Lisa, maar ook Silvia, Peter, Linda, Aise & Harish, vele malen dank voor alle hulp en de geweldige tijd! Alle (oud) leden van de Endo groep van Louis en Patrick met de fijne samenwerkingen, overleggen, feestjes en partijtjes, allen heel hartelijk bedankt voor de fijne sfeer waarin wetenschappelijk en vriendschappelijk sparren, maar vooral teamwork voorop stond. In het bijzonder Trea, voor je geduld met mijn positief (of was het negatief?) geladen karma.

De derde verdieping/HumGen, mijn tweede thuis. Mijn wisselende kamergenoten, met Sandra voor nou ja eigenlijk alles, Ludo voor de schrik-aanvallen, Marco, Eric & Kostas en de anderen, wat een productief feest! Daarnaast de groep Frants en de derde verdieping: zo divers onderzoek waar op eerste blik geen overeenkomsten zijn, maar later in mijn promotie zag ik steeds meer kruisbestuiving(smogelijkheden). Het is geweldig om persoonlijk een expert in vrijwel ieder gebied te kennen en daarmee te kunnen overleggen in een informele sfeer tijdens koffie-pauzes en lab-uitjes. The MGC committee 2013, superdeLux! Ook alle studenten in het lab, bedankt voor de frisse blik en het harde werken.

Ik wil Ben en Fred bedanken voor hun goede zorgen en hulp bij het belangrijke proefdier onderzoek.

The Metabolomics men and women, Martin, DP & Hulda but also Thomas, Amy, Marco, Can & Theo, you have taught me how to solve problems I didn't even know existed! I greatly enjoyed working with you all. Daarnaast heb ik kunnen helpen bij vele interessante

samenwerkingsprojecten, zoals met Bruno & Leonie aan insuline resistentie, met Maaike aan Duchenne, met TNO Leiden aan niacine, met Frank aan APOA5, met Rinke aan MBL, en met de TU/e onderzoekers Natal, Jeanine, Christiaan, Joep en Sharon. Allen bedankt!

Mijn vrienden en familie: allereerst Sabine, een lach, een traan, een dans, een dal en nog lang niet genoeg. En de andere UvB'ers Arno en Loes voor het samenwoon-plezier. De Scooby-gang, voor alle gezellige afleiding en luisterende oren (en Marcel voor de kaft!) De turners voor de diepgaande wetenschappelijke debatten. Bart, Brechtje, Eliane, Eva & Jos, ik ben heel blij jullie te kennen. De van der Geesten, voor jullie interesse en alle gezellige familiedagen. Rina & Michel voor de mooie momenten. Pap & mam, dankzij jullie kon ik uitgroeien tot wie ik ben en ik ben trots op jullie. Kien, mijn lieve zus, wat enorm fijn dat ik altijd op jou kan bouwen. Antoine, door dik en dun, contra el mundo. Je verdient je eigen bladzijde, maar ik moet volstaan met een gedichtje: 'Bij jou voel ik me krachtig en geweldig zoals een…' Nee, nee! 'Bij jou voel ik me krachtig en…' Nee, nee. 'Bij jou voel ik.'